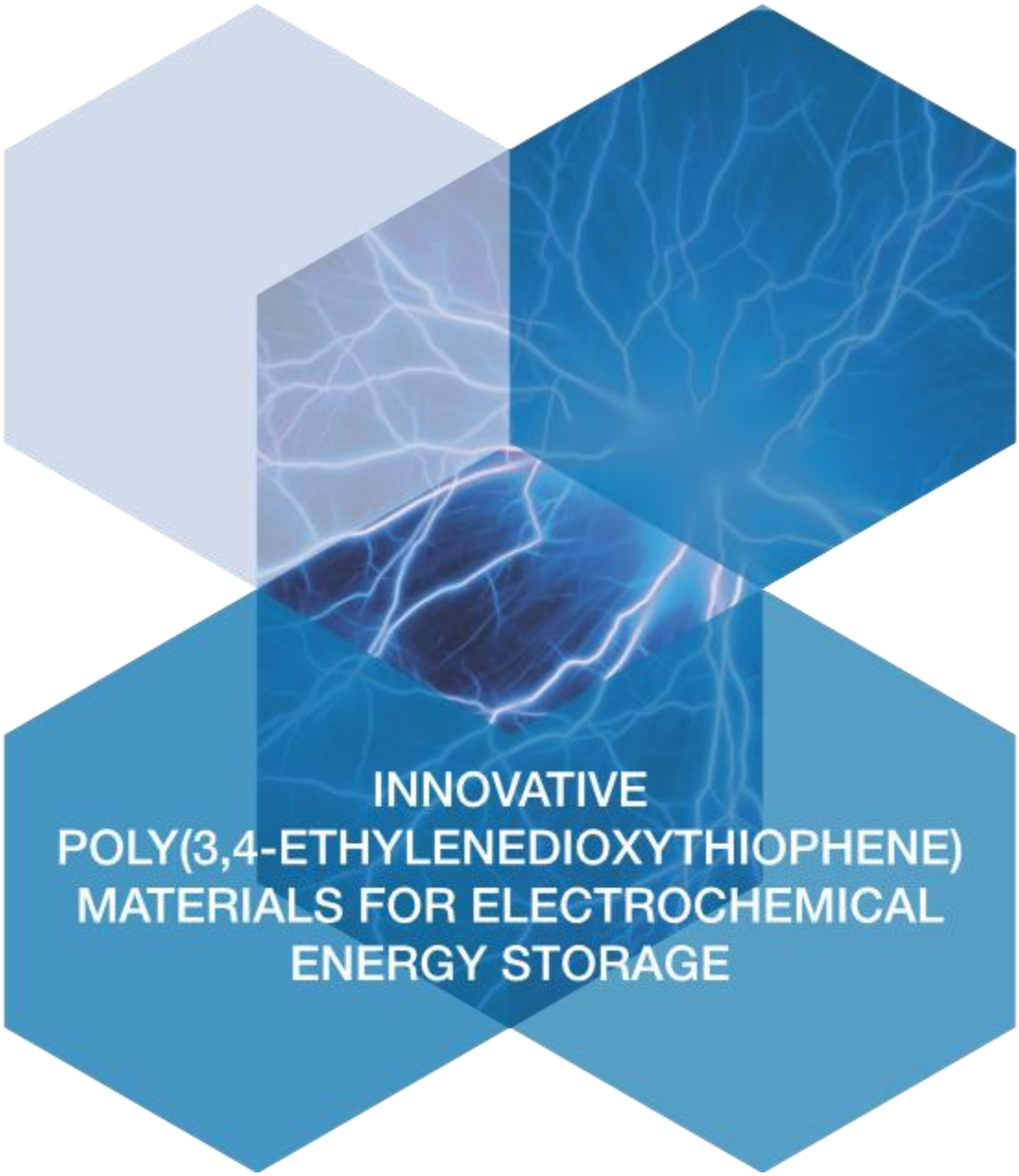

INNOVATIVE POLY(3,4-ETHYLENEDIOXYTHIOPHENE) MATERIALS FOR ELECTROCHEMICAL ENERGY STORAGE

NEREA CASADO PEREZ | PhD Thesis 2017

Universidad del País Vasco
Euskal Herriko Unibertsitatea

POLYMAT

Innovative Poly(3,4-ethylenedioxythiophene) Materials for Electrochemical Energy Storage

Nerea Casado Perez

University of the Basque Country UPV/EHU

Donostia-San Sebastián

2017

Contents

Chapter 2. PEDOT Radical Polymer with Synergetic Redox and Electrical Properties **41**

Chapter 3. High performance PEDOT/lignin biopolymer composites for electrochemical supercapacitors **71**

CHAPTER 1

Introduction

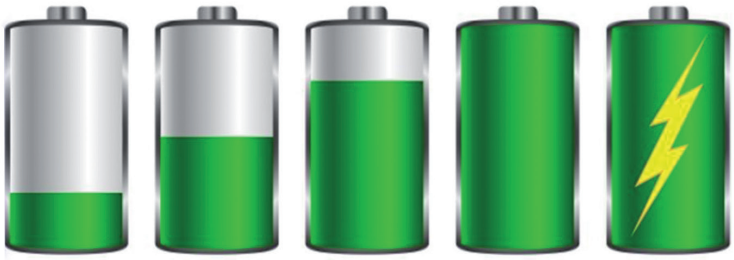

Chapter 1. Introduction

1.1. Electrochemical energy storage

Energy storage technologies are crucial in order to meet the global challenge of clean and efficient sustainable energy. During the last century, the development of improved energy storage systems has been intensely pursued in an effort to solve environmental problems related to pollution, depletion of fossil-fuel resources and the rapid development of portable electronics, electric vehicles and energy storage stations.[1,2]

The worldwide demand for electricity is predicted to double by 2050, which means the present energy production has to be doubled from 14 TW to 28 TW. This increase should be completed in a sustainable manner and not relying only in fossil fuel resources. The electrical energy will then be produced from renewable energy sources, such as solar, wind, hydropower or biomass. Due to the inherently intermittent character of these resources, good energy storage systems are necessary to make the best use of energy.[2] Although pumped hydroelectric systems represent the 98% of the worldwide storage power, electrochemical energy storage (EES) offers a well established strategy to improve portable electronics market, electrification of vehicles and grid utilization. Currently, researchers focus particularly on the development of not only high performance batteries and supercapacitors, but also on meeting the requirements of safety, cost, environmental friendliness and sustainability.[3-5]

Owing to their long cycle life, high energy and power densities, rechargeable lithium batteries have been one of the most important battery technologies in the last decades.[1] Lithium-ion batteries are appropriate for portable electronic devices; however, safety and cost issues should be further addressed in order to use them in large scale power systems, such as, electric vehicles and smart grids.[6] Consequently, researchers have shifted their attention to alternative battery chemistries, including Na-ion,[7] Li-S,[8] Li-O_2,[9] other metal-air chemistries[10,11] (Zn-air or Mg-air) and Li-organic batteries.[12] Figure 1.1 shows some of these current and future promising energy storage systems.[13]

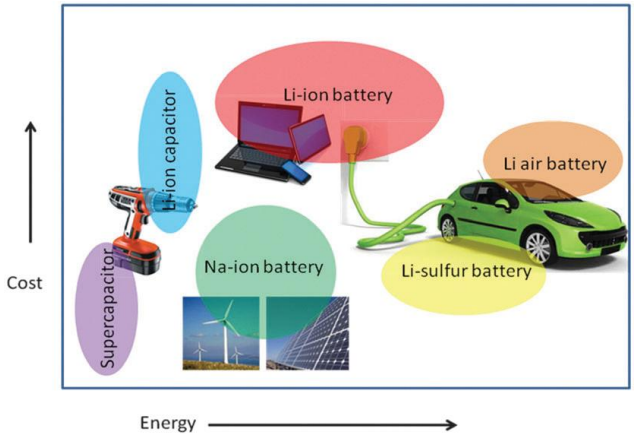

Figure 1.1. Cost vs. energy plot of different energy storage systems[13]

1.1.1. Electrochemical energy storage devices: batteries and capacitors

The main difference between batteries and capacitors, the two main types of EES devices, consist in the principle of storing charge. Batteries store energy through a reversible electrochemical reaction, while capacitors store energy electrostatically in electric fields.[14] A battery is made of two different electrodes with an ionic conductor electrolyte between, as represented in Figure 1.2a. During discharge, the negative electrode is oxidized, releasing electrons, while the positive electrode is reduced consuming these electrons. This source of electrons is driven through an external circuit to provide power. In the case of lithium ion batteries, the negative electrode is usually made of carbon based materials such as graphite and the positive electrode materials are typically lithium containing metal oxides or phosphates, such as lithium iron phosphate. Therefore, during the charging process, the cathode is oxidized releasing lithium ions and electrons. The lithium ions move into the anode through the electrolyte, storing energy during this process. When the battery is discharging, the lithium ions move back across the electrolyte to the cathode, and the electrons travel to the cathode through the external connection, generating an electric current.

Conventional capacitors store energy by electrostatic interactions in electric fields and in the case of electrochemical capacitors (supercapacitors) by means of ion adsorption of the electrolyte into the pores of the electrode. They are composed of two electrodes with an ionic conducting media in between (Figure 1.2.b). During charge, the cations of the electrolyte diffuse towards the negative electrode, while anions move towards the positive electrode. In

electrochemical capacitors the electrolyte forms a double layer on each electrode and consequently ions can be rapidly discharged.[15]

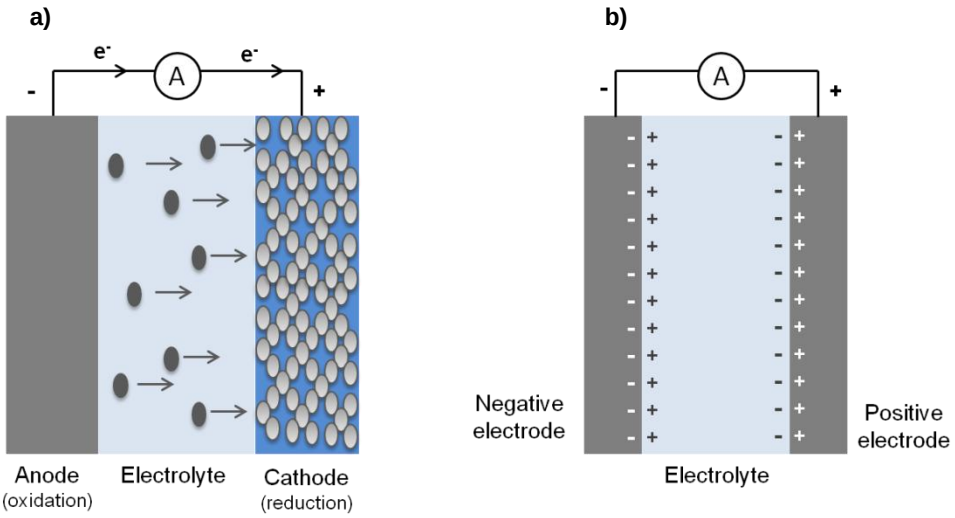

Figure 1.2. Scheme of a) a battery and b) a capacitor during discharge process

Electrochemical energy storage devices are characterized by the specific energy and specific power. Specific energy is the quantity of energy stored per unit of mass (Wh/Kg), while the specific power determines how fast that energy can be achieved. Figure 1.3 shows the Ragon plot of the current EES devices.[16] Batteries possess high specific energy but relatively low specific power, which means that they are able to provide high amount of energy but in long times. On the contrary, capacitors have high specific power but low specific energy, thus,

they provide low energy but in very short times. Electrochemical capacitors have intermediate properties between conventional capacitors and batteries.[5,15]

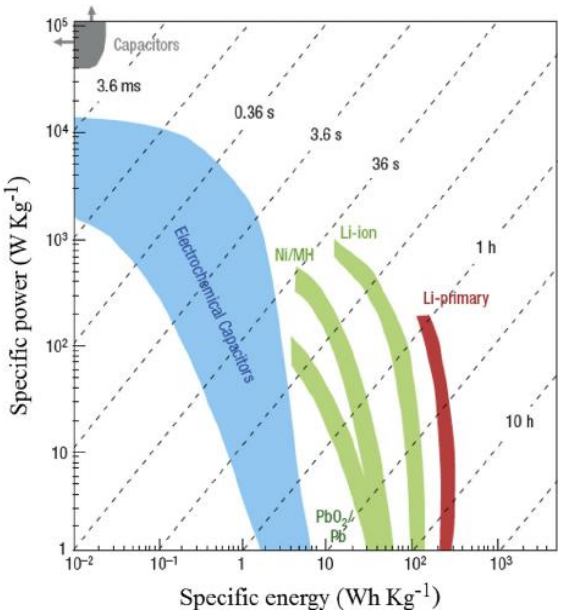

Figure 1.3. Ragone plot of current EES devices[17]

Another important difference between batteries and capacitors is their charging/discharging behaviour when a constant current is applied. The typical discharge voltage curves for a battery and capacitor are shown in Figure 1.4. Batteries rapidly reach a voltage plateau and function at a constant potential, at which the redox reaction of the electrodes occur. In the case of capacitors, as charges are stored electrostatically, the potential

is linearly changed as a function of time or charge, since inserting more charge becomes harder due to coulombic interactions.[18]

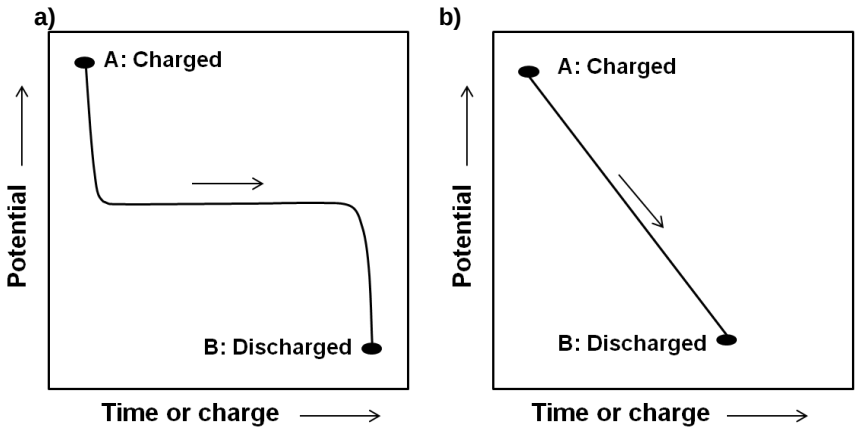

Figure 1.4. Typical discharge curve of a) a battery and b) a capacitor.

1.2. Conducting polymers

Since the discovery of conductive polyacetylene by Shirakawa and co-workers[19] in 1977, conducting polymers (CPs) have been widely investigated due to their interesting and tuneable properties. In general, conducting polymers possess high electrical conductivity, easy processability, flexibility, low weight, low cost and the possibility of large scale production.[20-22]

Therefore, CPs have been employed in a wide range of applications including actuators, organic light emitting diodes, photovoltaic devices, sensors, supercapacitors and batteries.[20-25]

The IUPAC definition for conducting polymer is an electrically conducting polymer composed of macromolecules having fully conjugated sequences of double bonds along the chains. Figure 1.5 shows the structures of the most studied conducting polymers due to their high conductivity and easy synthesis: polypyrrole (Ppy), polyaniline (PANI), polythiophene (PT) and poly(3,4-ethylenedioxythiophene) (PEDOT).

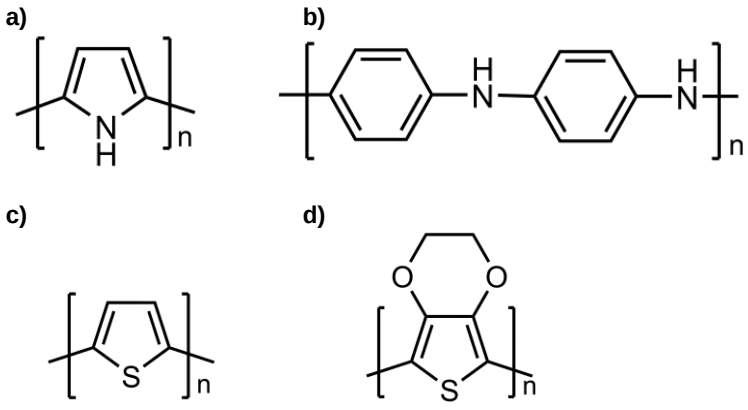

Figure 1.5. Chemical structures of a) polypyrrole, b) PANI, c) polythiophene and d) PEDOT conducting polymers.

Conducting polymers require partial oxidation or reduction processes to give rise to charged species. These charges are compensated by the appropriate counter ions, named dopants, to maintain the electroneutrality.[26] The partial oxidation and reduction are known as p-

doping and n-doping, respectively.[27] As a result of the doping process, charged defects such as *polarons* and *bipolarons* are introduced into the polymer chains, which are responsible for the electron conduction.

1.2.1. Poly(3,4-ethylenedioxythiophene)

Among all conducting polymers, poly(3,4-ethylenedioxythiophene) (PEDOT) (Figure 1.5d) has sparked much interest in various applications due to its high conductivity, good stability and easy processing. Since its discovery in the 1980s, which was chemically prepared by Jonas *et al.*[28] and electrochemically polymerized by Heinze *et al.*,[29] it has been applied in numerous applications starting from antistatic agent and photographic material[30] to state-of-the-art flexible supercapacitors.[31]

1.2.1.1. Electrochemical polymerization

There are three main types of polymerization reactions for the synthesis of PEDOT and its derivatives. Electrochemical polymerization is achieved by applying a potential to an electrode which is immersed in a monomer solution. The polymerization is usually carried out in a three electrode cell, consisting of a working, counter and reference electrode. During the polymerization process, the polymer is deposited onto the working electrode (Figure 1.6a).

EDOT can be electrochemically polymerized by cyclic voltammetry[32] (application of a linearly variable voltage), chronopotentiometry[33] (constant current) and chronoamperometry[22,34] (constant potential). The irreversible oxidation peak of EDOT occurs at 1.26 V while the

reversible redox process of electrodeposited PEDOT appears between -0.55 V and 0.1 V vs. Ag/AgCl.[35] Electrochemical polymerization allows controllable polymerization, since the selected technique and conditions affect the morphology and electrochemical properties of the polymer.[36] However, small amount of material is usually obtained through this method, limiting its use to specific applications.

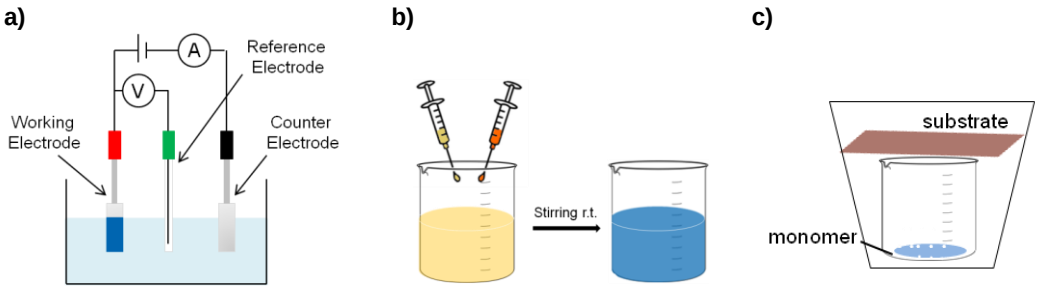

Figure 1.6. Schematic representation of a) electrochemical, b) oxidative chemical and c) vapour phase polymerization.

1.2.1.2. Oxidative chemical polymerization

In the oxidative chemical polymerization, monomers are oxidized by chemical oxidants that initiate the polymerization reaction (Figure 1.6b). This method leads to a polymer that precipitates out of solution, so it can be used to prepare high amounts of material.[37]

EDOT monomer and its derivatives can be polymerized using various oxidants. In the traditional method, $FeCl_3$ or $Fe(OTs)_3$ are employed as oxidizing agents. The overall polymerization reaction can be divided in two major steps (Figure 1.7). First, monomers are

polymerized through oxidative polymerization to give an undoped, neutral polymer (Figure 1.7a-d) and second, the polymer is doped due to the excess of oxidant yielding a conducting polymer (Figure 1.7e). In the same way, the oxidative polymerization step can be separated in three different steps. It starts by the oxidation of EDOT into a radical cation (Figure 1.7a), followed by coupling and re-aromatisation of free radicals forming dimer species (Figure 1.7b) and subsequent chain propagation by oxidation and recombination of oligomers (Figure 1.7c-d).[38] This method yields a black, insoluble PEDOT polymer with high conductivity compared to other polyetherocycles.[37]

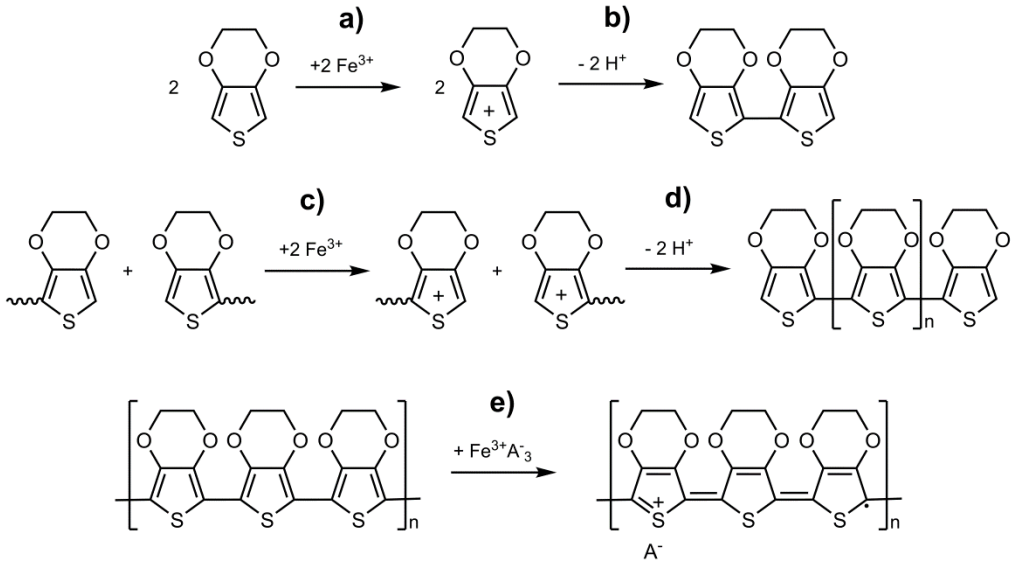

Figure 1.7. Scheme of the oxidative polymerization of PEDOT

Apart from Fe(III) compounds, persulfates are the most important group of oxidants, which are able to polymerize EDOT to form conductive PEDOT complexes. Sodium and ammonium persulfate salts are the most used ones.[39] Besides persulfate salts, the addition of a small amount of Fe(II) or Fe(III) salts as catalyst increases the rate of the polymerization.

1.2.1.3. Vapour phase polymerization

Vapour phase polymerization (VPP) was first described by Mohammadi *et al.*[40] as a chemical vapour deposition (CVD) process, for the polymerization of polypyrrole using $FeCl_3$ and H_2O_2 as oxidants. In VPP a substrate is coated with an oxidant, which is exposed to the EDOT monomer vapour and in this way, the polymerization takes place at the surface of the substrate, obtaining a PEDOT film (Figure 1.6c).[41,42] Several parameters affect the VPP process, such as, monomer concentration[43] or temperature.[44]

There are three different types of VPP for the synthesis of PEDOT: atmospheric VPP,[45] chemical vapour deposition (CVD)[44] and vacuum VPP.[43] Atmospheric VPP is performed under atmospheric conditions and apart from the oxidant ($FeCl_3$ or iron(III) tosylate), usually a base like pyridine is used to decrease the polymerization rate and obtain PEDOT with high conductivity.[46] In the case of CVD, vacuum conditions are applied in the polymerization chamber with high temperatures to sublime the oxidant ($FeCl_3$), which is placed in a crucible above the substrate. Like this, when the monomer is introduced as a vapour flow into the chamber, it gets oxidised by the oxidant vapour, initializing the polymerization process.[44] Vacuum VPP is carried out under higher pressures[43] than CVD. The substrate is coated by the

oxidant (as in atmospheric VPP), which then gets in contact with the monomer vapour, starting the polymerization process.

1.2.2. PEDOT:PSS

The solubility problem of PEDOT was surpassed by using a water soluble polyelectrolyte, poly(styrenesulfonic acid) (PSS), as counter ion and stabilizer of the positively charged PEDOT, forming the PEDOT:PSS complex (Figure 1.8).[47]

PEDOT:PSS is prepared by the oxidative polymerization of EDOT in presence of PSS in aqueous solution using $Na_2S_2O_8$ as oxidizing agent. PSS acts as charge balancing counter ion of PEDOT and it is also responsible for keeping PEDOT chains dispersed in the aqueous medium. In this way, a dark blue aqueous PEDOT:PSS dispersion is obtained, which is easy to process by drop-casting or spin coating.

It is worth to mention that the polymerized PEDOT segments are not very long, it is assumed from several measurements that the molecular weight of these segments is between 1000 and 2500 Da (6 to 18 repeating units).[48] Moreover, PEDOT:PSS complex is very stable. As an example, Inganäs and co-workers proved that $PEDOT^+$ and PSS^- cannot be separated by capillary electrophoresis.[49]

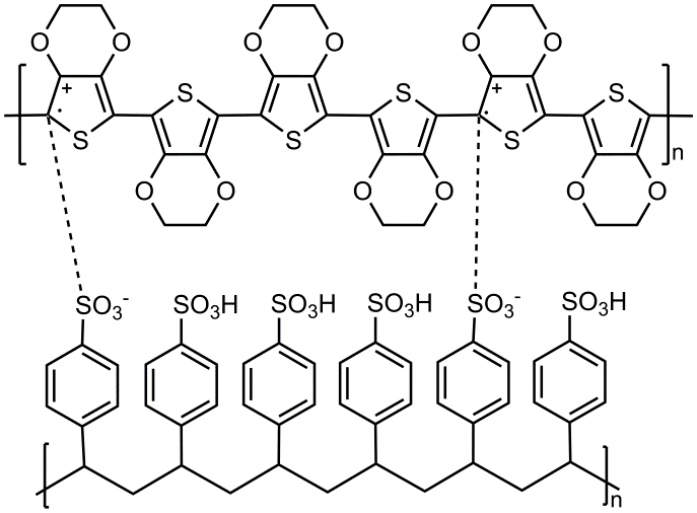

Figure 1.8. PEDOT:PSS structure

1.2.3. Conductivity of PEDOT and derivatives

Either electrochemically or chemically polymerized, PEDOT is obtained in its doped state and thus, in its electric conductor form. As mentioned in Section 1.2, the conductivity is caused by the movement of holes and electrons through the *polarons* and *bipolarons* of the polymer chains.

When electrochemical polymerization is used, the selection of the polymerization conditions as well as the dopant anion will define the morphology and properties of the final PEDOT films. Conductivity values of electropolymerized films, usually between 1-600 S/cm,

vary when changing the dopant anion. PEDOT has been electropolymerized using several dopant anions, such as ClO_4^-, PF_6^-, BF_4^- and $N(SO_2CF_3)_2^-$.[50-52] The highest conductivity values have been obtained with ClO_4^- as counter-ion (650 S/cm).[51]

The conductivity of PEDOT:PSS varies with PEDOT/PSS ratio, where an increase of PSS content reduces the conductivity. The PEDOT/PSS ratios of the commercial Baytron vary from 1:2.5 to 1:20 (PEDOT:PSS weight ratio) and the conductivity ranges from 1 to 10^{-5} S/cm. It has been observed that the particle size has also an influence on the conductivity; the bigger the particles, the higher the conductivity of the film.[48]

One method of increasing the conductivity of PEDOT:PSS is the incorporation of additives to the aqueous dispersion, such as several alcohols (ethylene glycol, sorbitol), organic solvents (dimethyl sulfoxide (DMSO), dimetylformamide), ionic liquids and salts.[53-56] In this way, an increase in conductivity is observed upon removal of the additive after the film formation. The highest increments have been observed with DMSO[57,58] and ethylene glycol[59,60] obtaining conductivity values up to 600 S/cm. Apart from adding organic solvents to PEDOT:PSS dispersion, the conductivity of PEDOT:PSS films can also be enhanced by post-treatment, immersing the films into polar organic compounds, inorganic acids or co-solvents.[23,53,61] As an example, Alemu *et al.* used methanol for post-treatment of PEDOT:PSS film, obtaining an increase in conductivity from 0.3 to 1362 S/cm.[62]

1.2.4. Electrochemistry of PEDOT and derivatives

PEDOT has a low oxidation potential and a relatively low bandgap, providing some especial electrochemical and spectroscopic properties. Owing to its low redox potential, it is very stable under ambient conditions in its oxidized state.

PEDOT has a pale blue transparent colour in its doped and conducting state, while in the reduced state has a deep blue colour. Due to its transparency in the doped state, it is suitable in applications such as electrochromic devices, antistatic transparent films and polymer light-emitting diodes.[20,23,24] A typical cyclic voltammogran of PEDOT film is depicted in Figure 1.9.[63] The oxidation potential peak appears at 0.1 V, while the reduction peak is at -0.5 V vs. Ag/AgCl. Depending on the synthesis conditions and scan rate, peaks can be slightly shifted and an additional oxidation peak could be observed at 0.4 V with a broad reduction process around 0 V. PEDOT is overoxidized at potentials higher than 2.2 V, where breakdown of the polymer occurs and the redox activity disappears.[64]

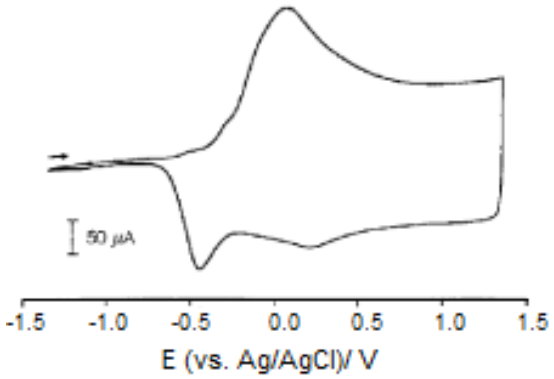

Figure 1.9. Cyclic voltammogram of PEDOT in 0.1 M $TBAPF_6$-propylene carbonate solution.[63]

One approach to enhance the electrochemical activity of conducting polymers is the attachment of redox moieties to the conducting polymer backbone[65,66] or the copolymerization with other redox active monomers.[67] As an example, Segura and co-workers functionalized an EDOT monomer with an anthraquinone moiety (Figure 1.10a) and they investigated its electrochemical polymerization and oxidation kinetics.[65] As shown in the cyclic voltammetry of this functionalized PEDOT derivative (Figure 1.10b), apart from the redox peaks of PEDOT backbone, an extra redox process is apparent due to the anthraquinone moiety, with oxidation and reduction potentials at -0.9 V and -1.1 V, respectively.

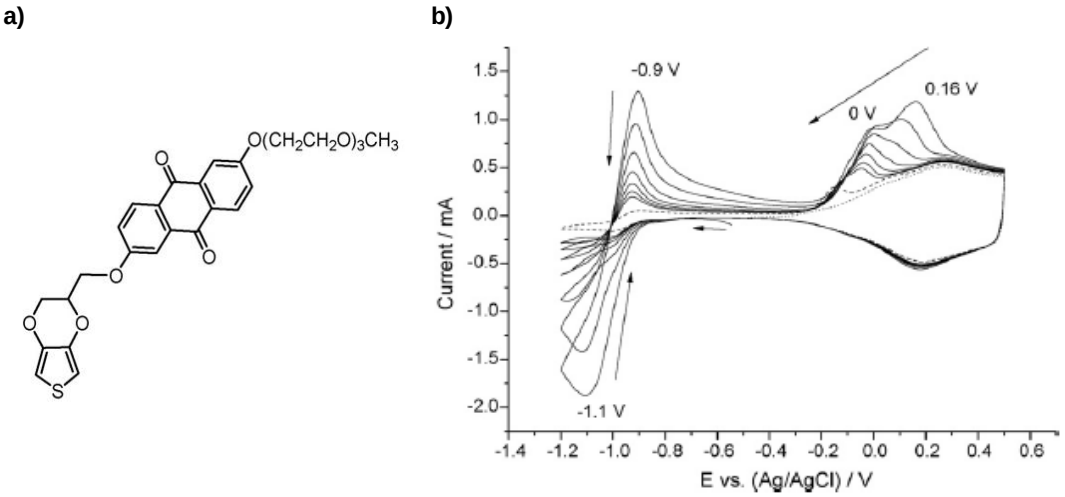

Figure 1.10. a) Structure of EDOT-anthraquinone monomer (AQ-EDOT) and b) cyclic voltammograms evolution of poly(AQ-EDOT) film in 0.1M $TBAPF_6$ acetonitrile solution at $50mVs^{-1}$.[65]

1.3. Applications of PEDOT derivatives in Electrochemical Energy Storage

PEDOT and several conducting polymers present outstanding chemical and physical properties such as high electrical conductivity, flexibility, easy nano-structuring, easy processability, high surface area and low cost.[68] Consequently, they have been employed in a wide range of applications.[20,23,24] In this section, their utilisation in electrochemical energy storage devices will be discussed.

1.3.1. Batteries

Polymers can have different functions in a battery. As mentioned in Section 1.1.1., batteries are composed of two electrodes, an anode and a cathode, with an ionic conductor electrolyte placed between them. At the same time, electrodes are made of three main components: a redox-active material (provides activity), a binder (structural integrity) and a conductive agent (facilitates electron transport). Current commercial electrode (cathode or anode) formulations include as the active redox material lithium inorganic oxides and phosphates, zinc, manganese oxide, silicon or graphite; a conductive additive such as carbon black and a polymeric binder.

Nowadays, conducting polymers have been widely investigated as conductive additives in electrodes. Although carbon is the most used conductive additive in electrodes, it decreases the overall energy density of the electrode, because it is bulky and inactive.[69] The replacement of carbon by conducting polymers has attracted much interest because apart from being

electronically conducting, it could also act as binder. Most of the works carried out with conducting polymers are based on the coating of other active species such as inorganic oxides [70-73] or sulfur.[74]

For example, Chen *et al.* reported the synthesis of sulfur/PEDOT core-shell nanoparticles to use as a cathode material for lithium-sulfur batteries.[75] The encapsulation of PEDOT shell can limit the polysulfide diffusion, as well as mitigate undesirable self-discharge and the shuttle effect, leading to Li-S batteries with enhanced cycling stability. PEDOT:PSS coating can also provide sufficient electrical conduction to electrodes and thus, it was used as coating of $LiFePO_4$ cathode material to improve the performance of the battery.[76] Wittstock *et al.* went a step further and use PEDOT:PSS as conductive binder for $LiFePO_4$ without any carbon and PVDF additives.[77] Recently, PEDOT:PSS has been used as conducting additive and binder for silicon anodes (Figure 1.11). Silicon anode has a considerably high theoretical capacity (3590 $mAhg^{-1}$), however, it suffers from 300% volume expansion during lithiation/delithiation processes. The use of PEDOT:PSS as conductive binder prevents the capacity losses that occur due to the physical separation of silicon and traditional conductive additives during lithiation.[78]

Apart from conductive additives, conducting polymers can be used as active material in electrodes due to their redox processes. The p-doped conducting polymers present high redox potentials (above 3.0 V), however, they have low capacities, usually between 80 and 150 mAh g^{-1}. There are different ways to improve these capacity values. For example, a redox-active chain, dopant or a side chain, can be introduced to increase the charge storage capacity of the polymer.[79] Some of the works reported include the attachment of redox moieties such as

anthraquinones[65] or phenylenediamines[80] to conducting polymer backbones in order to increase their redox properties.

Several studies have investigated conducting polymers as active materials in electrodes.[81-83] Recently, Zhan *et al.* used PEDOT as a cathode active material in lithium batteries. PEDOT shows a discharge plateau at 2.3 V and a discharge capacity of 350 mAh g^{-1}, which is promising and surprisingly higher than the theoretical value of PEDOT indicating a multi-electron electrode reaction.[84]

Zinc metal anode is an attractive alternative to lithium due to its ambient stability, low cost and natural abundance. PEDOT has been recently used as cathode active material for the development of zinc batteries with ionic liquid electrolytes (Figure 1.11). Although the capacity values are low (36 $mAhg^{-1}$ after 100 cycles), this novel Zn/PEDOT battery shows high efficiency and cycling stability over 320 cycles.[25]

PEDOT has been also investigated to develop for the first time an all polymer-air battery. The oxidation level of PEDOT in the anode is low, while in the cathode is in its fully oxidized state, leading to an open circuit voltage of about 0.5 V.[85]

The development of more sustainable batteries is nowadays an open challenge.[2] Redox active polymers in general are promising candidates due to their environmental friendliness, potential low cost and safety. In this field, Inganäs and coworkers have reported sustainable cathodes made of lignin biopolymer and polypyrrole.[86] Lignin has several quinone groups that can be used for electron and proton storage, whereas polypyrrole provides electrical

conductivity to the composite electrode. They found that quinone has higher charge storage properties than polypyrrole. However, these materials showed self-discharge behaviour and this should be solved before moving forward. Nevertheless, the synergic effect of both a natural redox polymer and a synthetic conducting polymer seems to be one of the most promising future directions.

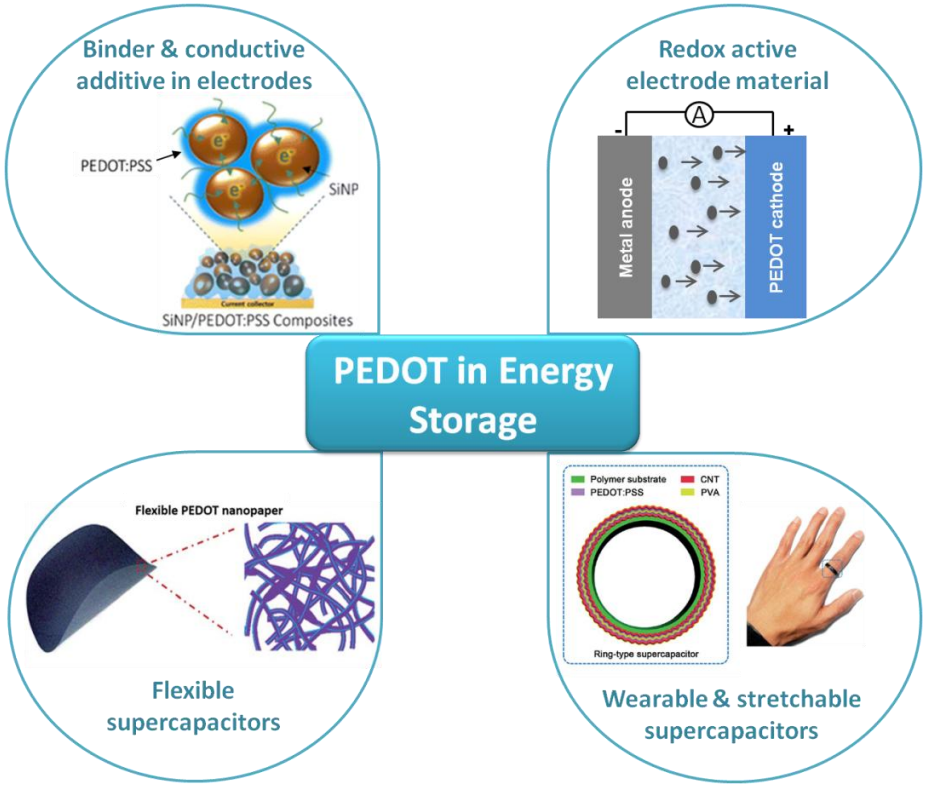

Figure 1.11. Main applications of PEDOT in energy storage: binder and conductive additive in electrodes,[78] redox active electrode material, flexible supercapacitors[31] and wearable and stretchable supercapacitors.[87]

1.3.2. Supercapacitors

There are two types of supercapacitors depending on the storage mechanism: pseudocapacitors and electric double layer capacitors (EDLC). In pseudocapacitors the energy is stored through Faradic mechanism, a redox reaction, taking place at the whole electrode and the electric charge is stored electrostatically. In the case of EDLC, charge is stored electrostatically by absorption of electrolyte ions in the pores of the electrodes.

Electrodes in pseudocapacitors are usually made of metal oxides (MnO_2, RuO_2),[88] polymer composites with metal oxides[21] or carbons,[89] polymer-coated carbon[90] or conducting polymers such as polypyrrole,[91] polyaniline,[92] polythiophene[93] and their derivatives. Conducting polymers are attractive supercapacitor electrode materials due to the known methods for their synthesis, low cost, flexibility and high electronic conductivity. Nevertheless, pure conducting polymer electrodes suffer from volume changes due to the doping process, being expanded during the doping process and shrunk when dedoped. This volume changes induce mechanical degradation and reduction of cycle life of electrodes. Therefore, different approaches have been taken to overcome this problem: fabrication of composite electrode materials, nanostructured conducting polymers such as nanorods, nanofibers, nanowires and nanotubes [94] or the use of carbons as negative electrodes.

PEDOT has been studied as electrode material in supercapacitors due to its high surface area, high conductivity in the p-doped state, good thermal and chemical stability, fast electrochemical switching and a wide potential window (1.4 V).[95] However, it possess a relatively low specific capacitance (around 100 F g^{-1}) taking into account its high molecular

weight and a doping level of 0.33.[96] As an example of nanostructured conducting polymers, Liu *et al.* developed PEDOT nanotube arrays and used them as positive and negative electrodes in symmetrical supercapacitors obtaining a specific capacitance of 140 F g^{-1} and high power density.[97] PEDOT nanofibers obtained by vapour-phase polymerization were also used in symmetric supercapacitors showing specific capacitance of 175 F g^{-1} and 92 % capacitance retention after 10000 cycles.[98]

Composite materials consisting of PEDOT and carbons[99,100] or metal oxides[21,101] have been also employed in supercapacitors. Recently, Karlsson *et al.* reported a symmetric supercapacitor using vapour-phase polymerized (VPP) PEDOT over carbon paper as electrodes and an ionic liquid as electrolyte. The VPP-PEDOT electrode showed a specific capacitance of 306 F g^{-1} and doping levels as high as 0.7 charges per monomer. The symmetric PEDOT cell exhibited a specific capacitance of 76.4 F g^{-1} and 19.8 Wh Kg^{-1} specific energy, as well as a good cycle life.[102]

Conducting polymers are promising materials for the development of flexible and wearable electronic devices due to their flexibility. Consequently, flexible supercapacitors have been made combining flexible substrates such as paper, metal foil or carbons with conducting polymers (Figure 1.11). For example, Wang *et al.* have recently reported a flexible nanostructured cellulose-PEDOT based supercapacitor. PEDOT was chemically polymerized in the presence of cellulose nanofibres obtaining a uniform PEDOT coating. The symmetric supercapacitor showed specific capacitance values of 90 F g^{-1} and a 93 % capacity retention after 15000 cycles.[31]

PEDOT:PSS has better affinity with polar groups, improving the supercapacitor performances when employing aqueous electrolytes. Huang *et al.* used different amounts of hydrous ruthenium oxide ($RuO_2 \cdot xH_2O$) with PEDOT:PSS to synthesize composite electrode materials. They observed that the specific capacitance increased when incrementing the amount of $RuO_2 \cdot xH_2O$ particles and a maximum specific capacitance of 653 F g^{-1} was obtained.[103] Recently, Weng *et al.* combined PEDOT:PSS with graphite oxide (16%) and carbon nanotubes (3%) by solution casting. The incorporation of these carbon materials improved both the energy (higher than 100 Wh kg^{-1}) and power (around 200 kW kg^{-1}) performances of the PEDOT:PSS electrode. The composite electrode showed a specific capacitance of 365 F g^{-1} over an operating potential window of 2.0 V with good cycling stability.[104] More recently, Weng *et al.* reported wearable and elastic ring type supercapacitors made by winding aligned carbon nanotube sheets with PEDOT:PSS onto an elastic polymer ring (Figure 1.11). The resulting supercapacitor exhibits high specific capacitance (134.8 F g^{-1}) with high flexibility and elasticity. Moreover, it can be moulded in different shapes with stable electrochemical properties under expansion and pressing.[87]

1.4. Motivation and objectives

Today, electrochemical energy storage systems play an important role in order to meet the global challenge of clean and efficient sustainable energy. During the last century, the development of improved energy storage systems has been intensely pursued in an effort to solve environmental problems related to pollution, depletion of fossil-fuel resources and the

rapid development of portable electronics, electric vehicles and energy storage stations. In the future, the elected energy storage technologies will consist of devices with superior safety and storage capabilities, as well as cost effective and easy to process materials.

In this context, conducting polymers appear as promising candidates to be implemented in energy storage devices due to their easy processing, high conductivity, light weight and good electrochemical properties. Moreover, they can play different roles to enhance the electrochemical properties of the device, for instance, as redox active electrode material or as conductive binder. Among different conducting polymers, PEDOT is the most promising one, because of its high conductivity and ambient stability. Thus, the main goal of this PhD thesis is to synthesize new PEDOT derivatives for the area of electrochemical energy storage systems.

Within this scope, the specific objectives of this thesis are:

- Synthesis and characterization of a new PEDOT derivative with enhanced redox properties by incorporation of a nitroxide radical to the polymer backbone.
- Development of sustainable organic electrode materials, by combining PEDOT and the biopolymer lignin through oxidative chemical polymerization.
- Synthesis of highly conductive PEDOT dispersions with a soft ionic conductor polyelectrolyte.
- Investigate the potential applications of these polymers in various energy storage systems: lithium-ion batteries, sodium-organic batteries and supercapacitors.

1.5. Outline of the thesis

In Chapter 1, after a brief introduction to electrochemical energy storage, an overview of conducting polymer PEDOT is presented, together with its most important applications in energy storage devices. The motivation and goals of this thesis are also presented in this chapter.

In Chapter 2, we show the synthesis and characterization of a new polymer which combines the present most successful conjugated polymer backbone and the most successful redox active side group, i.e. poly(3,4-ethylenedioxythiophene) (PEDOT) and a nitroxide stable radical. The new PEDOT-TEMPO radical polymer combines the electronic conductivity of conjugated polythiophene backbone and redox properties of the nitroxide group. As an example of application, this redox active polymer is used as conductive binder in lithium-ion batteries to replace both conductive carbon additive and inactive polymeric binders.

In Chapter 3, a novel sustainable organic electrode material is presented by the polymerization of EDOT in presence of lignin-sulfonate biopolymer. Composites with various PEDOT/lignin ratios are prepared in order to analyze the influence of each component in the electrochemical behaviour. The charge storage properties are investigated in aqueous solution for supercapacitor applications. It is demonstrated that the incorporation of lignin provides enhanced energy storage properties to PEDOT, by means of its redox active quinone moieties.

In Chapter 4, the electrochemical activity and cycling of PEDOT/lignin electrodes is investigated in a series of imidazolium and pyrrolidinium-based ionic liquids. The effects of water and sodium salt addition to the ionic liquids are studied in order to obtain optimum electrolyte systems for sodium batteries. Finally, the concept of a new battery cell presented by using PEDOT/lignin as cathode material, the optimized ionic liquid as electrolyte and sodium as anode. As a result, it is demonstrated that PEDOT/lignin composites can serve as low cost and sustainable cathode materials for sodium batteries.

In Chapter 5, we present the synthesis and characterization of highly conductive PEDOT/PSTFSI dispersions, which combine the electronic conductivity of PEDOT and the ionic conductivity of PSTFSI polyanion. For that, EDOT is polymerized by oxidative chemical polymerization in presence of PSTFSI using different EDOT:PSTFSI weight ratios. The properties of the obtained dispersions are investigated in detail, while the one with superior electric and electrochemical properties is investigated as additive in lithium iron phosphate cathodes, in order to improve the rate capability of these batteries.

In Chapter 6, the most relevant conclusions of this thesis are summarized.

1.6. References

(1) Armand M., Tarascon J. M. Building better batteries. *Nature*. **2008**;451:652-7.

(2) Larcher D., Tarascon J. M. Towards greener and more sustainable batteries for electrical energy storage. *Nat Chem*. **2015**;7:19-29.

(3) Dunn B., Kamath H., Tarascon J.-M. Electrical Energy Storage for the Grid: A Battery of Choices. *Science*. **2011**;334:928-35.

(4) Song Z., Zhou H. Towards sustainable and versatile energy storage devices: an overview of organic electrode materials. *Energy Environ. Sci.* **2013**;6:2280-301.

(5) Poizot P., Dolhem F. Clean energy new deal for a sustainable world: from non-CO2 generating energy sources to greener electrochemical storage devices. *Energy Environ. Sci.* **2011**;4:2003-19.

(6) Etacheri V., Marom R., Elazari R., Salitra G., Aurbach D. Challenges in the development of advanced Li-ion batteries: a review. *Energy Environ. Sci.* **2011**;4:3243-62.

(7) Palomares V., Casas-Cabanas M., Castillo-Martinez E., Han M. H., Rojo T. Update on Na-based battery materials. A growing research path. *Energy Environ. Sci.* **2013**;6:2312-37.

(8) Wang Z., Dong Y., Li H., Zhao Z., Bin Wu H., Hao C., Liu S., Qiu J., Lou X. W. Enhancing lithium–sulphur battery performance by strongly binding the discharge products on amino-functionalized reduced graphene oxide. *Nat. Commun.* **2014**;5:5002.

(9) Lu Y.-C., Gallant B. M., Kwabi D. G., Harding J. R., Mitchell R. R., Whittingham M. S., Shao-Horn Y. Lithium-oxygen batteries: bridging mechanistic understanding and battery performance. *Energy Environ. Sci.* **2013**;6:750-68.

(10) Zhang T., Tao Z., Chen J. Magnesium-air batteries: from principle to application. *Mater. Horiz.* **2014**;1:196-206.

(11) Xu M., Ivey D. G., Xie Z., Qu W. Rechargeable Zn-air batteries: Progress in electrolyte development and cell configuration advancement. *J. Power Sources*. **2015**;283:358-71.

(12) Liang Y., Tao Z., Chen J. Organic Electrode Materials for Rechargeable Lithium Batteries. *Adv. Energy Mater.* **2012**;2:742-69.

(13) Chou S.-L., Pan Y., Wang J.-Z., Liu H.-K., Dou S.-X. Small things make a big difference: binder effects on the performance of Li and Na batteries. *PCCP*. **2014**;16:20347-59.

(14) Chen K., Xue D. Materials chemistry toward electrochemical energy storage. *J. Mater. Chem. A*. **2016**;4:7522-37.

(15) Simon P., Gogotsi Y. Materials for electrochemical capacitors. *Nat Mater*. **2008**;7:845-54.

(16) Yoo H. D., Markevich E., Salitra G., Sharon D., Aurbach D. On the challenge of developing advanced technologies for electrochemical energy storage and conversion. *Mater. Today*. **2014**;17:110-21.

(17) Cao Z., Wei B. A perspective: carbon nanotube macro-films for energy storage. *Energy Environ. Sci.* **2013**;6:3183-201.

(18) Winter M., Brodd R. J. What Are Batteries, Fuel Cells, and Supercapacitors? *Chem. Rev.* **2004**;104:4245-70.

(19) Shirakawa H., Louis E. J., MacDiarmid A. G., Chiang C. K., Heeger A. J. Synthesis of electrically conducting organic polymers: halogen derivatives of polyacetylene, (CH). *J. Chem. Soc., Chem. Commun.* **1977**:578-80.

(20) Ouyang J., Chu C. W., Chen F. C., Xu Q., Yang Y. High-Conductivity Poly(3,4-ethylenedioxythiophene):Poly(styrene sulfonate) Film and Its Application in Polymer Optoelectronic Devices. *Adv. Funct. Mater.* **2005**;15:203-8.

(21) Sen P., De A., Chowdhury A. D., Bandyopadhyay S. K., Agnihotri N., Mukherjee M. Conducting polymer based manganese dioxide nanocomposite as supercapacitor. *Electrochim. Acta*. **2013**;108:265-73.

(22) Cong H.-P., Ren X.-C., Wang P., Yu S.-H. Flexible graphene-polyaniline composite paper for high-performance supercapacitor. *Energy Environ. Sci.* **2013**;6:1185-91.

(23) Xia Y., Ouyang J. PEDOT:PSS films with significantly enhanced conductivities induced by preferential solvation with cosolvents and their application in polymer photovoltaic cells. *J. Mater. Chem.* **2011**;21:4927-36.

(24) Elschner A., Bruder F., Heuer H. W., Jonas F., Karbach A., Kirchmeyer S., Thurm S., Wehrmann R. PEDT/PSS for efficient hole-injection in hybrid organic light-emitting diodes. *Synth. Met.* **2000**;111–112:139-43.

(25) Simons T. J., Salsamendi M., Howlett P. C., Forsyth M., MacFarlane D. R., Pozo-Gonzalo C. Rechargeable Zn/PEDOT Battery with an Imidazolium-Based Ionic Liquid as the Electrolyte. *ChemElectroChem*. **2015**;2:2071-8.

(26) Varela H., Torresi R. M. Ionic Exchange Phenomena Related to the Redox Processes of Polyaniline in Nonaqueous Media. *J. Electrochem. Soc.* **2000**;147:665-70.

(27) Ishiguro Y., Inagi S., Fuchigami T. Gradient Doping of Conducting Polymer Films by Means of Bipolar Electrochemistry. *Langmuir*. **2011**;27:7158-62.

(28) Jonas F., Heywang G., Schmidtberg W. DE 38 13 589 A1, (Bayer AG), **1988**.

(29) Heywang G., Jonas F., Heinze J., Dietrich M. De 38 43 412 A1, (Bayer AG), **1988**.

(30) Jonas F., Krafft W. EP 440 957, (Bayer AG), **1990**.

(31) Wang Z., Tammela P., Huo J., Zhang P., Stromme M., Nyholm L. Solution-processed poly(3,4-ethylenedioxythiophene) nanocomposite paper electrodes for high-capacitance flexible supercapacitors. *J. Mater. Chem. A*. **2016**;4:1714-22.

(32) Tamburri E., Orlanducci S., Toschi F., Terranova M. L., Passeri D. Growth mechanisms, morphology, and electroactivity of PEDOT layers produced by electrochemical routes in aqueous medium. *Synth. Met.* **2009**;159:406-14.

(33) Zhou Z., He D., Guo Y., Cui Z., Wang M., Li G., Yang R. Fabrication of polyaniline–silver nanocomposites by chronopotentiometry in different ionic liquid microemulsion systems. *Thin Solid Films*. **2009**;517:6767-71.

(34) Sekine S., Ido Y., Miyake T., Nagamine K., Nishizawa M. Conducting Polymer Electrodes Printed on Hydrogel. *J. Am. Chem. Soc.* **2010**;132:13174-5.

(35) Zhang C., Xu Y., Wang N., Xu Y., Xiang W., Ouyang M., Ma C. Electrosyntheses and characterizations of novel electrochromic copolymers based on pyrene and 3,4-ethylenedioxythiophene. *Electrochim. Acta*. **2009**;55:13-8.

(36) Wolfart F., Dubal D. P., Vidotti M., Holze R., Gómez-Romero P. Electrochemical supercapacitive properties of polypyrrole thin films: influence of the electropolymerization methods. *J. Solid State Electrochem.* **2016**;20:901-10.

(37) Heywang G., Jonas F. Poly(alkylenedioxythiophene)s—new, very stable conducting polymers. *Adv. Mater.* **1992**;4:116-8.

(38) Elschner A., Kirchmeyer S., Lovenich W., Merker U., Reuter K. The In Situ Polymerization of EDOT to PEDOT. PEDOT: CRC Press; 2010. p. 91-111.

(39) Mumtaz M., Cloutet E., Labrugere C., Hadziioannou G., Cramail H. Synthesis of hybrid semiconducting polymer-metal latexes. *Polym. Chem.* **2013**;4:615-22.

(40) Mohammadi A., Hasan M. A., Liedberg B., Lundström I., Salaneck W. R. Chemical vapour deposition (CVD) of conducting polymers: Polypyrrole. *Synth. Met.* **1986**;14:189-97.

(41) Lawal A. T., Wallace G. G. Vapour phase polymerisation of conducting and non-conducting polymers: A review. *Talanta*. **2014**;119:133-43.

(42) Winther-Jensen B., Winther-Jensen O., Forsyth M., MacFarlane D. R. High Rates of Oxygen Reduction over a Vapor Phase–Polymerized PEDOT Electrode. *Science*. **2008**;321:671-4.

(43) Fabretto M., Autere J.-P., Hoglinger D., Field S., Murphy P. Vacuum vapour phase polymerised poly(3,4-ethyelendioxythiophene) thin films for use in large-scale electrochromic devices. *Thin Solid Films*. **2011**;519:2544-9.

(44) Lock J. P., Im S. G., Gleason K. K. Oxidative Chemical Vapor Deposition of Electrically Conducting Poly(3,4-ethylenedioxythiophene) Films. *Macromolecules*. **2006**;39:5326-9.

(45) Winther-Jensen B., West K. Vapor-Phase Polymerization of 3,4-Ethylenedioxythiophene: A Route to Highly Conducting Polymer Surface Layers. *Macromolecules*. **2004**;37:4538-43.

(46) Winther-Jensen B., Chen J., West K., Wallace G. Vapor Phase Polymerization of Pyrrole and Thiophene Using Iron(III) Sulfonates as Oxidizing Agents. *Macromolecules*. **2004**;37:5930-5.

(47) Jonas F., Krafft W. EP 440 957, (Bayer AG), **1990**.

(48) Kirchmeyer S., Reuter K. Scientific importance, properties and growing applications of poly(3,4-ethylenedioxythiophene). *J. Mater. Chem.* **2005**;15:2077-88.

(49) Ghosh S., Inganäs O. Self-assembly of a conducting polymer nanostructure by physical crosslinking: applications to conducting blends and modified electrodes. *Synth. Met.* **1999**;101:413-6.

(50) Aubert P. H., Groenendaal L., Louwet F., Lutsen L., Vanderzande D., Zotti G. In situ conductivity measurements on polyethylenedioxythiophene derivatives with different counter ions. *Synth. Met.* **2002**;126:193-8.

(51) Groenendaal L., Zotti G., Jonas F. Optical, conductive and magnetic properties of electrochemically prepared alkylated poly(3,4-ethylenedioxythiophene)s. *Synth. Met.* **2001**;118:105-9.

(52) Giurgiu I., Zong K., Reynolds J. R., Lee W. P., Brenneman K. R., Saprigin A. V., Epstein A. J., Hwang J., Tanner D. B. Dioxypyrrole and dioxythiophene based conducting polymers: properties and applications. *Synth. Met.* **2001**;119:405-6.

(53) Ouyang J., Xu Q., Chu C.-W., Yang Y., Li G., Shinar J. On the mechanism of conductivity enhancement in poly(3,4-ethylenedioxythiophene):poly(styrene sulfonate) film through solvent treatment. *Polymer*. **2004**;45:8443-50.

(54) Timpanaro S., Kemerink M., Touwslager F. J., De Kok M. M., Schrader S. Morphology and conductivity of PEDOT/PSS films studied by scanning–tunneling microscopy. *Chem. Phys. Lett.* **2004**;394:339-43.

(55) Döbbelin M., Marcilla R., Salsamendi M., Pozo-Gonzalo C., Carrasco P. M., Pomposo J. A., Mecerreyes D. Influence of Ionic Liquids on the Electrical Conductivity and Morphology of PEDOT:PSS Films. *Chem. Mater.* **2007**;19:2147-9.

(56) Xia Y., Ouyang J. Salt-Induced Charge Screening and Significant Conductivity Enhancement of Conducting Poly(3,4-ethylenedioxythiophene):Poly(styrenesulfonate). *Macromolecules*. **2009**;42:4141-7.

(57) Lim K., Jung S., Lee S., Heo J., Park J., Kang J.-W., Kang Y.-C., Kim D.-G. The enhancement of electrical and optical properties of PEDOT:PSS using one-step dynamic etching for flexible application. *Org. Electron.* **2014**;15:1849-55.

(58) Lee S. H., Park H., Son W., Choi H. H., Kim J. H. Novel solution-processable, dedoped semiconductors for application in thermoelectric devices. *J. Mater. Chem. A*. **2014**;2:13380-7.

(59) Wichiansee W., Sirivat A. Electrorheological properties of poly(dimethylsiloxane) and poly(3,4-ethylenedioxy thiophene)/poly(stylene sulfonic acid)/ethylene glycol blends. *Materials Science and Engineering: C*. **2009**;29:78-84.

(60) Yan H., Jo T., Okuzaki H. Highly Conductive and Transparent Poly(3,4-ethylenedioxythiophene)/Poly(4-styrenesulfonate) (PEDOT/PSS) Thin Films. *Polym. J*. **2009**;41:1028-9.

(61) Jalili R., Razal J. M., Innis P. C., Wallace G. G. One-Step Wet-Spinning Process of Poly(3,4-ethylenedioxythiophene):Poly(styrenesulfonate) Fibers and the Origin of Higher Electrical Conductivity. *Adv. Funct. Mater.* **2011**;21:3363-70.

(62) Alemu D., Wei H.-Y., Ho K.-C., Chu C.-W. Highly conductive PEDOT:PSS electrode by simple film treatment with methanol for ITO-free polymer solar cells. *Energy Environ. Sci.* **2012**;5:9662-71.

(63) Dietrich M., Heinze J., Heywang G., Jonas F. Electrochemical and spectroscopic characterization of polyalkylenedioxythiophenes. *J. Electroanal. Chem.* **1994**;369:87-92.

(64) Kvarnström C., Neugebauer H., Blomquist S., Ahonen H. J., Kankare J., Ivaska A. In situ spectroelectrochemical characterization of poly(3,4-ethylenedioxythiophene). *Electrochim. Acta*. **1999**;44:2739-50.

(65) Arias-Pardilla J., Otero T. F., Blanco R., Segura J. L. Synthesis, electropolymerization and oxidation kinetics of an anthraquinone-functionalized poly(3,4-ethylenedioxythiophene). *Electrochim. Acta*. **2010**;55:1535-42.

(66) Lowe M. A., Kiya Y., Henderson J. C., Abruña H. D. Pendant thioether polymer for redox capacitor cathodes. *Electrochem. Commun.* **2011**;13:462-5.

(67) Nie G., Qu L., Xu J., Zhang S. Electrosyntheses and characterizations of a new soluble conducting copolymer of 5-cyanoindole and 3,4-ethylenedioxythiophene. *Electrochim. Acta*. **2008**;53:8351-8.

(68) Elschner A., Kirchmeyer S., Lovenich W., Merker U., Reuter K. *PEDOT Principles and Applications of an Intrinsically Conductive Polymer*: CRC Press; 2010.

(69) Chen Z., Dahn J. R. Reducing Carbon in LiFePO4 / C Composite Electrodes to Maximize Specific Energy, Volumetric Energy, and Tap Density. *J. Electrochem. Soc.* **2002**;149:A1184-A9.

(70) Qie L., Yuan L.-X., Zhang W.-X., Chen W.-M., Huang Y.-H. Revisit of Polypyrrole as Cathode Material for Lithium-Ion Battery. *J. Electrochem. Soc.* **2012**;159:A1624-A9.

(71) Wang G. X., Yang L., Chen Y., Wang J. Z., Bewlay S., Liu H. K. An investigation of polypyrrole-LiFePO4 composite cathode materials for lithium-ion batteries. *Electrochim. Acta*. **2005**;50:4649-54.

(72) Cintora-Juarez D., Perez-Vicente C., Ahmad S., Tirado J. L. Improving the cycling performance of LiFePO4 cathode material by poly(3,4-ethylenedioxythiopene) coating. *RSC Advances*. **2014**;4:26108-14.

(73) Shi J.-Y., Yi C.-W., Kim K. An Investigation of LiFePO4/Poly(3,4-ethylenedioxythiophene) Composite Cathode Materials for Lithium-Ion Batteries. *Bull. Korean Chem. Soc.* **2010**;31:2698-700.

(74) Wang L., He X., Sun W., Li J., Gao J., Tian G., Wang J., Fan S. Organic polymer material with a multi-electron process redox reaction: towards ultra-high reversible lithium storage capacity. *RSC Advances*. **2013**;3:3227-31.

(75) Chen H., Dong W., Ge J., Wang C., Wu X., Lu W., Chen L. Ultrafine Sulfur Nanoparticles in Conducting Polymer Shell as Cathode Materials for High Performance Lithium/Sulfur Batteries. *Sci. Rep.* **2013**;3:1910.

(76) Cintora-Juarez D., Perez-Vicente C., Kazim S., Ahmad S., Tirado J. L. Judicious design of lithium iron phosphate electrodes using poly(3,4-ethylenedioxythiophene) for high performance batteries. *J. Mater. Chem. A*. **2015**;3:14254-62.

(77) Das P. R., Komsiyska L., Osters O., Wittstock G. PEDOT: PSS as a Functional Binder for Cathodes in Lithium Ion Batteries. *J. Electrochem. Soc.* **2015**;162:A674-A8.

(78) Higgins T. M., Park S.-H., King P. J., Zhang C., McEvoy N., Berner N. C., Daly D., Shmeliov A., Khan U., Duesberg G., Nicolosi V., Coleman J. N. A Commercial Conducting Polymer as Both Binder and Conductive Additive for Silicon Nanoparticle-Based Lithium-Ion Battery Negative Electrodes. *ACS Nano*. **2016**;10:3702-13.

(79) Mike J. F., Lutkenhaus J. L. Electrochemically Active Polymers for Electrochemical Energy Storage: Opportunities and Challenges. *ACS Macro Letters*. **2013**;2:839-44.

(80) Conte S., Rodriguez-Calero G. G., Burkhardt S. E., Lowe M. A., Abruna H. D. Designing conducting polymer films for electrochemical energy storage technologies. *RSC Adv.* **2013**;3:1957-64.

(81) Killian J. G., Coffey B. M., Gao F., Poehler T. O., Searson P. C. Polypyrrole Composite Electrodes in an All-Polymer Battery System. *J. Electrochem. Soc.* **1996**;143:936-42.

(82) Wang C. Y., Tsekouras G., Wagner P., Gambhir S., Too C. O., Officer D., Wallace G. G. Functionalised polyterthiophenes as anode materials in polymer/polymer batteries. *Synth. Met.* **2010**;160:76-82.

(83) Sultana I., Rahman M. M., Wang J., Wang C., Wallace G. G., Liu H.-K. All-polymer battery system based on polypyrrole (PPy)/para (toluene sulfonic acid) (pTS) and polypyrrole (PPy)/indigo carmine (IC) free standing films. *Electrochim. Acta*. **2012**;83:209-15.

(84) Zhan L., Song Z., Zhang J., Tang J., Zhan H., Zhou Y., Zhan C. PEDOT: Cathode active material with high specific capacity in novel electrolyte system. *Electrochim. Acta*. **2008**;53:8319-23.

(85) Xuan Y., Sandberg M., Berggren M., Crispin X. An all-polymer-air PEDOT battery. *Org. Electron.* **2012**;13:632-7.

(86) Milczarek G., Inganäs O. Renewable Cathode Materials from Biopolymer/Conjugated Polymer Interpenetrating Networks. *Science*. **2012**;335:1468-71.

(87) Wang L., Wu Q., Zhang Z., Zhang Y., Pan J., Li Y., Zhao Y., Zhang L., Cheng X., Peng H. Elastic and wearable ring-type supercapacitors. *J. Mater. Chem. A*. **2016**;4:3217-22.

(88) Wei W., Cui X., Chen W., Ivey D. G. Manganese oxide-based materials as electrochemical supercapacitor electrodes. *Chem. Soc. Rev.* **2011**;40:1697-721.

(89) Frackowiak E., Khomenko V., Jurewicz K., Lota K., Béguin F. Supercapacitors based on conducting polymers/nanotubes composites. *J. Power Sources*. **2006**;153:413-8.

(90) Zhang L. L., Li S., Zhang J., Guo P., Zheng J., Zhao X. S. Enhancement of Electrochemical Performance of Macroporous Carbon by Surface Coating of Polyaniline†. *Chem. Mater.* **2009**;22:1195-202.

(91) Sun W., Zheng R., Chen X. Symmetric redox supercapacitor based on micro-fabrication with three-dimensional polypyrrole electrodes. *J. Power Sources*. **2010**;195:7120-5.

(92) Cho S., Shin K.-H., Jang J. Enhanced Electrochemical Performance of Highly Porous Supercapacitor Electrodes Based on Solution Processed Polyaniline Thin Films. *ACS Applied Materials & Interfaces*. **2013**;5:9186-93.

(93) Laforgue A., Simon P., Fauvarque J.-F. Chemical synthesis and characterization of fluorinated polyphenylthiophenes: application to energy storage. *Synth. Met.* **2001**;123:311-9.

(94) Cho S. I., Lee S. B. Fast Electrochemistry of Conductive Polymer Nanotubes: Synthesis, Mechanism, and Application. *Acc. Chem. Res.* **2008**;41:699-707.

(95) Lota K., Khomenko V., Frackowiak E. Capacitance properties of poly(3,4-ethylenedioxythiophene)/carbon nanotubes composites. *J. Phys. Chem. Solids*. **2004**;65:295-301.

(96) Snook G. A., Chen G. Z. The measurement of specific capacitances of conducting polymers using the quartz crystal microbalance. *J. Electroanal. Chem.* **2008**;612:140-6.

(97) Liu R., Cho S. I., Lee S. B. Poly(3,4-ethylenedioxythiophene) nanotubes as electrode materials for a high-powered supercapacitor. *Nanotechnology*. **2008**;19:215710.

(98) D'Arcy J. M., El-Kady M. F., Khine P. P., Zhang L., Lee S. H., Davis N. R., Liu D. S., Yeung M. T., Kim S. Y., Turner C. L., Lech A. T., Hammond P. T., Kaner R. B. Vapor-Phase Polymerization of Nanofibrillar Poly(3,4-ethylenedioxythiophene) for Supercapacitors. *ACS Nano*. **2014**;8:1500-10.

(99) Ghaffari M., Kosolwattana S., Zhou Y., Lachman N., Lin M., Bhattacharya D., Gleason K. K., Wardle B. L., Zhang Q. M. Hybrid supercapacitor materials from poly(3,4-ethylenedioxythiophene) conformally coated aligned carbon nanotubes. *Electrochim. Acta*. **2013**;112:522-8.

(100) Pandey G. P., Rastogi A. C., Westgate C. R. All-solid-state supercapacitors with poly(3,4-ethylenedioxythiophene)-coated carbon fiber paper electrodes and ionic liquid gel polymer electrolyte. *Journal of Power Sources*. **2014**;245:857-65.

(101) Hou Y., Cheng Y., Hobson T., Liu J. Design and Synthesis of Hierarchical MnO2 Nanospheres/Carbon Nanotubes/Conducting Polymer Ternary Composite for High Performance Electrochemical Electrodes. *Nano Lett.* **2010**;10:2727-33.

(102) Karlsson C., Nicholas J., Evans D., Forsyth M., Strømme M., Sjödin M., Howlett P. C., Pozo-Gonzalo C. Stable Deep Doping of Vapor-Phase Polymerized Poly(3,4-ethylenedioxythiophene)/Ionic Liquid Supercapacitors. *ChemSusChem*. **2016**;9:2112-21.

(103) Huang L.-M., Lin H.-Z., Wen T.-C., Gopalan A. Highly dispersed hydrous ruthenium oxide in poly(3,4-ethylenedioxythiophene)-poly(styrene sulfonic acid) for supercapacitor electrode. *Electrochim. Acta*. **2006**;52:1058-63.

(104) Weng Y.-T., Wu N.-L. High-performance poly(3,4-ethylene-dioxythiophene):polystyrenesulfonate conducting-polymer supercapacitor containing hetero-dimensional carbon additives. *J. Power Sources*. **2013**;238:69-73.

CHAPTER 2

PEDOT Radical Polymer with Synergetic Redox and Electrical Properties

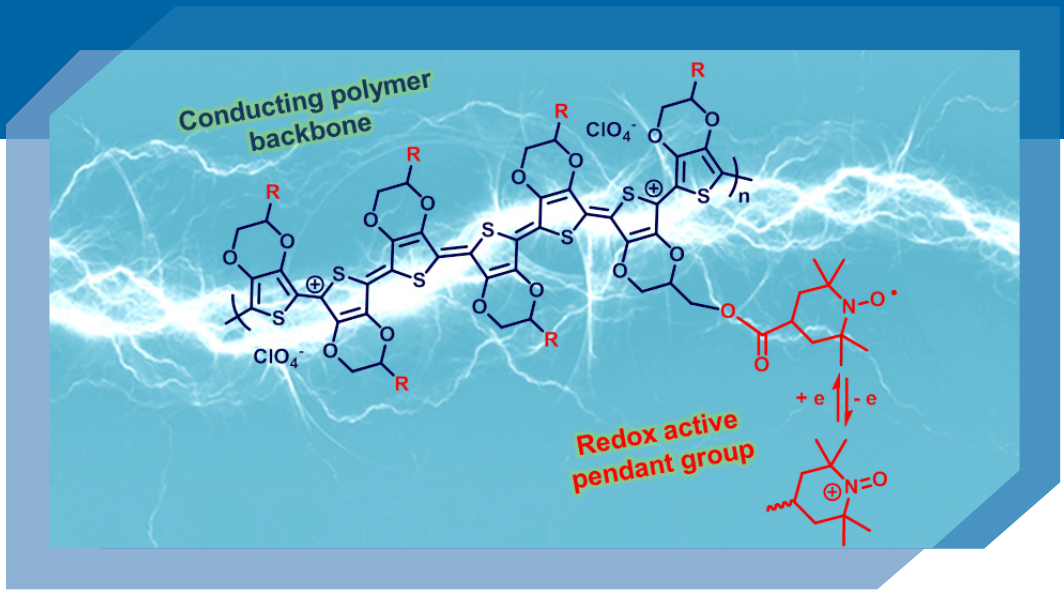

Chapter 2. PEDOT Radical Polymer with Synergetic Redox and Electrical Properties

2.1. Introduction

Redox active polymers have attracted much interest due to the capability to change their chemical, electronic, optical or mechanical properties depending on the redox state.[1] The reversibility of the redox process makes these polymers target materials for different applications such as electrochromic devices, organic solar cells, batteries, biosensors, bioactuators and nanomedicine.[2-7] Polymers with redox properties are those with the ability of changing their electrochemical properties with the oxidation state due to the loss (oxidation) or gain (reduction) of electrons. The IUPAC definition for a redox polymer is a polymer containing groups that can be reversibly reduced or oxidized. Reversible redox reactions can take place in the polymer main chain, as in the case of conducting polymers such as polyaniline,[8] or in side-groups, as in the case of a polymer carrying ferrocene side-groups. In this chapter, we show the synthesis and characterization of a new polymer which combines both the most successful redox active conjugated polymer backbone and the most successful side group, i.e. poly(3,4-ethylenedioxythiophene) (PEDOT) and a nitroxide stable radical.

As it has been explained in Chapter 1, poly(3,4-ethylenedioxythiophene) (PEDOT) is a commercially available and widely used conducting polymer having a redox active conjugated backbone.[9] PEDOT can be synthesized by electrochemical polymerization[10] or by oxidative chemical polymerization to obtain aqueous dispersions stabilized by a water soluble polyelectrolyte, i.e. poly(styrene sulphonate). PEDOT is characterized by its high electrical conductivity (up to 10^3 S/cm), good transparency and excellent electrochemical and thermal stability.[11-14] As an example of applications, PEDOT and other conducting polymers have been used as cathode and anode materials in batteries.[15-17] However, they posses relatively low specific energy density, hence several recent works have reported the attachment of redox moieties such as anthraquinones to increase its performance.[18]

Polymers containing stable organic radical moieties as pendant groups or radical polymers are attracting much attention for their high charge transfer reactions and the possibility to create p-type and n-type radical polymers depending on the functional pendant group.[19-21] Nishide and coworkers first developed polymers containing stable nitroxide radicals such as 2,2,6,6-tetramethylpiperidine-1-oxyl (TEMPO).[22] Batteries with these organic radical polymers have good cycling stability, fast charge-discharge rates and high power density.[23,24] Most of the radical polymers have non-conjugated macromolecular backbones. Actual trends include the attachment of different types of stable radicals, development of new macromolecular architectures such as block copolymers or the further physico-chemical understanding and new applications of these polymers in optoelectronics. It is worth to mention that Aydin *et al.* have recently reported the synthesis of a polymer having a semiconjugated

backbone and a nitroxide pendant group which showed a limited performance in a battery probably due to the low stability of the chosen polymer backbone.[25]

In this chapter, we present the synthesis and characterization of a new polymer which combines both a poly(3,4-ethylenedioxythiophene) (PEDOT) backbone and a nitroxide stable radical (TEMPO) side chain. For that purpose, the synthesis of 3,4-ethylenedioxythiophene derivative monomer bearing TEMPO nitroxide radical was carried out. Its electrochemical polymerization and the characterization of the obtained redox active and electrically conductive PEDOT-TEMPO polymer were investigated. The PEDOT-TEMPO polymer shows a unique combination of redox and electrical properties. As a potential application the results of the use of the polymer as conductive binder in $LiFePO_4$ batteries are presented.

2.2. Monomer synthesis and characterization

The new EDOT bearing TEMPO monomer was synthesized via esterification reaction between EDOT-MeOH and 4-carboxy-TEMPO in the presence of dicyclohexylcarbodiimide (DCC) and dimethylaminopyridine (DMAP) in dry dichloromethane with a high yield (Figure 2.1).

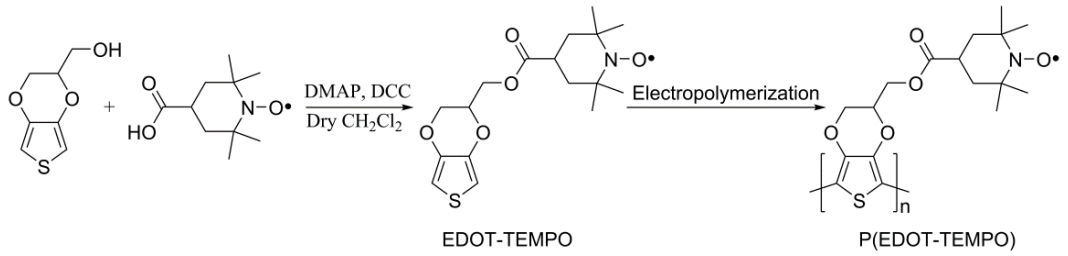

Figure 2.1. Synthesis of EDOT-TEMPO monomer and its electrochemical polymerization.

The esterification reaction was proven by ATR-FTIR spectroscopy, MALDI-TOF mass spectrometry and elemental analysis. ATR-FTIR spectroscopy (Figure 2.2a) shows absorption at 1724 cm^{-1} due to the presence of the carbonyl stretching which is higher than the reactant carboxylic acid (1685 cm^{-1}) and a lack of O-H stretching band at around 3200 cm^{-1}. The UV-Vis spectrum of EDOT-TEMPO monomer shows absorption at 239 and 256 nm related to EDOT group (Figure 2.2b). The monomer was characterized by MALDI-TOF mass spectrometry using positive-ion reflectron mode. Figure 2.3a shows an enlargement of the obtained MALDI spectral peaks for the monomer and the comparison with theoretical isotopic distribution. Electron Spin Resonance (ESR) spectrum of the monomer in toluene solution shows a triplet with nitrogen hyperfine splitting constant of 14.4 G (Figure 2.3b) which is characteristic of TEMPO nitroxide radicals.

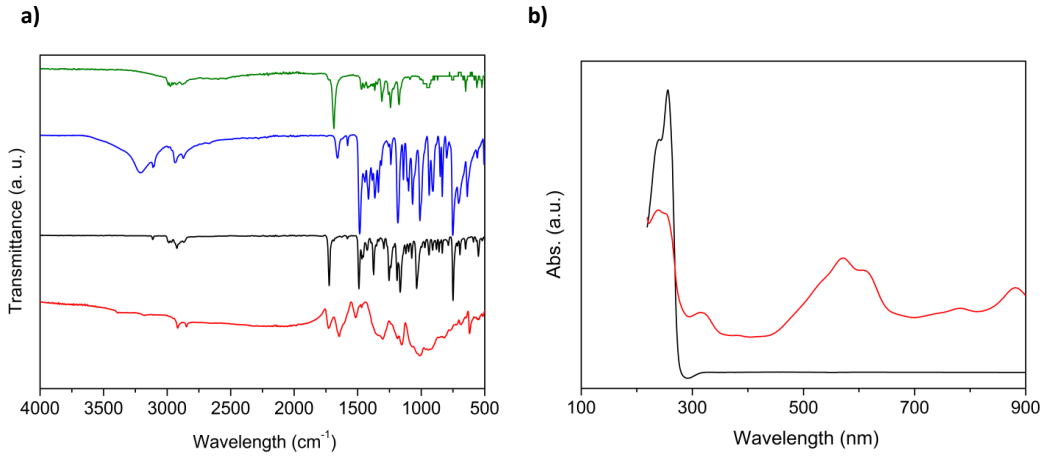

Figure 2.2. a) ATR-FTIR spectra of 4-carboxy-TEMPO (green), hydroxymethyl-EDOT (blue), EDOT-TEMPO monomer (black) and PEDOT-TEMPO polymer (red). (B) UV-Vis spectra of EDOT-TEMPO monomer before electropolymerization (black) and electropolymerized PEDOT-TEMPO polymer in $TBAPF_6$/acetonitrile solution.

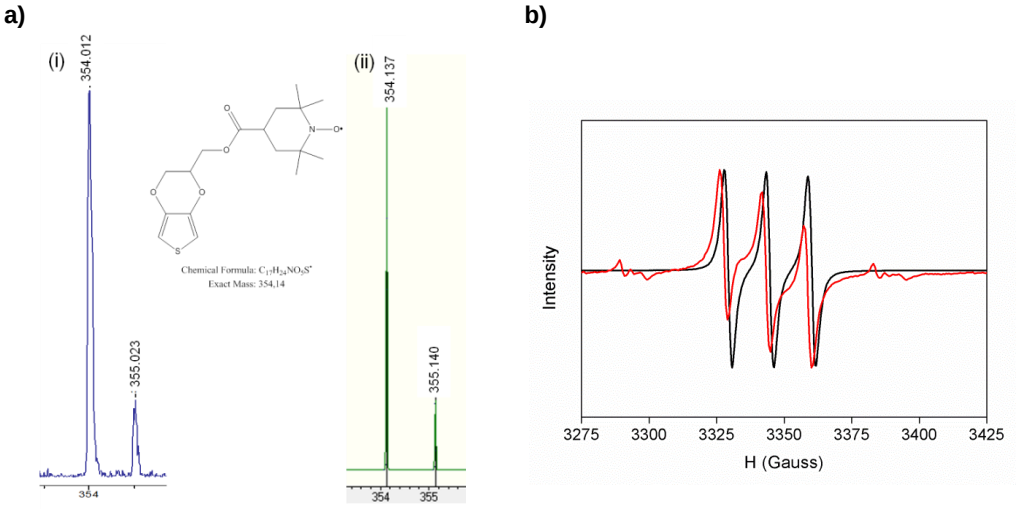

Figure 2.3. a) Isotopic distribution and structure of EDOT-TEMPO monomer, (i) experimental peaks and (ii) theoretical values. b) X-band ESR spectra of EDOT-TEMPO monomer (black line) and polymer (red line).

2.3. Electrochemical polymerization

The electrochemical polymerization of EDOT-TEMPO monomer was investigated by cyclic voltammetry in acetonitrile and dichloromethane at 20 mV s^{-1} scan rate, switching the potential between 0.0 V and 1.5 V. When the electrochemical polymerization was carried out in acetonitrile (Figure 2.4a), the nitroxide group was oxidized at 0.75 V and reduced at 0.65 V, while the thiophene ring was oxidized at potentials higher than 1.40 V, leading to the polymerization. During the polymerization, the material that was forming onto the electrode was simultaneously dissolved in the electrolyte leading to a blue coloured solution, as shown in the inset of Figure 2.4a.

When the electropolymerization was carried out in dichloromethane solution (Figure 2.4b), the polymerization started at 1.35 V with the oxidation of EDOT, while the TEMPO group of the monomer was oxidized and reduced at 0.95 V and 0.62 V, respectively. When increasing the number of cycles, the current and the potential of the maxima increased showing the growing amount of polymer electrodeposited onto the electrode during every sweep. The potential of the oxidation peak maxima varies from the first to the second cycle, in the case of EDOT from 1.42 V to 1.34 V and from 0.95V to 0.82 V for TEMPO. This behavior is usual in conducting polymers since the oxidation on the coated polymer electrode needs lower potential than the oxidation on the platinum electrode.

Due to the electrochromic characteristics of PEDOT polymers that are colourless in their oxidized state and coloured in their reduced state, it was not possible to observe the formation and growth of the film during the anodic electropolymerization, only during reduction the blue

film was observed. The colour change from colourless to blue was observed at potentials lower than 0.2 V.

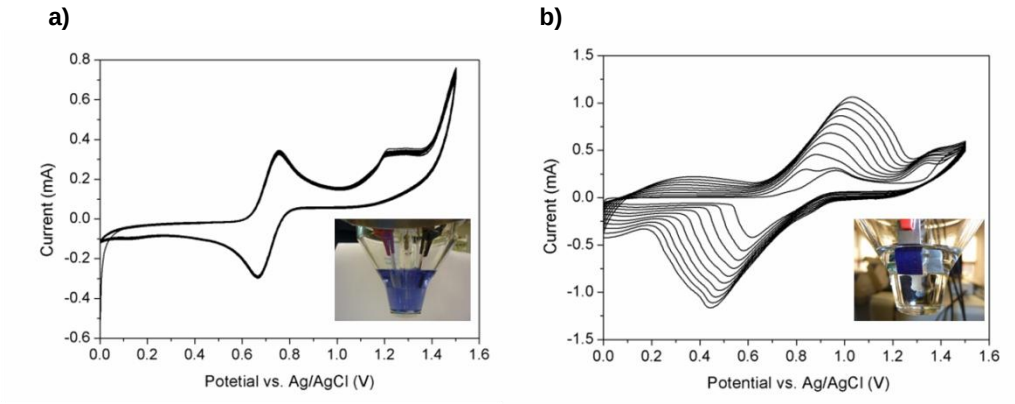

Figure 2.4. Cyclic voltammograms of the electrochemical polymerization in 10^{-3} M EDOT-TEMPO and 0.1 M $LiClO_4$ acetonitrile solution (a), and in 0.1 M $TBAPF_6$ dichloromethane solution (b), using a 1 cm^2 electrode, switching potential from 0.0 V to 1.5 V at a 20 mV s^{-1} scan rate. Insets show the pictures of the cell after the electropolymerization.

The electropolymerization was also investigated by applying constant current flows of 0.10, 0.15, 0.20 and 0.25 mA through previously cleaned platinum electrodes for 60 s (Figure 2.5a). When 0.10 mA constant current was applied, 60 s were not sufficient for the electropolymerization, since the potential reached was lower than the onset of the monomer oxidation. For higher currents, the electropolymerization occurred at almost constant potential between 1.3 and 1.4 V, which is the oxidation potential of the monomer and the voltage plateau was higher when the applied current was increased.

The electropolymerization was also carried out by potential steps from 0 V to different potentials ranging between 1.4 V and to 1.8 V, which are higher than the onset of the monomer oxidation (Figure 2.5b). In the chronoamperograms obtained at the potential steps of 1.4 and 1.5 V, after an initial current leap a minimum and a shoulder are present which are representative of a nucleation process of PEDOT-TEMPO on the platinum electrode. When higher potentials are applied, a high initial peak is followed by a fast current decrease. The stationary current obtained after the initial peak, is higher when applying a higher anodic potential. The electrochemical characterization of the formed films showed a similar voltammogram to the one obtained by electropolymerization by cyclic voltammetry, indicating that the electropolymerization occurs via the same mechanism.

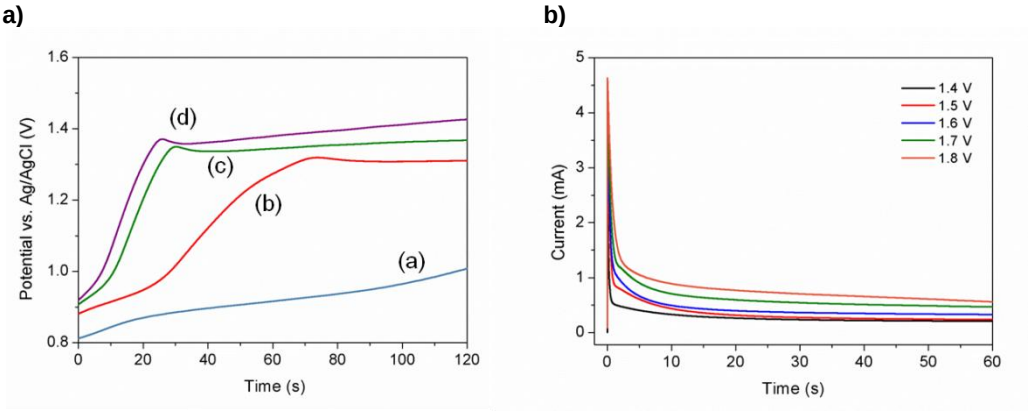

Figure 2.5. a) Chronopotentiograms obtained from a 10^{-3} M EDOT-TEMPO and 0.1 M $TBAPF_6$ dichloromethane solution at constant currents of (a) 0.10, (b) 0.15, (c) 0.20, (d) 0.25 mA. b)Chronoamperograms obtained from the same monomeric solution at potential steps between 1.4 and 1.8 V, using a 1 cm^2 electrode.

The electrodeposited PEDOT-TEMPO film in dichloromethane was later electrochemically characterized in a monomer free 0.1 M $TBAPF_6$ dichloromethane solution.

The cyclic voltammograms of the polymer obtained when sweeping the potential between -0.5 V and 1.8 V at different scan rates are shown in Figure 2.7a. The polymer shows two redox processes (Figure 2.6); the first one related to the PEDOT backbone which is oxidized at 0.3 V and reduced at around -0.2 V and the second one to TEMPO group that is oxidized and reduced at 0.92 V and 0.6 V, respectively at 5 mV s^{-1} scan rate. The cathodic and anodic peak currents of TEMPO show a linear dependence on the scan rate indicating that the redox processes are not diffusion limited (Figure 2.7a). The electrochemical behaviour of a cathode consisting of 70 % of PEDOT-TEMPO electropolymerized in acetonitrile and 30 % of carbon was investigated versus lithium anode by sweeping the potential between 2.8 V and 4.2 V at different scan rates (Figure 2.7b). In the same manner of the film, PEDOT-TEMPO cathode shows two main redox processes. The TEMPO group shows its oxidation and reduction at 3.65 V and 3.55 V, respectively while PEDOT backbone redox activity is observed around 3.0 V.

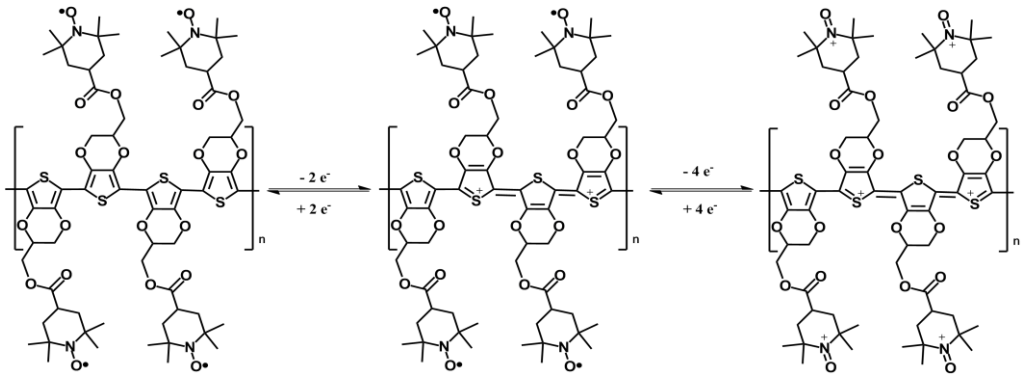

Figure 2.6. Scheme of redox reactions of PEDOT-TEMPO polymer.

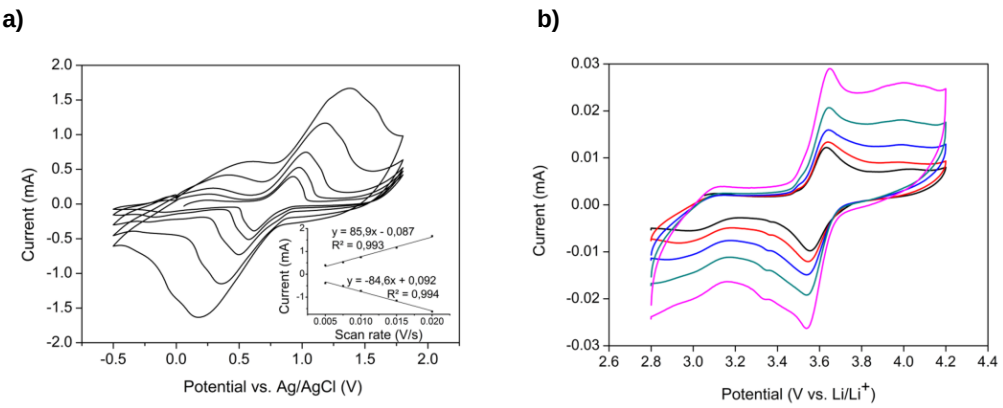

Figure 2.7. a) Cyclic voltammograms of PEDOT-TEMPO film in 0.1 M $TBAPF_6$ dichloromethane solution at 5, 7.5, 10, 15 and 20 mV s^{-1}. Inset graph shows the relationship between the oxidation and reduction peak currents vs scan rate. b) Cyclic voltammograms of PEDOT-TEMPO/C (70/30) electrode with 1 M $LiPF_6$ in EC:DMC electrolyte at 0.05, 0.1, 0.2, 0.4, 0.8 mV s^{-1}.

2.4. Copolymerization with EDOT

In order to be able to tune the redox and electrical properties of the final polymer, copolymerization of EDOT-TEMPO with EDOT monomer is desirable. Consequently, electrochemical copolymerization of EDOT-TEMPO monomer with EDOT was investigated by cyclic voltammetry in dichloromethane solution. The EDOT/EDOT-TEMPO molar ratios studied were 75/25 and 85/15, as well as PEDOT homopolymer for comparison.

The electrochemical copolymerization was carried out in dichloromethane solution (Figure 2.8) by switching the potential between 0.0 V and 1.5 V at 20 mV s^{-1} scan rate. Figure 2.8a shows the first cyclic voltammogram for the different compositions. The cyclic voltammetry of EDOT shows one irreversible oxidation at 1.26 V, while the mixture of the two monomers

exhibit the irreversible oxidation of EDOT together with the oxidation and reduction of TEMPO group. The EDOT oxidation potential of the copolymerization solutions shifts to higher potentials due to the presence of EDOT-TEMPO monomer, whose thiophene group oxidation appears at 1.35V. The redox peaks related to TEMPO have the same onset potential for the two copolymerizations, 0.78 V for the oxidation and 0.88 V for the reduction, while the peak maxima vary due to the different concentrations of EDOT-TEMPO in the solutions. Figure 2.8b shows the 10 cyclic voltammograms of each copolymerization. It can be observed that the current and the potential of the maxima increases due to the growing amount of copolymer electrodeposited onto the electrode during every sweep.

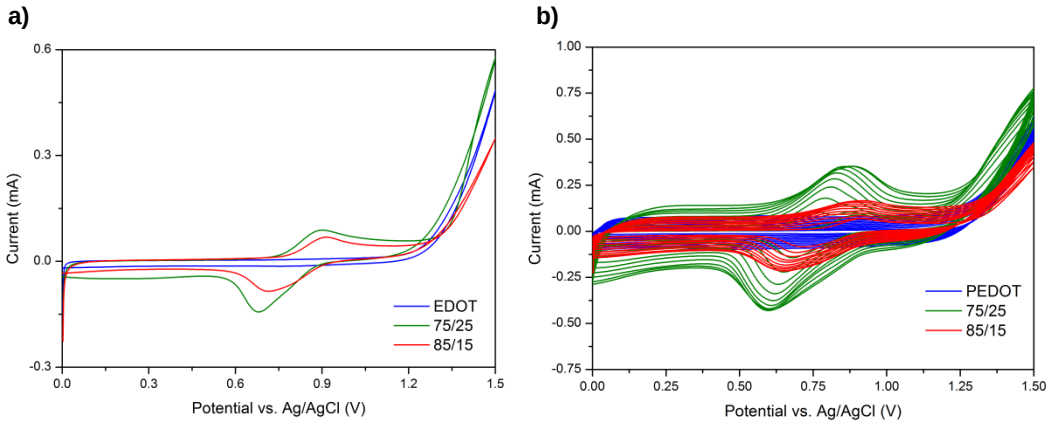

Figure 2.8. Cyclic voltammograms of the electrochemical copolymerization in 0.1 M $TBAPF_6$ dichloromethane solution with EDOT/EDOT-TEMPO molar ratio of 100/0 (blue), 85/15 (red) and 75/25 (green). a) First cycle and b) 10 cycles of electropolymerization.

The electrodeposited films of the copolymers were later electrochemically characterized in a monomer free 0.1 M $TBAPF_6$ dichloromethane solution. The cyclic voltammograms obtained at 10 mV s^{-1} scan rate for the two copolymers and PEDOT are shown in Figure 2.9.

PEDOT homopolymer shows one redox process related to the oxidation and reduction of the polymer backbone, with oxidation peak maximum at 0.12 V and reduction at -0.69 V. On the other hand, copolymers exhibit three redox processes, the first two related to the thiophene backbone and the last one associated with TEMPO group. Both copolymers present cyclic voltammograms with similar shape and redox potentials. The oxidation peaks appear at -0.44 V (A_1), 0.04 V (A_2) and 0.83 V (A_3) while the reduction peaks occur at -0.90 V (C_1), -0.60 V (C_2) and 0.65 V (C_3). When comparing the two copolymers, we can observed that the intensity of the first two redox processes related to PEDOT backbone is higher with the higher amount of EDOT in the copolymerization solution (85%). Therefore, we can conclude that copolymerization of EDOT-TEMPO with EDOT is possible trough cyclic voltammetry and that the concentration relation of the two monomers in the starting solution and in the final copolymer is proportional.

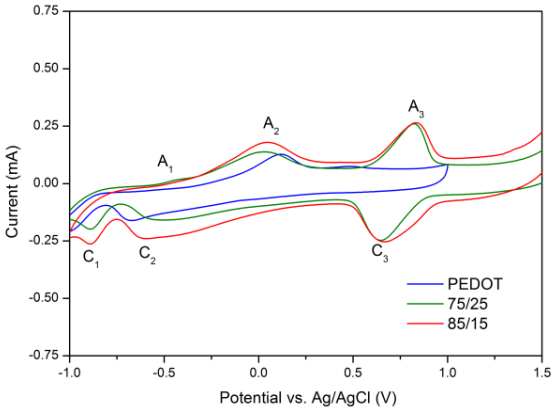

Figure 2.9. Cyclic voltammograms of PEDOT homopolymer and 75/25, 85/15 copolymers (EDOT/EDOT-TEMPO) in 0.1 M $TBAPF_6$ dichloromethane solution at 10 mV s^{-1}.

2.5. PEDOT-TEMPO characterization

Taking advantage of the solubility of PEDOT-TEMPO electropolymerized in acetonitrile, its structural and electric properties were further characterized. The nature of the PEDOT backbone was confirmed by FTIR and UV spectroscopies shown in Figure 2.2. The typical bands associated with thiophene ring vibrations were identified in the FTIR spectrum of the polymer (1517, 1355, 1304 cm^{-1}) as well as the carbonyl (1727 cm^{-1}) and nitroxide (1362 cm^{-1}) bands. The UV-Vis spectrum of EDOT-TEMPO monomer shows absorption at 239 and 256 nm. The latter peak related to EDOT group shifts to higher wavelengths during the polymerization, as the π system conjugation becomes longer. UV-Vis spectrum of the polymer soluble in acetonitrile shows absorption at 312 nm related to oligomeric units, absorption at 567 and 609 nm corresponding to π-π* transitions in PEDOT backbone and the typical polaronic-bipolaronic bands with maximum absorption at 776 and 875 nm.

Interestingly, MALDI-TOF mass spectrometry was used to analyze the molar mass distributions of the electropolymerized PEDOT-TEMPO. Using positive ion linear mode, the molar mass distribution (MMD) and the number of monomeric units were determined. The obtained MMD values for PEDOT-TEMPO are: Mn = 1759, Mw = 2033 and polydispersity (Đ) of 1.16. The correct repeating unit of 352 Da is observed between the peaks of different series, and oligomers up to 15 monomeric units are detected. Figure 2.10 shows the spectra of PEDOT-TEMPO in two different mass ranges. In order to avoid the ion suppression effect at low molecular weight (LMW) and achieve detecting peaks in high molecular weight (HMW) it was necessary to do deflection of the sample below 600 and 1000 Da. The red arrows show

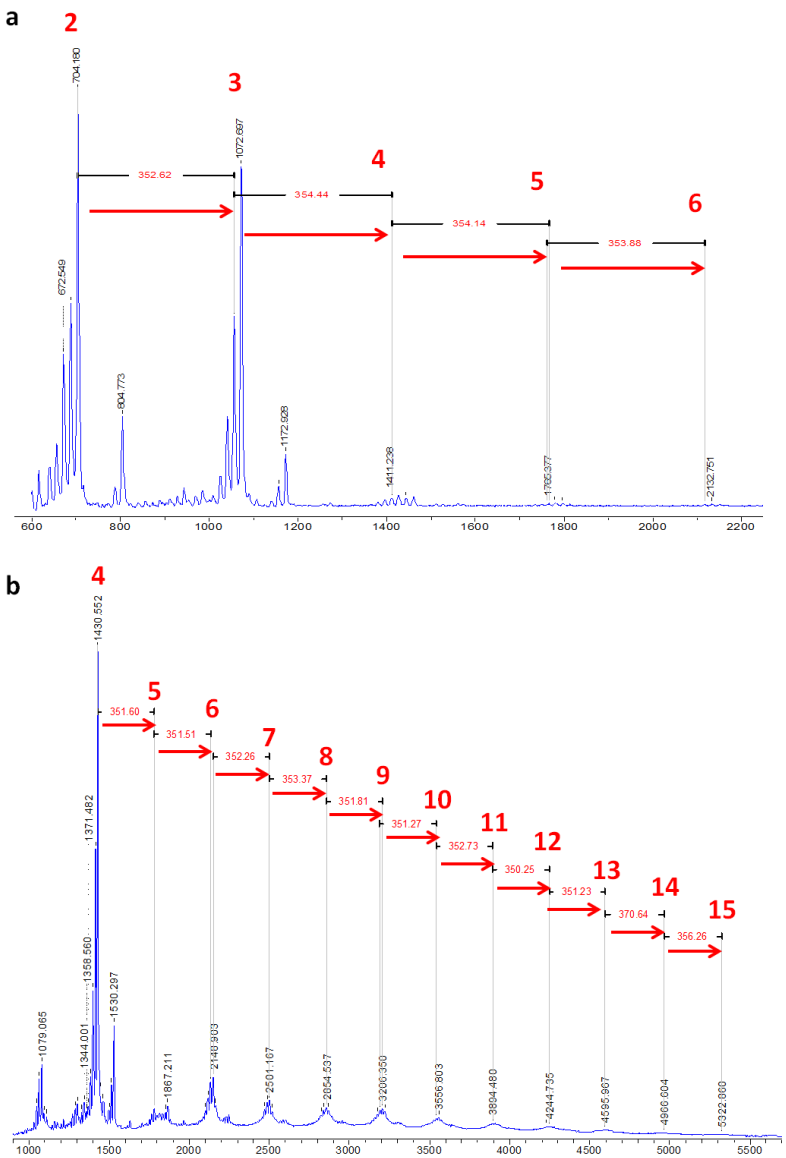

Figure 2.10. MALDI-TOF mass spectra of PEDOT-TEMPO in positive ion linear mode in different mass ranges (a) 600- 2200 Da (deflection below 600 Da) and (b) 1000-5500 Da (deflection below 1000 Da).

the increment of a monomeric unit in the oligomer. The number above the peaks denotes the total number of monomer units in the oligomer.

Furthermore, the presence of the radical nitroxide in the obtained PEDOT-TEMPO polymer was investigated by ESR. The ESR spectrum of the polymer was recorded in acetone solution (Figure 2.3). The polymer shows a triplet similar to the monomer spectrum, with the usual hyperfine coupling constant of 14.4 G, which indicates that the polymer is bearing nitroxide radicals. As the measurement was done in acetone solution, the spectrum shows signals of Mn^{2+} ion hyperfine structure coming from the capillary.

The electrical conductivity of electropolymerized PEDOT-TEMPO was measured by the four-point probe technique. For the measurements, the obtained polymer in acetonitrile was drop casted on glass slides to obtain films of around 10 μm thickness. The average conductivity value of three films was 5.7×10^{-2} S/cm. This value is relatively low when compared to PEDOT conductivity (1×10^{3} S/cm) but similar to the electrical conductivity reported for other PEDOT derivatives based on substituted EDOT monomers.[26] On the other hand, this value compares very favourably with the conductivity of conventional radical polymers which show conductivity values between 10^{-5}-10^{-7} S/cm.[19]

The redox nature and activity of the polymer was confirmed by ESR and electrochemical characterization, while the chemical structure and electrical properties were studied by FTIR, UV-Vis, MALDI-TOF MS and four-point probe. Altogether, the different characterizations carried out confirmed the synthesis of a PEDOT radical polymer with synergetic redox and electrical properties.

2.6. Application in lithium-ion batteries

A first attempt was done using the redox active PEDOT-TEMPO as cathode active material for organic-lithium batteries. However, the obtained capacities were very small. Therefore, as a potential application, PEDOT-TEMPO was used as conductive binder in lithium-ion batteries. Conventional lithium-ion cathodes are usually made of three main components: an active material ($LiFePO_4$, $LiCoO_2$ etc.), a conductive additive such as carbon and a polymeric binder. As it has been seen in Chapter 1, conductive polymers have been mostly applied as conductive coatings of current Li-ion insolating inorganic cathode materials such as $LiCoO_2$ or $LiFePO_4$.[27-29] On the other hand, Gohy and collaborators have recently shown that the presence of radical polymers allowed to increase the electron transfer kinetics of $LiFePO_4$ electrodes and cycling ability of the batteries at high C rates.[30,31] Furthermore, in order to obtain high energy density batteries, the use of conductive additives and binders that are not redox active should be decreased so as to have the maximum active material into a fixed volume of electrode. So in principle, PEDOT-TEMPO polymer may be ideally suited to be used as conducting binder due to its synergetic properties.

The performance of PEDOT-TEMPO as conductive binder was investigated in $LiFePO_4$ (LFP) cathodes and compared to its counterpart cathode containing a conventional binder, poly(vinylidene fluoride) (PVDF). Cell performance of the cathode without carbon added consisting of 85 % LFP and 15 % PEDOT-TEMPO is shown in Figure 2.11a. The charge/discharge capacity of the cell containing PEDOT-TEMPO is higher than the counterpart having PVDF as binder, whose capacity decreases drastically in the first cycles due to a lack of

electron transport between cathode components. This confirms that PEDOT-TEMPO can act as conductive binder providing high coulombic efficiency (98 %), however, the discharge capacity is not completely stable. After addition of a minimum amount of carbon, stable discharge capacity of PEDOT-TEMPO cell was obtained (95 % capacity retention after 50 cycles) together with high coulombic efficiency (>99 %) at 0.1 C rate.

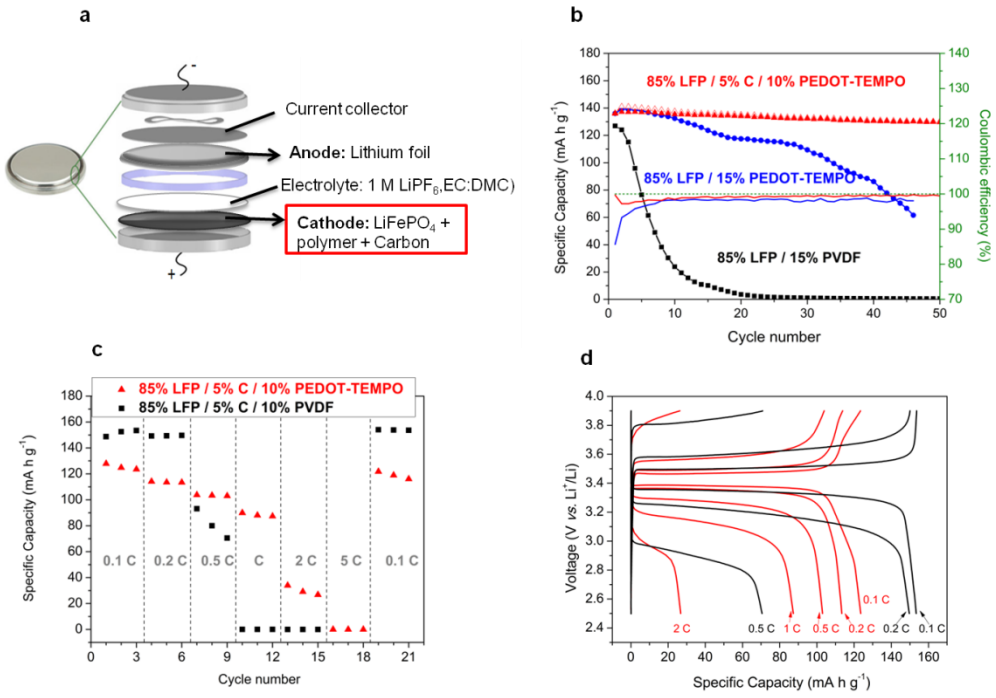

Figure 2.11. a) Schematic diagram of the battery components and cell performance of LFP cathodes: b) Discharge capacity and coulombic efficiency at 0.1 C with (●)15% PEDOT-TEMPO, (▲)10% PEDOT-TEMPO and 5% carbon and (■)15% PVDF; c) C-rate capability and d) voltage profile at different C rates for 10% PEDOT-TEMPO and 5% carbon (red line) and 10% PVDF and 5% carbon (black line).

The rate capability of the cells with the latter configuration was also investigated (Figure 2.11b). Although cathode with PVDF binder provides higher capacity deliverance at low C rates (0.1 C and 0.2 C), higher C rate performance (0.5C, 1C and 2C) was dominated by cathode with PEDOT-TEMPO binder with a capacity of 90 mA hg^{-1} at 1 C rate. The voltage profiles at different rates are shown in Figure 2.11c where the polarization of the cathode containing PVDF binder at C rates higher than 0.2 C is noticeable.

2.7. Conclusions

In conclusion, the synthesis of a novel EDOT derivative bearing a TEMPO nitroxide radical has been presented in this chapter. The monomer has been polymerized by electrochemical techniques and the obtained polymer presents combined properties of both groups, electronic conductivity of PEDOT backbone together with the redox activity of TEMPO moiety. Interestingly, the electropolymerization in acetonitrile leaded to a soluble polymer. These properties make PEDOT-TEMPO a good candidate to be used as conductive binder in batteries. Its performance as binder was investigated in $LiFePO_4$ batteries and compared to conventional PVDF binder. Good cycling stability with high coulombic efficiency and increased C rate capability were obtained with 85%LFP/5%C/10%PEDOT-TEMPO cathode configuration. Therefore, PEDOT-TEMPO can act as a conductive binder thus replacing the conventional binder and reducing the amount of high surface area carbon additive generally required to improve electrical conductivity in insulating cathode materials.

2.8. Experimental part

2.8.1. Materials

4-carboxy-TEMPO (97 %), hydroxymethyl EDOT (95 %), 4-(dimethylamino)pyridine (DMAP, ≥ 99 %), *N, N´*-dicyclohexylcarbodiimide (DCC, 99 %), dry lithium perchlorate ($LiClO_4$, 99.99 %) and dry tetrabutylammonium hexafluorophosphate ($TBAPF_6$, ≥ 99 %) were obtained from Sigma-Aldrich and used as received.

Anhydrous dichloromethane (DCM), anhydrous acetonitrile (ACN), hexane and ethyl acetate were purchased from Sigma-Aldrich and used as received.

2.8.2. Methods

Attenuated Total Reflectance Fourier Transform Infrared Spectroscopy measurements (ATR-FTIR) were conducted on a Bruker ALPHA Spectrometer.

UV-Vis spectra were acquired at room temperature on a PerkinElmer UV/Vis/NIR Lambda 950 spectrometer.

Electron paramagnetic resonance (ESR) spectra were recorded on a Bruker ESP300 spectrometer operating at the X-band and Q-band and equipped with standard Oxford Instruments low-temperature devices (ESR900/ITC4), at room temperature in the solid state and in acetone solution at 140 K.

Matrix Assisted Laser Desorption Ionization Time of Flight Mass Spectrometry (MALDI-TOF MS) measurements were carried out on a Bruker Autoflex Speed system (Bruker, Germany). The instrument was equipped with a 355 nm Nd:YAG laser. All spectra were acquired in the positive-ion linear and reflectron modes. The samples were dissolved in acetonitrile just before analysis at 2 g L^{-1}. Approximately 0.25 µL of the dissolved sample were hand spotted onto a PACII target. This target contains α-cyano-4-hydroxycinnamic acid (CHCA, Aldrich) matrix. When the sample was air dried, the MALDI sample plate was inserted into the spectrometer and spectra were acquired under high vacuum conditions. For each spectrum, 5000 laser shots were accumulated.

Conductivity measurements were performed on a FPP Veeco/Miller FPP5000 using layer resistivity function, sampling in different zones of the film more than five times and doing the reciprocal. Thickness of polymer film was measured with a Digimatic micrometer from Mitutoyo Corporation.

The electrochemical polymerization and characterization was performed on an Autolab PGSTAT302N by using the standard three-electrode configuration where platinum sheets (with an area of 1 cm^2) were used as working and counter electrodes and an Ag/AgCl (3 M KCl) as reference electrode.

Cathodes were prepared mixing Carbon Black (Csp-Imerys®) and lithium iron phosphate ($LiFePO_4$, Alees3, Taiwan) by hand-milling and adding the mixture to the dissolved polymer in acetonitrile. The obtained slurry was drop casted onto aluminum foil discs with 11 mm diameter. The electrodes were dried under vacuum at 45 °C for 4 hours. Coin cells

(CR2032) were assembled in an argon-filled glove box. The anode was a disk of lithium metal foil (Rockwood lithium) and it was separated from the cathode by a glass fiber (Glass fiber GFD/55, Whatman) soaked in a solution of 1 M $LiPF_6$ in EC:DMC (1:1 vol. %) (Solvionic). Cells were probed using a MACCOR® battery tester and cycled between 2.8 V and 3.9 V.

2.8.3. Synthesis of (2,3-dihydrothieno[3,4-b][1,4]dioxin-2-yl)methyl 2,2,6,6-tetramethylpiperidine-1-oxyl-4-carboxilate (EDOT-TEMPO)

4-Carboxy-2,2,6,6-tetramethylpiperidine 1-oxyl (4-carboxy-TEMPO, 0.28 g, $1.4 \cdot 10^{-3}$ mol) was added to a solution of (2,3-Dihydrothieno[3,4-b][1,4]dioxin-2-yl)methanol (EDOT-MeOH, 0.38 g, $2.18 \cdot 10^{-3}$ mol, 1.6 eq.) and dimethylaminopyridine (DMAP, 0.017 g, $1.34 \cdot 10^{-4}$ mol, 0.1 eq.) in 10 mL of dry DCM at 0 ºC. After 5 min stirring at 0 ºC, dicyclohexylcarbodiimide (DCC, 0.31 g, $1.52 \cdot 10^{-3}$ mol, (1.1 eq.) was added in 4 mL of dry DCM. After 3 days stirring at room temperature, the solution was stored in the freezer overnight and the white precipitate was filtered. The filtrate was washed with H_2O (80 mL) four times, dried over $MgSO_4$ and filtered. Crude monomer was purified by column chromatography using the elution 3/1 Hexane/EtOAc to yield an orange solid (64%). The presence of the nitroxide free radical makes imposible to measure the NMR spectrum of the monomer, therefore, it was reduced with phenylhydrazine to obtain its hydroxylamine derivative. M.p. 98-101 °C. ^{1}H NMR (400 MHz, $CDCl_3$, ppm): 6.40 (d, *J*= 4.5 Hz, 2 H), 4.44-4.23 (m, 5H), 2.76 (m, 1H), 1.86 (m, 2H), 1.74 (m, 2H), 1.27 (s, 6H), 1.19 (s, 6H) (Figure 2.12). FTIR-ATR (cm^{-1}): 3011 (C-H thiophene stretching), 2987, 2967, 2923, 2870 (C-H aliphatic stretching), 1725 (C=O stretching), 1490, 1466, 1457, 1424, 1375 (N-O stretching), 1255, 1239, 1190, 1164, 1122, 1100 (C-O stretching), 1075, 1035 (=C-H bending).

MALDI-TOF: *m/z* = 354.14 Da, (theoretical *m/z* = 354.44 Da). Elemental analysis: $C_{17}H_{24}NO_5S\cdot$ (theoretical); C: 57.61; H: 6.82; N: 3.95; S: 9.05; (found); C: 57.57; H: 6.93; N: 3.95; S: 8.68. ESR ($C_6H_5CH_3$ solution): three peaks with a_N = 14.4 G.

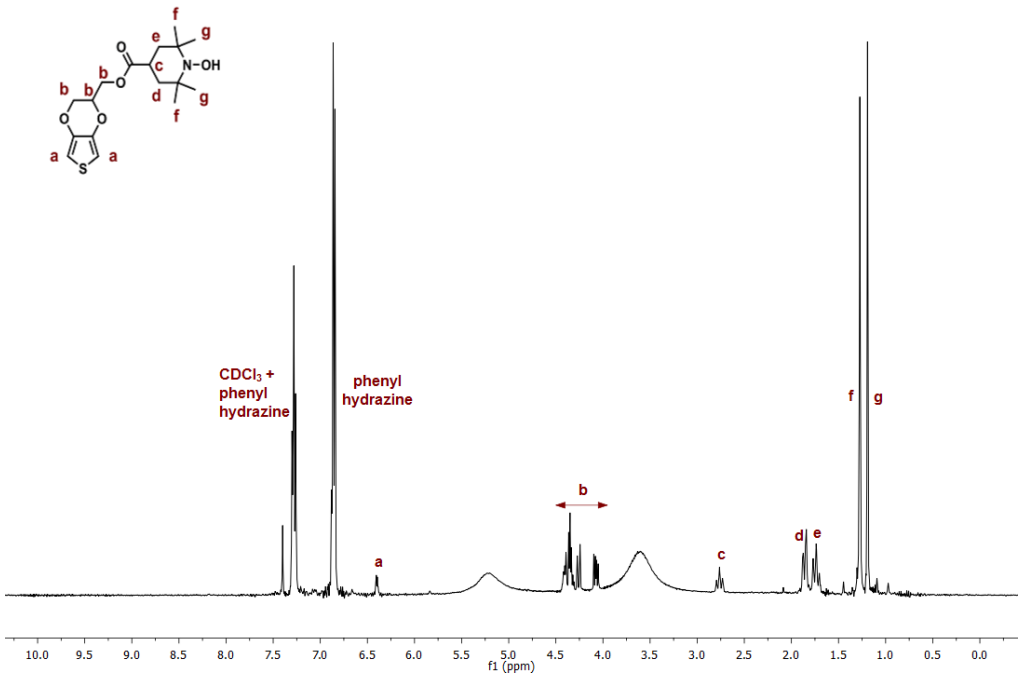

Figure 2.12. ^{1}H NMR spectra of EDOT-TEMPO monomer with phenyl hydrazine in $CDCl_3$.

2.8.4. Electrochemical polymerization of EDOT-TEMPO and copolymes

The electrochemical polymerization of EDOT-TEMPO monomer was investigated by cyclic voltammetry, potential step and constant current methods. Electrochemical polymerization by cyclic voltammetry was studied in two organic media: 0.1 M $LiClO_4$ acetonitrile and 0.1 M $TBAPF_6$ dichloromethane solutions and switching the potential between 0.0 V and 1.5 V at 20 mV s^{-1} scan rate. Electropolymerization by potential step and constant current were carried out in 0.1 M $TBAPF_6$ dichloromethane solution, applying potentials between 1.4 and 1.8 V for 60 s and constant currents of 0.10, 0.15, 0.20, 0.25 mA for 120s, respectively. The monomer concentration was 10^{-3} M for all the cases.

The electrochemical copolymerizations of EDOT-TEMPO with EDOT were investigated by cyclic voltammetry in 0.1 M $TBAPF_6$ dichloromethane solution, switching the potential between 0.0 V and 1.5 V at 20 mV s^{-1} scan rate. The total monomer concentration was 10^{-3} M for both cases: 75/25 (7.5 10^{-4} M EDOT / 2.5 10^{-4} M EDOT-TEMPO) and 85/15 (8.5 10^{-4} M EDOT / 1.5 10^{-4} M EDOT-TEMPO).

2.9. References

(1) Gracia R., Mecerreyes D. Polymers with redox properties: materials for batteries, biosensors and more. *Polym. Chem.* **2013**;4:2206-14.

(2) Macaya D. J., Nikolou M., Takamatsu S., Mabeck J. T., Owens R. M., Malliaras G. G. Simple glucose sensors with micromolar sensitivity based on organic electrochemical transistors. *Sens. Actuators B-Chem.* **2007**;123:374-8.

(3) Zhang F., Johansson M., Andersson M. R., Hummelen J. C., Inganäs O. Polymer Photovoltaic Cells with Conducting Polymer Anodes. *Adv. Mater.* **2002**;14:662-5.

(4) Janoschka T., Hager M. D., Schubert U. S. Powering up the Future: Radical Polymers for Battery Applications. *Adv. Mater.* **2012**;24:6397-409.

(5) Huo M., Yuan J., Tao L., Wei Y. Redox-responsive polymers for drug delivery: from molecular design to applications. *Polym. Chem.* **2014**;5:1519-28.

(6) Mike J. F., Lutkenhaus J. L. Electrochemically Active Polymers for Electrochemical Energy Storage: Opportunities and Challenges. *ACS Macro Lett.* **2013**;2:839-44.

(7) Casado N., Hernández G., Sardon H., Mecerreyes D. Current trends in redox polymers for energy and medicine. *Prog. Polym. Sci.* **2015**.

(8) Vlad A., Arnould K., Ernould B., Sieuw L., Rolland J., Gohy J.-F. Exploring the potential of polymer battery cathodes with electrically conductive molecular backbone. *J. Mater. Chem. A*. **2015**;3:11189-93.

(9) Elschner A., Kirchmeyer S., Lövenich W., Merker U., Reuter K. PEDOT Principles and Applications of an Intrinsically Conductive Polymer. 1st ed. Boca Raton: CRC Press Taylor & Francis Group; 2010. p. 377.

(10) Liu J., Wei B., Sloppy J. D., Ouyang L., Ni C., Martin D. C. Direct Imaging of the Electrochemical Deposition of Poly(3,4-ethylenedioxythiophene) by Transmission Electron Microscopy. *ACS Macro Lett.* **2015**;4:897-900.

(11) Okuzaki H., Suzuki H., Ito T. Electromechanical Properties of Poly(3,4-ethylenedioxythiophene)/Poly(4-styrene sulfonate) Films. *J. Phys. Chem. B*. **2009**;113:11378-83.

(12) Karlsson R. H., Herland A., Hamedi M., Wigenius J. A., Åslund A., Liu X., Fahlman M., Inganäs O., Konradsson P. Iron-Catalyzed Polymerization of Alkoxysulfonate-Functionalized 3,4-Ethylenedioxythiophene Gives Water-Soluble Poly(3,4-ethylenedioxythiophene) of High Conductivity. *Chem. Mater.* **2009**;21:1815-21.

(13) Fabretto M. V., Evans D. R., Mueller M., Zuber K., Hojati-Talemi P., Short R. D., Wallace G. G., Murphy P. J. Polymeric Material with Metal-Like Conductivity for Next Generation Organic Electronic Devices. *Chem. Mater.* **2012**;24:3998-4003.

(14) Mueller M., Fabretto M., Evans D., Hojati-Talemi P., Gruber C., Murphy P. Vacuum vapour phase polymerization of high conductivity PEDOT: Role of PEG-PPG-PEG, the origin of water, and choice of oxidant. *Polymer*. **2012**;53:2146-51.

(15) Zhan L., Song Z., Zhang J., Tang J., Zhan H., Zhou Y., Zhan C. PEDOT: Cathode active material with high specific capacity in novel electrolyte system. *Electrochim. Acta*. **2008**;53:8319-23.

(16) Wang C. Y., Tsekouras G., Wagner P., Gambhir S., Too C. O., Officer D., Wallace G. G. Functionalised polyterthiophenes as anode materials in polymer/polymer batteries. *Synt. Met.* **2010**;160:76-82.

(17) Chen J., Liu Y., Minett A. I., Lynam C., Wang J., Wallace G. G. Flexible, Aligned Carbon Nanotube/Conducting Polymer Electrodes for a Lithium-Ion Battery. *Chem. Mater.* **2007**;19:3595-7.

(18) Arias-Pardilla J., Otero T. F., Blanco R., Segura J. L. Synthesis, electropolymerization and oxidation kinetics of an anthraquinone-functionalized poly(3,4-ethylenedioxythiophene). *Electrochim. Acta*. **2010**;55:1535-42.

(19) Tomlinson E. P., Hay M. E., Boudouris B. W. Radical Polymers and Their Application to Organic Electronic Devices. *Macromolecules*. **2014**;47:6145-58.

(20) Sukegawa T., Kai A., Oyaizu K., Nishide H. Synthesis of Pendant Nitronyl Nitroxide Radical-Containing Poly(norbornene)s as Ambipolar Electrode-Active Materials. *Macromolecules*. **2013**;46:1361-7.

(21) Oyaizu K., Nishide H. Radical Polymers for Organic Electronic Devices: A Radical Departure from Conjugated Polymers? *Adv. Mater.* **2009**;21:2339-44.

(22) Nakahara K., Oyaizu K., Nishide H. Organic Radical Battery Approaching Practical Use. *Chem. Lett.* **2011**;40:222-7.

(23) Huang Q., Choi D., Cosimbescu L., Lemmon J. P. Multi-electron redox reaction of an organic radical cathode induced by a mesopore carbon network with nitroxide polymers. *Phys. Chem. Chem. Phys.* **2013**;15:20921-8.

(24) Oyaizu K., Kawamoto T., Suga T., Nishide H. Synthesis and Charge Transport Properties of Redox-Active Nitroxide Polyethers with Large Site Density. *Macromolecules*. **2010**;43:10382-9.

(25) Aydın M., Esat B., Kılıç Ç., Köse M. E., Ata A., Yılmaz F. A polythiophene derivative bearing TEMPO as a cathode material for rechargeable batteries. *Eur. Polym. J.* **2011**;47:2283-94.

(26) Krishnamoorthy K., Ambade A. V., Mishra S. P., Kanungo M., Contractor A. Q., Kumar A. Dendronized electrochromic polymer based on poly(3,4-ethylenedioxythiophene). *Polymer*. **2002**;43:6465-70.

(27) Her L.-J., Hong J.-L., Chang C.-C. Preparation and electrochemical characterizations of poly(3,4-dioxyethylenethiophene)/LiCoO2 composite cathode in lithium-ion battery. *J. Power Sources*. **2006**;157:457-63.

(28) Cintora-Juarez D., Perez-Vicente C., Ahmad S., Tirado J. L. Improving the cycling performance of LiFePO4 cathode material by poly(3,4-ethylenedioxythiopene) coating. *RSC Adv.* **2014**;4:26108-14.

(29) Grygiel K., Lee J.-S., Sakaushi K., Antonietti M., Yuan J. Thiazolium Poly(ionic liquid)s: Synthesis and Application as Binder for Lithium-Ion Batteries. *ACS Macro Lett.* **2015**:1312-6.

(30) Kim J.-M., Park H.-S., Park J.-H., Kim T.-H., Song H.-K., Lee S.-Y. Conducting Polymer-Skinned Electroactive Materials of Lithium-Ion Batteries: Ready for Monocomponent Electrodes without Additional Binders and Conductive Agents. *ACS Appl. Mater. Interfaces*. **2014**;6:12789-97.

(31) Vlad A., Singh N., Rolland J., Melinte S., Ajayan P. M., Gohy J. F. Hybrid supercapacitor-battery materials for fast electrochemical charge storage. *Sci. Rep.* **2014**;4:4315.

CHAPTER 3

High Performance PEDOT/lignin Biopolymer Composites for Electrochemical Supercapacitors

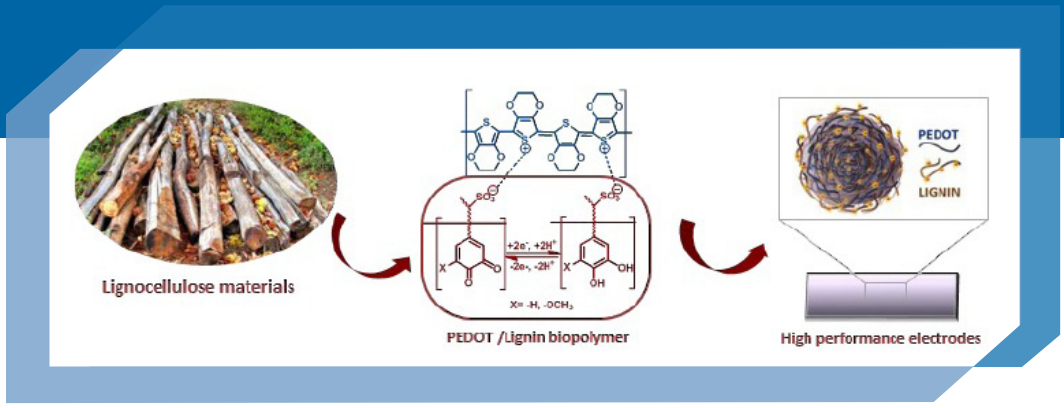

Chapter 3. High performance PEDOT/lignin biopolymer composites for electrochemical supercapacitors

3.1. Introduction

The development of energy storage devices based on sustainable bio-inspired components is nowadays heavily researched.[1] Lignin, the second most abundant biopolymer on earth, contains a large variety of redox-active phenolic type functional groups that enable storage of charge.[2] The development of charge storage devices based on lignin would be a large step towards the development of sustainable devices. Lignin is also a side product in the processing of wood for paper, and is mainly burnt to get process heat. It is used as a surfactant in processing of cement, but such uses only cover a small fraction of the waste product use. It is therefore a cheap and scalable material. However, lignin in itself is an insulating material. Accordingly, it is necessary to incorporate lignin into a matrix consisting of a conducting material, in order to allow charge transport.[3,4] In this way, the conductor will transport charge to the lignin moiety, where charge can be stored in a reversible redox reaction between the hydroquinone and quinone forms. The first example of this approach utilized a combination of lignin and polypyrrole.[5] In addition, various combinations of lignin and conductors such as reduced graphene oxide[6] or carbon nanotubes[7] have been investigated since then.

The use of conducting polymers is attractive as properties can be modified by variations in polymer structure. We already mentioned that PEDOT is one of the most successful conducting polymers due to its high conductivity and electrochemical and thermal stability.[8] Moreover, the polymerization of EDOT monomer is facile; but the low solubility of PEDOT makes processing of the material challenging. This drawback can be overcome by polymerizing EDOT in the presence of a water-soluble polyelectrolyte, such as polystyrenesulfonate (PSS).[9-13] Lignin can be processed into a so called lignosulfonate, containing sulfonate groups that, in a similar manner to the sulfonate groups in PSS, could enable the lignosulfonate to act as both counter ion and dispersing agent.[14] It could thus be considered that lignosulfonate could disperse EDOT in aqueous solution and upon EDOT polymerization a PEDOT/lignosulfonate composite would form. Such PEDOT/lignin (PEDOT/Lig) composites can in principle be synthesized by two different approaches: chemical polymerization or electrochemical polymerization. Chemical polymerization allows bulk production of polymeric dispersions, which makes chemical polymerization the method of choice for large scale production and commercial applications. On the other hand, electrochemical polymerization allows the deposition of homogeneous films onto the working electrode with a well-controlled thickness and morphology.[15]

Therefore, the aim of this chapter is to investigate chemically synthesized PEDOT/Lig composites and study their redox behaviour, electrochemical stability and surface morphology.

3.2. PEDOT/lignin synthesis

PEDOT/Lig composites were synthesized by oxidative chemical polymerization, as represented in Figure 3.1. The resulting PEDOT/Lig biomaterial is an ionic complex composite where both PEDOT and lignosulfonates are closely combined, similar to interpenetrating polymer networks.

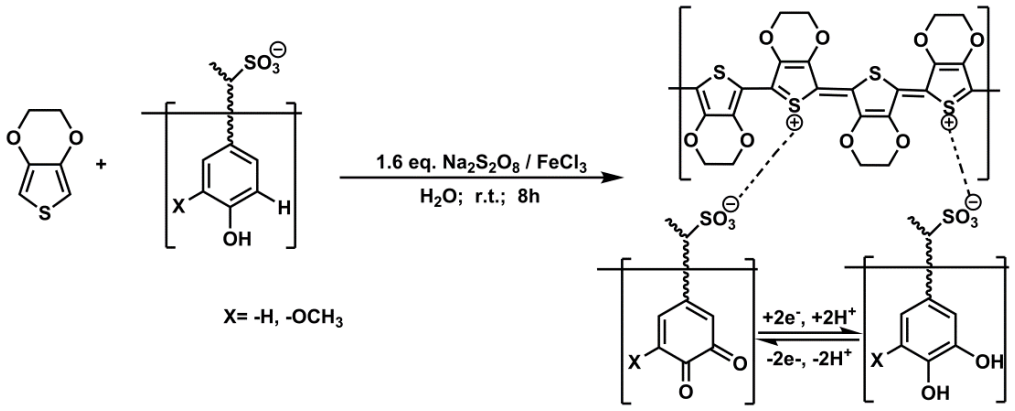

Figure 3.1. Oxidative chemical polymerization of PEDOT/Lig composite.

PEDOT/Lig composites were synthesized via chemical oxidative polymerization of EDOT in presence of lignin, using an iron redox agent in a catalytic amount and a primary oxidant, sodium persulfate (Figure 3.1).

The synthetic strategy of preparation of PEDOT/Lig composite was carried out containing different EDOT/Lignin mass ratios (6:1; 7:4; 3:2; 5:4; 2:3; 1:3). The final

PEDOT/lignin ratio was calculated from lignin quantification by UV-Vis.[16] First, a lignin calibration curve was obtained by measuring the absorbance at 202 nm of different lignin standards with concentrations between 0.0025 and 0.20 g/L (Figure 3.2). Then, the absorbance of PEDOT/lignin dispersions was measured and the lignin concentration on the dispersion was calculated with the calibration curve. The calculated final ratio of the composites and the relation between the feed and product ratios are shown in Figure 3.3b, the product ratio is quite similar to the initial feed. When PEDOT is synthesized through oxidative polymerization with oxidizing agents such as persulfate or iron (III) salts, the typical molecular weight of PEDOT is not higher than 1000 to 2500 Da (6-18 repeating units), therefore, we assume that the molecular weight of PEDOT molecules in the composites is in the same range.[17]

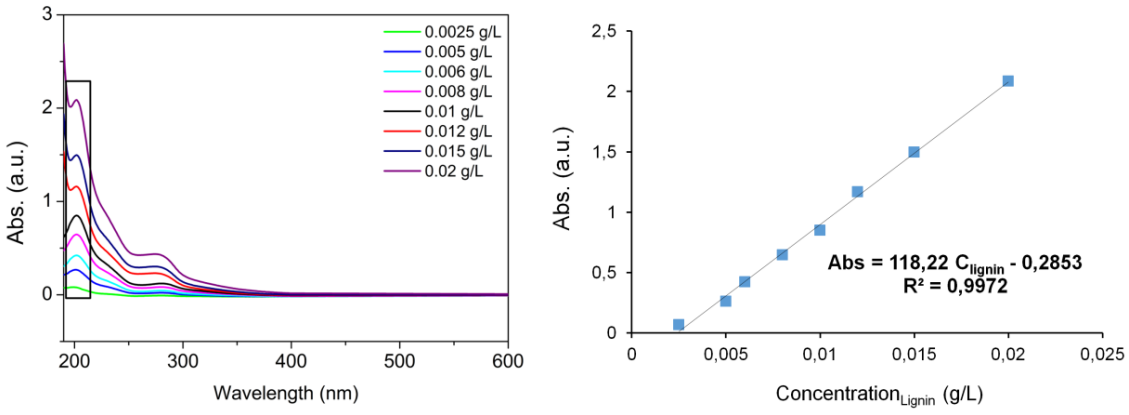

Figure 3.2. Calibration curve of lignin at 202 nm wavelength.

The formation of PEDOT/lignosulfonate composites might be understood as a rearrangement and clustering process during the polymerization synthesis giving rise to easier charge transport. Moreover, as sulfonates in lignin carry negative charge, they are expected to act as a charge balancing counter-ion to the positively doped PEDOT chains facilitating the association of PEDOT chains with lignin via electrostatic interaction during the polymerization.

PEDOT/Lig composites can also be polymerized by electrochemical techniques such as galvanostatic conditions. Electrochemical polymerization offers some advantages over chemical polymerization, regarding the control of thickness and morphology of the deposited film. However, chemical polymerization has other clear advantages since it allows controlling the ratio between PEDOT and lignin in the final composites. Furthermore, it allows the production of PEDOT/Lig composites in large scale comparing to electrochemical routes. In the next sections, we will characterize the different PEDOT/Lig composites obtained by oxidative chemical polymerization.

3.3. Characterization of PEDOT/lignin composites

PEDOT/Lig composites synthesized by chemical oxidative polymerization were obtained in the form of dark blue aqueous dispersions, having different PEDOT/Lig ratios. The UV/Vis spectra of the resulting PEDOT/Lig dispersions (as well as, for reference, the spectra of lignin and EDOT) are shown in Figure 3.3a. The lignin-sulfonate spectrum has two distinctive peaks. The peak at 202 nm which is assigned to the conjugated C=C of the aromatic structure and another one at 280 nm which correspond to *p*-substituents in phenolic groups depending on

the different monolignols units (coumaryl, coniferyl and sinapyl) in lignin due to their electron donating character.[18,19] The absorption spectrum of PEDOT depends on the redox-state of the polymer. Neutral PEDOT has an absorption band at 600 nm, caused by π-π* transitions. On the other hand, the absorption spectra of doped PEDOT has absorption maxima located at 800 nm and ~1100 nm which are attributed to polaronic and bipolaronic states.[20] The absorbance spectra of PEDOT/Lig dispersions display transitions typical of both lignin (202, 283 nm) and doped PEDOT (800 nm, <1000 nm). The appearance of UV-Vis spectra thus confirms that EDOT has been successfully polymerized in presence of lignosulfonate, obtaining an oxidized PEDOT which is stabilized by lignosulfonate.

The EDOT monomer shows a maximum absorption at 260 nm, which shifts to higher wavelengths during the polymerization, as the π system conjugation is extended as the polymer is formed.[21] Since EDOT does not show absorption at 202 nm, all PEDOT/Lig spectra in Figure 3.3a have been normalized with respect to the lignin absorption peak at 202 nm. Therefore, the absorption intensity of the bands between 600 and 1300 nm reveals the relative proportion of PEDOT to Lignin in the dispersions. Inspection of the spectra accordingly allows us to confirm that a polymerization carried out with higher relative ratio of EDOT to lignosulfonate results in an increase of PEDOT band intensity.

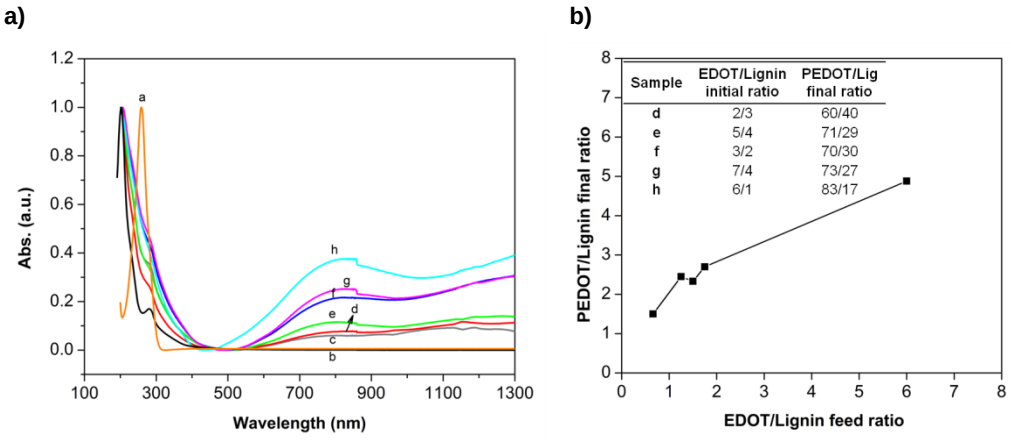

Figure 3.3. a) UV–Vis-NIR absorption spectra of EDOT (a), lignin (b) and normalized PEDOT/Lig composites, obtained from different weight ratios of EDOT/Lignin 1:3 (c); 2:3 (d); 5:4 (e); 3:2 (f); 7:4 (g); 6:1 (h). b) PEDOT/lignin final ratio vs. EDOT/lignin feed ratio. The inset shows a table with the summary of EDOT/lignin synthesis ratio, PEDOT/Lig final ratio calculated from lignin quantification by UV-Vis.

The thermal behaviour of PEDOT/Lig composites was investigated by thermogravimetric analysis (TGA), performed under nitrogen atmosphere, measuring the weight loss as a function of temperature (Figure 3.4). The signal of lignin alone is considered as a control in order to compare the different PEDOT/Lig composites.[12,22] TGA curves show that all the PEDOT/Lig composites are stable up to 250 ºC, similar to the control lignin. The most noticeable degradation occurs between 300 °C and 400 °C, and is attributed to the decomposition of PEDOT. The control lignin shows residual traces of 52% of the total mass however the residual traces decrease as the content of PEDOT increases. Therefore, the TGA results are consistent with the final PEDOT/lignin composition.

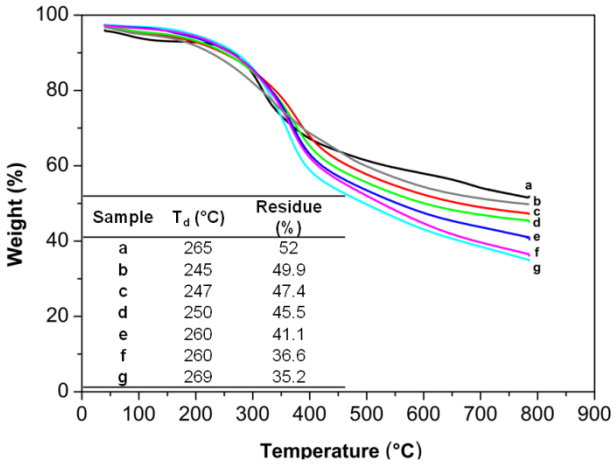

Figure 3.4. Thermogravimetric analysis (TGA) of lignin (a) and PEDOT/Lig composites, obtained from different weight ratios of EDOT and Lignin 1:3 (b); 2:3 (c); 7:4 (d); 3:2 (e); 7:4 (f); 6:1 (g). The inset shows a table with the degradation temperature (T_d) and residual mass obtained from TGA at a heating rate of 10 °C/min under nitrogen atmosphere.

FT-Infrared (FTIR) spectra of Lignin and 6:1, 3:2 PEDOT/Lig composites are shown in Figure 3.5. Lignin spectrum shows peaks at 1600 and 1505 cm^{-1} attributed to the vibrations of aromatic ring, and bands at 1460 and 1422 cm^{-1} related to the aromatic ring vibrations combined with methyl and methylene C-H deformations. A broad peak is observed at 1215 cm^{-1} due to C—C and C—O stretching vibrations merged aromatic ring stretching modes and a strong peak at 1040 cm^{-1} attributed to C—O—C stretching vibrations. These results are in agreement with the previously reported lignin spectra.[23] On the other hand, all PEDOT/Lig composites show similar spectra exhibiting bands related to both PEDOT and lignin structures. PEDOT/Lig composites show peaks at 1500, 1380 and 1340 cm^{-1} corresponding to aromatic

ring vibrations in lignin and thiophene ring. Bands at 1197, 1089, 1055 cm^{-1} are attributed to C—O—C stretching modes in the composites, and the peak at 838 cm^{-1} is related to C—S stretching vibration of thiophene ring. These results are consistent with electrochemically and chemically synthesized PEDOT.[24,25]

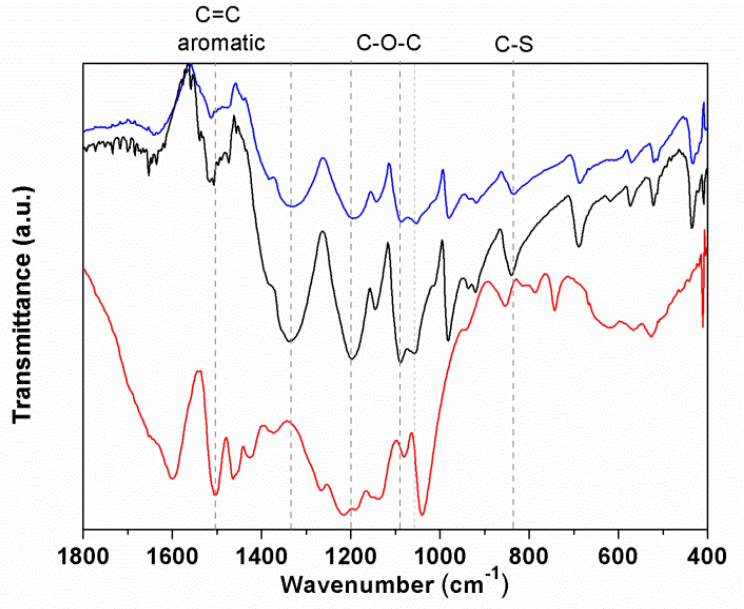

Figure 3.5. FTIR spectra of lignin (red line) and PEDOT/Lig composites of 6:1 (black line) and 3:2 (blue line) mass ratios.

The electrochemical performance of an electrode is largely dependent on the morphology and surface area of the electrode material. Therefore, Scanning Electron Microscopy (SEM) and Transmission Electron Microscopy (TEM) were used to investigate the

surface morphology of PEDOT/Lig composites. SEM images of the chemically polymerized biocomposites of 3:2 and 7:4 mass ratio exhibit a granular-spongy morphology (Figure 3.6a-b). PEDOT/Lig composite of 6:1 mass ratio shows the formation of aggregates because of the existence of higher content of PEDOT (Figure 3.6c). Figure 3.7 shows TEM images of the chemically polymerized PEDOT/Lig composites with (a) 3:2; (b) 7:4; (c) 6:1 EDOT:lignin mass ratios. TEM images reveal that PEDOT/Lig composites form aggregates of various sizes, the majority being 200-400 nm size. It seems that these aggregates consist of various tangles which have a PEDOT rich inner part and a lignin rich outer part.

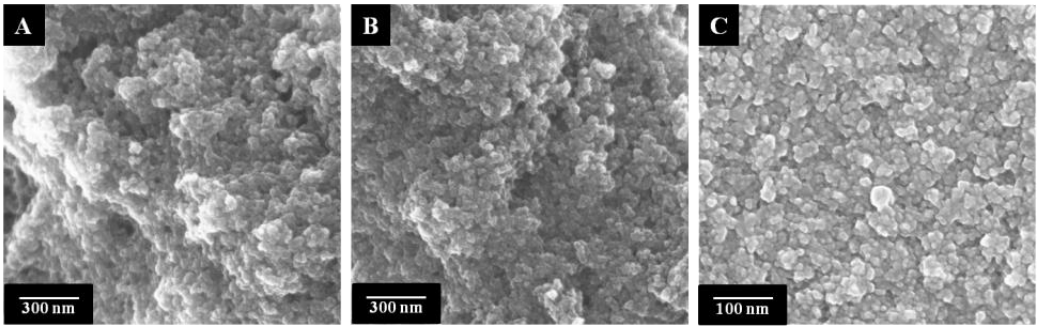

Figure 3.6. SEM images of PEDOT/Lig composites chemically polymerized with the following EDOT:lignin mass ratios: a) 3:2; b) 7:4 and c) 6:1.

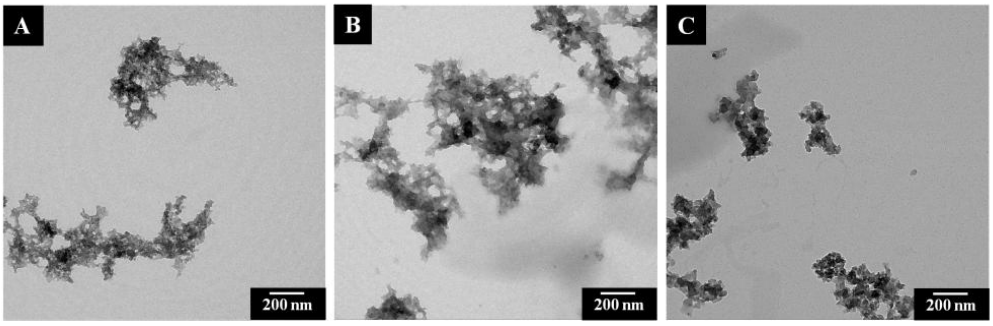

Figure 3.7. TEM images of PEDOT/Lig composites chemically polymerized with the following EDOT:lignin mass ratios a) 3:2; b) 7:4; c) 6:1.

We can therefore hypothesize that the influence of a larger content of lignin in the chemical polymerized biocomposites leads to greater roughness, leading to a larger surface area which provides more accessible electroactive ions during electrochemical processes.

3.4. Electrochemical characterization

The electrochemical characterization of PEDOT/Lig composite films was carried out in 0.1 M $HClO_4$ aqueous solution. The polymer films were prepared by casting the dispersions onto the working electrodes. Cyclic voltammetry measurements were performed on composites having different PEDOT/Lig ratios in order to examine the electrochemical behaviour and evaluate the charge storage properties. The voltage range was held from −0.2 to 0.8 V and a scan rate of 100 mV/s was employed. The resulting cyclic voltammograms are shown in Figure

3.8a. It is apparent that the electrochemical performance can be tuned by varying the PEDOT/Lig ratio. The cyclic voltammograms of composites show two characteristic redox regions. The first region corresponds to the PEDOT doped state (-0.2 to 0.35 V) and the second one corresponds to the quinone groups formed in lignin (ca 0.58 V). The sample where the content of lignin is three times higher than EDOT (1:3), showed no charge transport. This is probably due to the insulating character of lignin, which dominates the oxidative polymerization giving a non-conducting composite. The stored charge of quinones in lignin was estimated considering the integration area of the quinone peaks and the total charge which is stored in each PEDOT/Lig composites (Figure 3.8b), achieving an optimum relation for the 3:2 (40% of lignin), 7:4 (36% of lignin) and 5:4 (44% of lignin) ratio of PEDOT/Lig composites. The charge storing behaviour of 3:2 and 7:4 ratio of PEDOT/Lig composites exhibit comparable redox activity showing well defined redox peaks with higher capacity over all biocomposites electrode materials. Nevertheless, it is worth noticing the contribution of redox quinone activity in lignin for 5:4 ratio. As the content of PEDOT is higher than the content of lignin for the 6:1 ratio, the hydroquinone/quinone redox peaks of lignin decrease while PEDOT region increases. The increase of PEDOT content clearly shows typical capacitor performance with improved charge propagation.

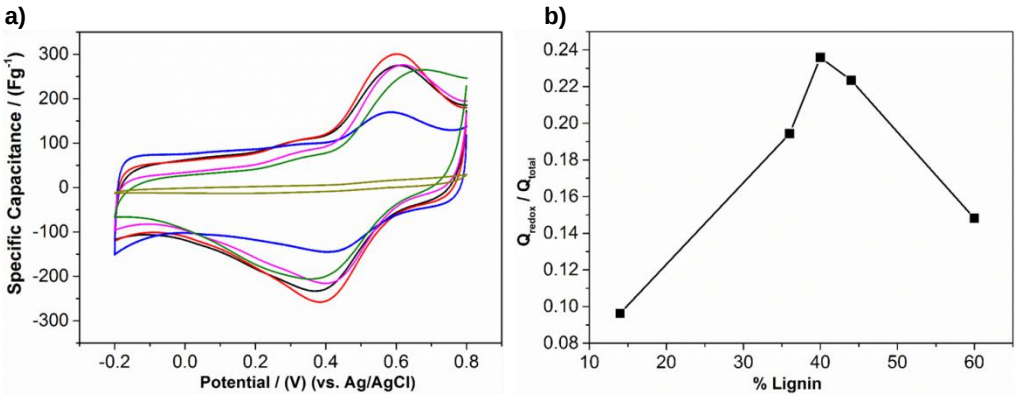

Figure 3.8. a) Cyclic voltammograms of drop-casted films of PEDOT/Lig composites at different mass ratios, 6:1 (blue line); 7:4 (black line); 3:2 (red line); 5:4 (pink line); 2:3 (green line); 1:3 (olive line) within the potential range of -0.2 V and 0.8 V at scan rate of 100 mV s^{-1} in 0.1 M $HClO_4$ aqueous solution. b) Ratio between charge of quinones and total charge in the PEDOT/Lig composites.

Given the electrochemical properties of PEDOT/Lig, the feed mass ratios 3:2, 7:4 and 6:1 were chosen to further analyze the redox activities of the composite materials. Figure 3.9 shows the galvanostatic charge/discharge curves of PEDOT/Lig composites performed at a current density of 1A g^{-1} within the potential window of 0.1 to 0.7 V. It can be clearly seen that the 3:2 and 7:4 PEDOT/Lig mass ratios have very similar specific charge values of 28.0 mAh g^{-1} and 27.6 mAh g^{-1}, respectively. In contrast, the 6:1 ratio has a specific charge of 18.5 mAh g^{-1}. The charge storage capacity can thus be modified by varying the PEDOT/Lig ratio. At the optimum content of lignin, the charge storage capacity of the conducting polymer/biopolymer composite is improved up to 40% compared to the 6:1 PEDOT/Lig ratio. Moreover the discharge curves show a plateau between 0.55 V and 0.35 V, which can be explained by the

Faradaic reactions of quinones. Furthermore, it is worth noting how the charge is stored following the capacitive behaviour of PEDOT.

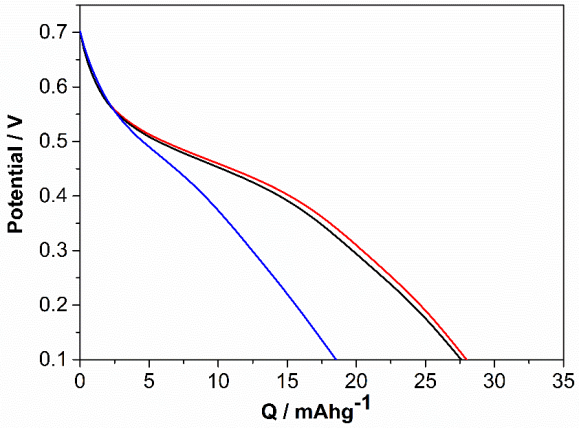

Figure 3.9. Galvanostatic discharge curves of PEDOT/Lig composite polymerized at different mass ratios, 6:1 (blue line); 7:4 (black line); 3:2 (red line); at a current density of 1A g^{-1}.

The discharge properties of each system at different current densities were also studied (Figure 3.10). As expected, the charge stored at 1 A g^{-1} is larger than at higher current densities, however PEDOT/Lig composites of mass ratios 6:1, 7:4 and 3:2 show a retention of 95%, 82% and 85% respectively at 16 A g^{-1}, suggesting a good rate capability of the biocomposite material.

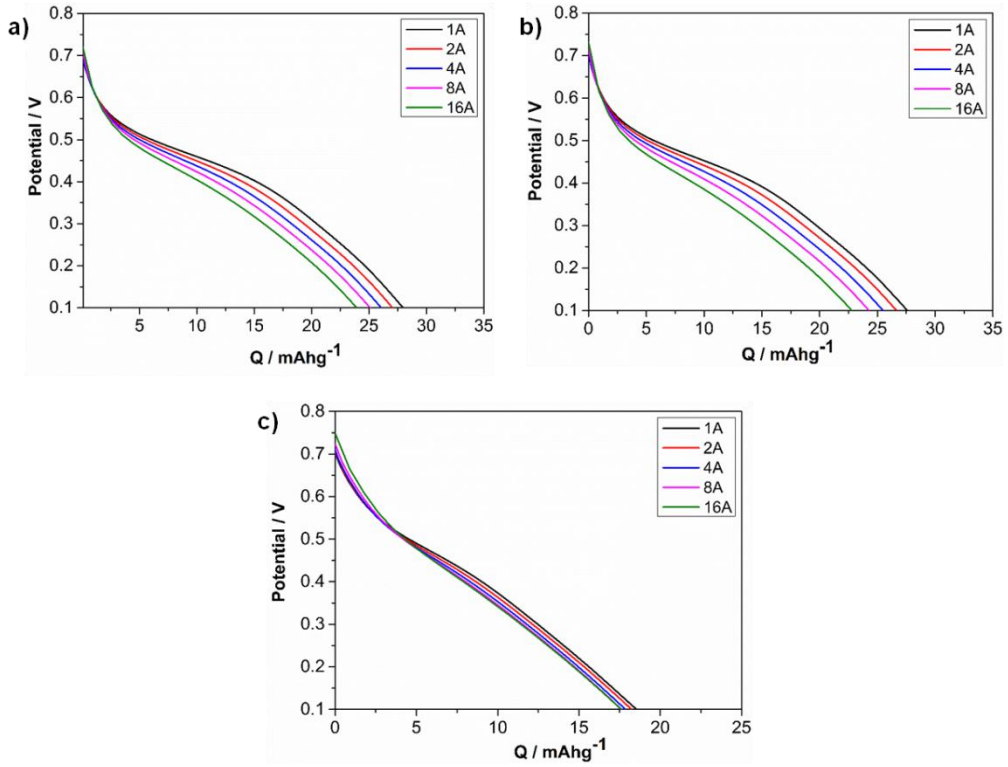

Figure 3.10. Discharge curves at different currents of PEDOT/Lig composites: a) 3:2, b) 7:4, c) 6:1.

Cycling stability is one of the most important parameters for the performance of a supercapacitor electrode. For this reason, the charge–discharge cycle life of PEDOT/Lig composites was tested applying potential from 0.1 to 0.7 V for up to 1000 cycles (Figure 3.11 and Figure 3.12). Upon cycling, the PEDOT/Lig composites showed a decrease in the initial capacitance, which was less than 20% after 1000 cycles. The main loss occurred during the first 100 cycles, as shown in Figure 3.11. After that the specific capacitance values of the

original capacitor were retained by more than 90%. This loss of capacity can be explained by degradation of the quinone groups in lignin, resulting in a loss of redox activity. The specific capacitance and capacitance retention upon cycling are shown in Figure 3.12. PEDOT/Lig composites for the mass ratios of 6:1, 7:4 and 3:2 show specific capacitances of 100 F g^{-1}, 135 F g^{-1} and 138 F g^{-1} respectively at a discharge current of 8 A g^{-1} (Figure 3.12). The capacity retention at 8 Ag^{-1} current density after 1000 cycles was 87 %, 83 % and 83 % for mass ratios of 6:1, 7:4 and 3:2.

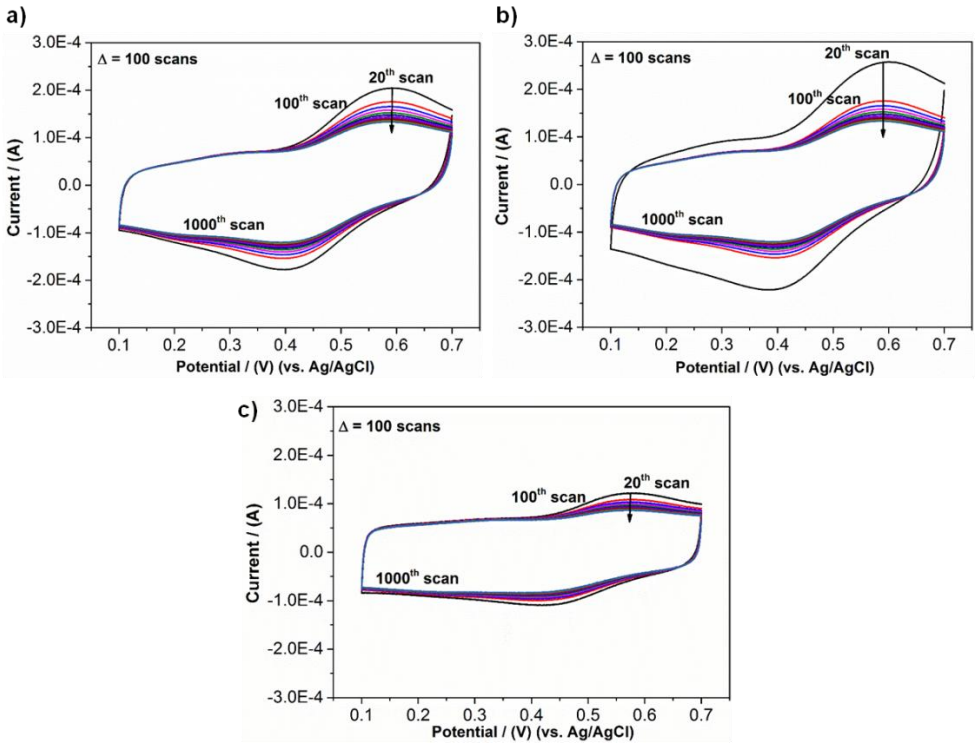

Figure 3.11. Cyclic voltammograms of PEDOT/Lig composites polymerized at different mass ratios: a) 3:2, b) 7:4, c) 6:1 within the potential range of 0.1 V and 0.7 V at scan rate of 100 mV s^{-1}.

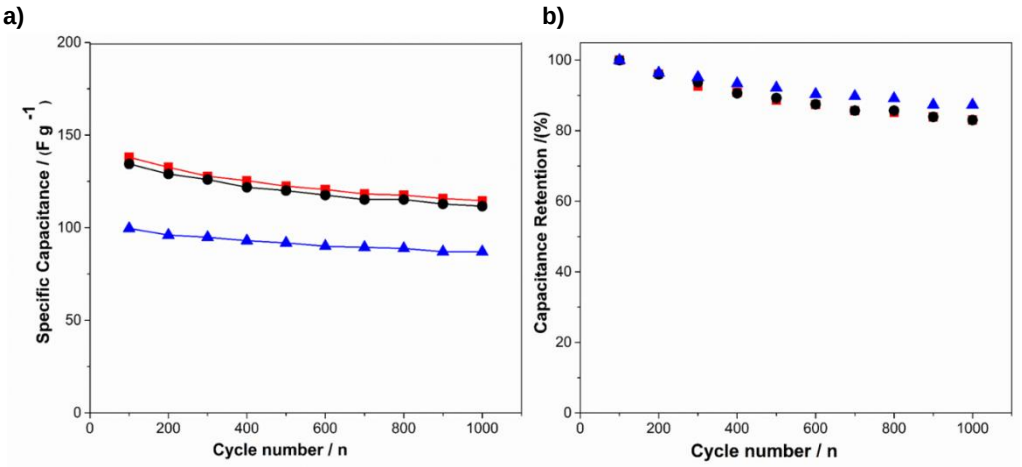

Figure 3.12. a) Specific capacitance and b) capacitance retention over 1000 cycles of PEDOT/Lig composites polymerized at different mass ratios 6:1 (blue), 7:4 (black), and 3:2 (red), measure at a current density of 8 Ag^{-1}.

3.5. Self-discharge

Self discharge is one of the main problems of conducting polymers and energy storage devices made out of them.[26,27] Figure 3.13 shows self-discharge with open circuit potential in a three electrode system, decaying to ca. 0.40 V for the three PEDOT/Lig composites after 16 h. The maximum self discharge is observed for PEDOT/Lig composite with highest PEDOT content (6:1). Consequently, we can say that the incorporation of lignin to the composites alleviates the self-discharge problems of conducting polymer electrodes.

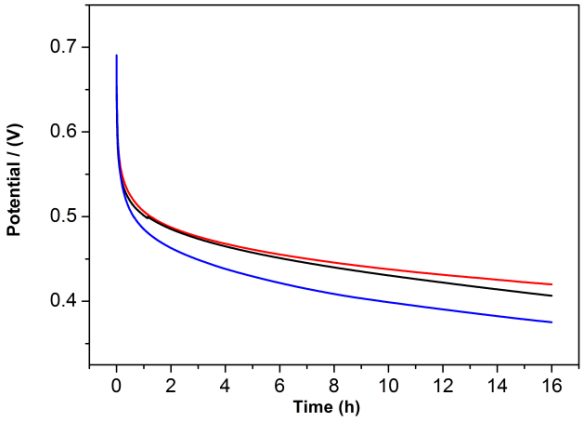

Figure 3.13. Self-discharge behaviour of PEDOT/Lig composites polymerized at different mass ratios 6:1 (blue), 7:4 (black), and 3:2 (red).

3.6. Influence of pH

The electrochemistry of quinone moieties is pH dependent due to the H^+ exchange during redox reactions. Hence, it is possible to confirm the reversibility of hydroquinone/quinone conversion during the redox process by testing it within a broad pH range. The redox activity of PEDOT/Lig composite (polymerized at 3:2 ratio) across different pH (over the pH range 1.0-8.0) as measured by cyclic voltammetry is shown in Figure 3.14. It was observed that the peak potentials are shifted negatively with the increase of pH, while no significant decrease of peak current was observed at higher pH. The linear relationship between the peak potential and the pH value has a slope of -0.057 V/pH, very close to the theoretical Nernstian value.[7] Taken together, these data indicate that the redox behaviour of

PEDOT/Lig electrodes is governed by two-electron two-proton processes that oxidize hydroquinones into quinones.

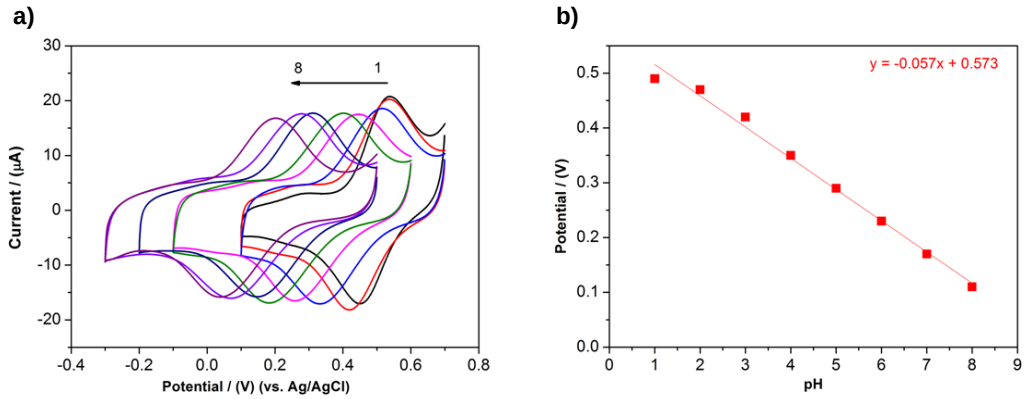

Figure 3.14. a) Cyclic voltammograms of PEDOT/Lig composites polymerized at 3:2 mass ratio at different pHs (1.0 to 8.0) and b) corresponding calibration curve of potential versus pH.

3.7. Comparative analysis between chemically and electrochemically polymerized PEDOT/lignin composites

PEDOT/Lig composites can be also polymerized by electrochemical techniques such as galvanostatic conditions, as we have recently reported.[28] The quality of the electropolymerized conducting polymer layer is usually higher compared to that obtained after casting the dispersions. This is noticeable when comparing the specific capacitance values of

electrochemically and chemically prepared composites. A comparison of the performance of the chemically and electrochemically polymerized PEDOT/Lig composites together with bare PEDOT is shown in Figure 3.15. The highest specific capacitance of electrochemically polymerized composites was found to be 170 F g^{-1} compared to the 138 F g^{-1} obtained for the best chemically polymerized composite. It is worth to mention that in both cases enhanced specific capacitance values were obtained as compared to the standard PEDOT polymer (80.4 F g^{-1}). Both electrochemically and chemically polymerized PEDOT/Lig composites exhibit similar capacitance retention upon cycling, which was lower than the one observed for bare PEDOT. On the other hand, all PEDOT/Lig composites, whether obtained by chemical or electrochemical polymerization, showed similar self-discharge profiles, as well as comparable redox activity among different pH values (pH range 1.0-8.0).

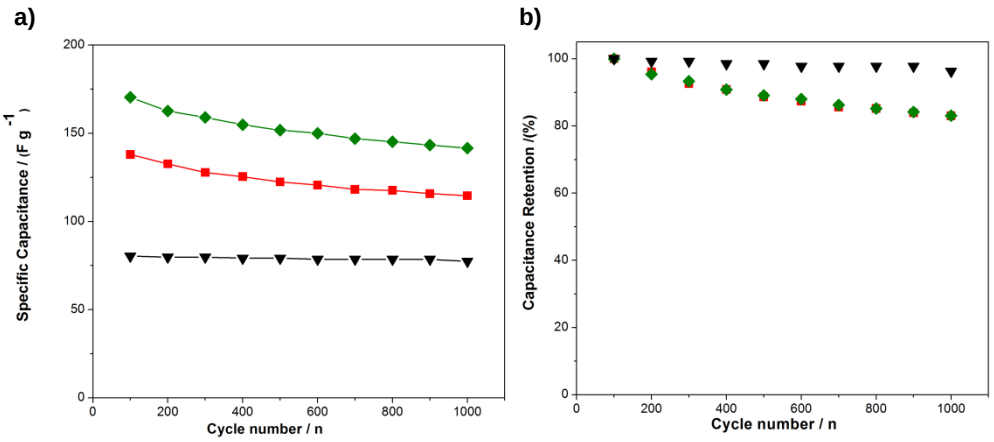

Figure 3.15. a) Specific capacitance and b) capacitance retention over 1000 cycles of electrochemically polymerized PEDOT (black) and PEDOT/Lig composites obtained by electrochemical polymerization (green) and chemical polymerization at 3:2 ratio (red) measure at a current density of 8 Ag^{-1}.

3.8. Conclusions

In conclusion, PEDOT/lignin composites were prepared by chemical polymerization of PEDOT in presence of lignin using different EDOT:lignin mass ratios. The characterization of the different PEDOT/Lig composites was presented, together with their electrochemical behaviour in aqueous solution, which demonstrated the importance of the addition of hydroquinone/quinone redox couple of lignin within the chemical structure of PEDOT to accomplish a significant improvement in charge storage properties.

The highest specific capacitance obtained for the chemically polymerized PEDOT/Lig biocomposite was 138 F g^{-1}, acquired for the composite polymerized at 3:2 mass ratio. All PEDOT/Lig composites retained 83 % of capacity after 1000 cycles and exhibit more than 95 % of coulombic efficiency. The evidence of higher stability values for PEDOT/Lig composites reinforces the idea that an important synergic effect exists between both polymers compared to the previously studied Polypyrrole/Lignin composites, where strong degradation was observed upon cycling. Hence, PEDOT/Lig composites exhibit higher capacitive performance which is advantageous over the performance of PEDOT without lignin for further applications.

The encouraging findings open up the possibility of scaling up PEDOT/Lig production thanks to the chemical synthesis, satisfying the requirements of inexpensiveness, environmental friendliness and easy processability for potential charge storage material in supercapacitors and supercabatteries.

3.9. Experimental part

3.9.1. Materials

3, 4-Ethylenedioxythiophene (EDOT, 99%, Acros organics), lignin derivative in the form of lignosulfonates (LC30, M_w=13400, MeadWestvaco), sodium persulfate ($Na_2S_2O_8$), iron (III) chloride ($FeCl_3$), acetonitrile (MeCN) and perchloric acid ($HClO_4$) (Sigma-Aldrich), were used as received. The aqueous solutions were prepared with ultrapure deionised water (Millipore).

3.9.2. Methods

The electrochemical characterization of PEDOT/Lig was evaluated by using the standard three-electrode configuration where a platinum wire, an Ag/AgCl (KCl sat.) and glassy carbon electrode (GC, with area of 0.07 cm^2) were used as counter (CE), reference (RE) and working electrodes, respectively (Bioanalytical Systems Inc. USA). The potential window of the cyclic voltammetry (CV) was cycled from - 0.2 V to 0.8 V vs Ag/AgCl by applying 20 cycles at 100 mV s^{-1}. On the other hand, the cycling stability was measured within the potential range of 0.1 V to 0.7 V vs Ag/AgCl at 100 mV s^{-1}. Galvanostatic charge-discharge cycles were measured applying different current densities (1-16 A g^{-1}) within the potential range of 0.1 V to 0.7 V. For the galvanostatic method, the specific capacitance (F g^{-1}) was determined from the change in potential and discharge time using the equation:

$$C = (I \Delta t)/(m \Delta E)$$

where I is the charge–discharge current, Δt is the time for discharge, m is the mass of the active material and ΔE is the potential change during discharge.

The calculation of the capacitance was based on the mass of the whole PEDOT/lignin composite obtained by balance weight determination.

UV-Vis spectra were acquired at room temperature on a PerkinElmer UV/Vis/NIR Lambda 950 spectrometer.

The thermal stability of the samples was investigated by thermo-gravimetric analysis (TGA) performed on a TGA Q500 from TA Instruments. Measurements were carried out by heating the sample at 10 °C min^{-1} under nitrogen atmosphere from room temperature to 800 °C.

Fourier Transform Infrared Spectroscopy (FTIR) measurements were performed at room temperature using a Thermo scientific model Nicolet 6700 FT-IR spectrometer, applying 10 scans in transmission mode using KBr pellets.

Scanning electron microscopy (SEM) images were collected using a Zeiss Leo 1550 Gemini Scanning Electron Microscope with an acceleration voltage of 5 kV. Before imaging the organic film (deposited onto gold evaporated onto a silicon wafer with titanium as an adhesive layer) was coated with a 15 Å W using a Leica EM SCD500 sputter coater.

Transmission electron microscopy (TEM) images were collected using a FEI TECNAI G2 20 TWIN TEM, operating at an accelerating voltage of 200 KeV in a bright-field image

mode. Samples were prepared by drop-casting the dispersions on a Carbon film Copper grid, which was previously hydrophilized by a glow discharge process.

3.9.3. Chemical synthesis of PEDOT/lignin composites

The polymerization of PEDOT/lignin was accomplished by drop-wise addition of an aqueous mixture of $Na_2S_2O_8$ (1.5 eq. EDOT) and a catalytic amount of $FeCl_3$ as oxidant to a solution of EDOT and lignin in water, yielding a dispersion of the biocomposite material. The oxidative polymerization was carried out under mechanical stirring at r.t. for 8 h and the concentration of the solution was kept constant at 1% (w/v). Instantaneously upon addition of the oxidant mixture, the EDOT/Lignin solution turned from brownish to deep blue coloured solution. Finally, the obtained PEDOT/Lig dispersions were dialyzed with deionised water for 48 hours using a 1000 g/mol cut-off membrane and freeze-dried, yielding PEDOT/Lig as a dark bluish powder. The overall yield of the polymerization was 85 %.

3.9.4. Electrode preparation

200 µl of homogeneous mixtures of the different chemically polymerized PEDOT/Lig materials were deposited by drop casting onto glass, dried in the oven and finally weighed using balance (Sartorius BP 210D). Afterwards, 1 µl of homogeneous dispersion was deposited by drop-casting onto the prior polished GC electrodes. The deposited mass of the different PEDOT/Lig solutions were 8.6 µg (6:1), 10.9 µg (7:4), 7.9 µg (3:2), 8.0 µg (5:4), 7.5 µg (2:3) and 5.5 µg (1:3), respectively.

3.10. References

(1) Zhang L., Liu Z., Cui G., Chen L. Biomass-derived materials for electrochemical energy storages. *Prog. Polym. Sci.* **2015**;43:136-64.

(2) Milczarek G. Lignosulfonate-Modified Electrodes: Electrochemical Properties and Electrocatalysis of NADH Oxidation. *Langmuir*. **2009**;25:10345-53.

(3) Huskinson B., Marshak M. P., Suh C., Er S., Gerhardt M. R., Galvin C. J., Chen X., Aspuru-Guzik A., Gordon R. G., Aziz M. J. A metal-free organic-inorganic aqueous flow battery. *Nature*. **2014**;505:195-8.

(4) Kim Y. J., Wu W., Chun S.-E., Whitacre J. F., Bettinger C. J. Catechol-Mediated Reversible Binding of Multivalent Cations in Eumelanin Half-Cells. *Adv. Mater.* **2014**;26:6572-9.

(5) Milczarek G., Inganäs O. Renewable Cathode Materials from Biopolymer/Conjugated Polymer Interpenetrating Networks. *Science*. **2012**;335:1468-71.

(6) Kim S.-K., Kim Y. K., Lee H., Lee S. B., Park H. S. Superior Pseudocapacitive Behavior of Confined Lignin Nanocrystals for Renewable Energy-Storage Materials. *ChemSusChem*. **2014**;7:1094-101.

(7) Milczarek G., Nowicki M. Carbon nanotubes/kraft lignin composite: Characterization and charge storage properties. *Mater. Res. Bull.* **2013**;48:4032-8.

(8) Okuzaki H., Suzuki H., Ito T. Electromechanical Properties of Poly(3,4-ethylenedioxythiophene)/Poly(4-styrene sulfonate) Films. *J. Phys. Chem. B*. **2009**;113:11378-83.

(9) Louwet F., Groenendaal L., Dhaen J., Manca J., Van Luppen J., Verdonck E., Leenders L. PEDOT/PSS: synthesis, characterization, properties and applications. *Synth. Met.* **2003**;135–136:115-7.

(10) Groenendaal L., Jonas F., Freitag D., Pielartzik H., Reynolds J. R. Poly(3,4-ethylenedioxythiophene) and Its Derivatives: Past, Present, and Future. *Adv. Mater.* **2000**;12:481-94.

(11) Charba A., Mumtaz M., Brochon C., Cramail H., Hadziioannou G., Cloutet E. Preparation of Water-Free PEDOT Dispersions in the Presence of Reactive Polyisoprene Stabilizers. *Langmuir*. **2014**;30:12474-82.

(12) Roy S., Fortier J. M., Nagarajan R., Tripathy S., Kumar J., Samuelson L. A., Bruno F. F. Biomimetic Synthesis of a Water Soluble Conducting Molecular Complex of Polyaniline and Lignosulfonate. *Biomacromolecules*. **2002**;3:937-41.

(13) Harman D. G., Gorkin Iii R., Stevens L., Thompson B., Wagner K., Weng B., Chung J. H. Y., in het Panhuis M., Wallace G. G. Poly(3,4-ethylenedioxythiophene):dextran sulfate (PEDOT:DS) – A highly processable conductive organic biopolymer. *Acta Biomater.* **2015**;14:33-42.

(14) Yang C., Liu P. Water-Dispersed Conductive Polypyrroles Doped with Lignosulfonate and the Weak Temperature Dependence of Electrical Conductivity. *Ind. Eng. Chem. Res.* **2009**;48:9498-503.

(15) Heinze J., Frontana-Uribe B. A., Ludwigs S. Electrochemistry of Conducting Polymers—Persistent Models and New Concepts. *Chem. Rev.* **2010**;110:4724-71.

(16) Lee R. A., Bédard C., Berberi V., Beauchet R., Lavoie J.-M. UV–Vis as quantification tool for solubilized lignin following a single-shot steam process. *Bioresour. Technol.* **2013**;144:658-63.

(17) Kirchmeyer S., Reuter K. Scientific importance, properties and growing applications of poly(3,4-ethylenedioxythiophene). *J. Mater. Chem.* **2005**;15:2077-88.

(18) Li Z., Ge Y. Extraction of lignin from sugar cane bagasse and its modification into a high performance dispersant for pesticide formulations. *J. Braz. Chem. Soc.* **2011**;22:1866-71.

(19) Cyril Heitner D. D., John Schmidt. *Lignin and Lignans: Advances in Chemistry*: CRC Press; 2010.

(20) Park B.-w., Yang L., Johansson E. M. J., Vlachopoulos N., Chams A., Perruchot C., Jouini M., Boschloo G., Hagfeldt A. Neutral, Polaron, and Bipolaron States in PEDOT Prepared by Photoelectrochemical Polymerization and the Effect on Charge Generation Mechanism in the Solid-State Dye-Sensitized Solar Cell. *J. Phys. Chem. C*. **2013**;117:22484-91.

(21) Apperloo J. J., Groenendaal L. B., Verheyen H., Jayakannan M., Janssen R. A. J., Dkhissi A., Beljonne D., Lazzaroni R., Brédas J.-L. Optical and Redox Properties of a Series of 3,4-Ethylenedioxythiophene Oligomers. *Chem. Eur. J.* **2002**;8:2384-96.

(22) Lima R. B., Raza R., Qin H., Li J., Lindstrom M. E., Zhu B. Direct lignin fuel cell for power generation. *RSC Adv.* **2013**;3:5083-9.

(23) Ajjan F. N., Jafari M. J., Rebis T., Ederth T., Inganas O. Spectroelectrochemical investigation of redox states in a polypyrrole/lignin composite electrode material. *J. Mater. Chem. A*. **2015**;3:12927-37.

(24) Kvarnström C., Neugebauer H., Ivaska A., Sariciftci N. S. Vibrational signatures of electrochemical p- and n-doping of poly(3,4-ethylenedioxythiophene) films: an in situ attenuated total reflection Fourier transform infrared (ATR-FTIR) study. *J. Mol. Struct.* **2000**;521:271-7.

(25) Zhan L., Song Z., Zhang J., Tang J., Zhan H., Zhou Y., Zhan C. PEDOT: Cathode active material with high specific capacity in novel electrolyte system. *Electrochim. Acta*. **2008**;53:8319-23.

(26) Novák P., Müller K., Santhanam K. S. V., Haas O. Electrochemically Active Polymers for Rechargeable Batteries. *Chem. Rev.* **1997**;97:207-82.

(27) Olsson H., Jämstorp Berg E., Strømme M., Sjödin M. Self-discharge in positively charged polypyrrole–cellulose composite electrodes. *Electrochem. Commun.* **2015**;50:43-6.

(28) Ajjan F. N., Casado N., Rebis T., Elfwing A., Solin N., Mecerreyes D., Inganas O. High performance PEDOT/lignin biopolymer composites for electrochemical supercapacitors. *J. Mater. Chem. A*. **2016**;4:1838-47.

CHAPTER 4

Electrochemical behaviour of PEDOT/lignin in ionic liquid electrolytes: suitable cathode/electrolyte system for sodium batteries

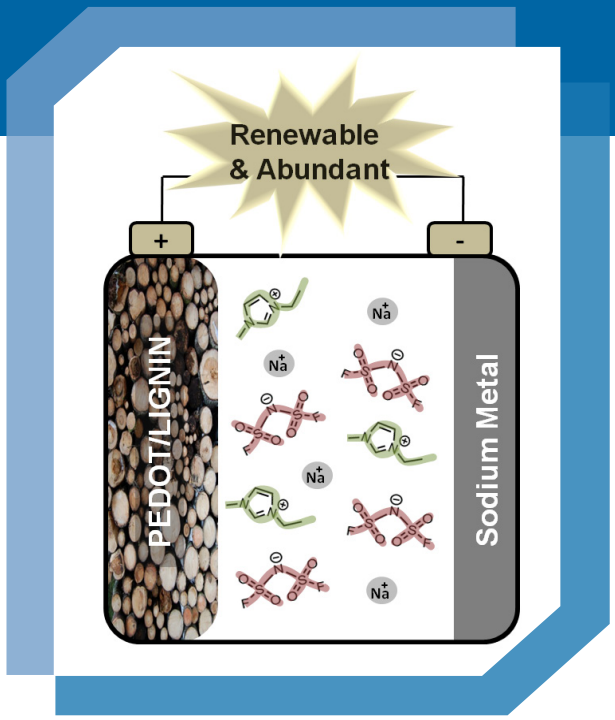

Chapter 4. Electrochemical behaviour of PEDOT/lignin in ionic liquid electrolytes: suitable cathode/electrolyte system for sodium batteries

4.1. Introduction

In the previous chapter, a new organic electrode material based on PEDOT conducting polymer and lignin biopolymer was developed, named PEDOT/lignin. Redox active polymers are good candidates to meet the challenging demand of green batteries due to their low toxicity, low cost, processability and recyclability.[1,2] However, they also present some drawbacks such as low energy density, self-discharge and low cyclability.

Recently, various conducting polymer/lignin composites have been developed and many studies have focused on the improvement of their charge storage properties,[3-6] however, their electrochemical behaviour has been just investigated in aqueous acidic media such as 0.1 M $HClO_4$[7] and 0.5 M H_2SO_4.[6] For this reason, these materials have only been applied so far in supercapacitors[6] and electrochemical sensors.[8]

Ionic liquids (ILs) have been widely investigated as electrolyte materials for batteries due to the outstanding properties and structure versatility. In general, ionic liquids show good ionic conductivity, low vapour pressure, low flammability, excellent chemical and thermal stability and wide electrochemical window.[9,10] They are being investigated as electrolytes not only in lithium batteries but also in other technologies such as supercapacitors, sodium batteries, flow batteries or metal air batteries.

Sodium secondary batteries have gained great interest due to the lower price and significantly greater abundance of sodium compared to lithium. Imidazolium and pyrrolidinium based ILs have been studied as potential electrolytes for sodium batteries, which demonstrated sodium deposition and dissolution with good efficiency.[11,12] Moreover, conducting polymers have been proven to be good electroactive materials for sodium batteries due to their flexible structure to reversibly host Na ions.[13]

The goal of this chapter is to investigate the electrochemical behaviour of PEDOT/lignin biopolymers in a series of imidazolium and pyrrolidinium-based ionic liquids. The effects of the nature of the ionic liquid, type of cation/anion, water and sodium salt addition are investigated in detail, in order to achieve the best electrode/electrolyte combination. It is expected that the use of ionic liquids as electrolyte in comparison to the studied aqueous acidic solutions will provide lower ionic conductivity but an enhancement of the electrochemical and thermal stability of the device, as well as a higher output voltage.[14] Previous works indicate a good electrochemical behaviour of both PEDOT and quinone/hydroquinone moieties in ionic liquids, showing reversible redox processes in aprotic ionic liquids.[15-17] The final goal of this chapter is to demonstrate the concept of a new battery cell using PEDOT/lignin as cathode material, the

optimized ionic liquid as electrolyte and a sodium anode. To the best of our knowledge this is the first conducting polymer/lignin sodium battery. We envisioned that this cell configuration could lead to high cycling stabilities and satisfactory storage capacities, with an average voltage higher than 2.5 V.

4.2. Selection of PEDOT/lignin composite

Figure 4.1 shows the chemical structure of PEDOT/lignin polymer and the ionic liquids investigated in this chapter. PEDOT/lignin composites were obtained by oxidative polymerization as in the previous chapter, but it has to be mentioned that the lignin used in this chapter comes from another supplier. As lignins are polyphenolic compounds with no exact regular structure and varying chemical and physical properties depending on the biological source,[18] the final PEDOT/lignin properties will not be totally identical to the previous ones. In this case, PEDOT/lignin composites of two different weight ratios, 80/20 (PEDOTLig8020) and 60/40 (PEDOTLig6040), have been investigated in a series of 4 ionic liquids composed of the combination of an imidazolium ($EMIm^+$) and pyrrolidinium ($BMPyr^+$) cation with bis(trifluoromethylsulfonyl)imide ($TFSI^-$) and bis(fluorosulfonyl)imide (FSI^-) anion.

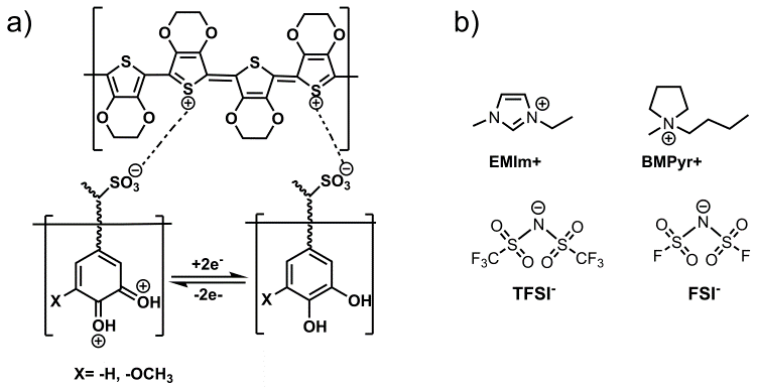

Figure 4.1. Chemical structure of a) PEDOT/lignin biopolymer and b) cationic and anionic species of the ionic liquids used in this chapter.

First, the electrochemical properties of PEDOT/lignin composites were compared to their single constituents, PEDOT and lignin, in BMPyrTFSI ionic liquid. Electrochemical stability of the biocomposites was studied by subsequent scans. Figure 4.2 shows the 20th cycle corresponding to PEDOTLig8020, PEDOTLig6040, PEDOT and lignin in BMPyrTFSI (Figure 4.2a-b) and EMImFSI (Figure 4.2c-d) ionic liquids. PEDOT/lignin composites exhibit three oxidation peaks, A_1-A_3, and three reduction processes C_1-C_3. The first oxidation process in BMPyrTFSI for PEDOTLig8020 at -0.90 V (A_1) is not very pronounced, which is followed by another at -0.30 V (A_2) and the third one at 0.90 V (A_3). Comparing to the single constituents we can observe that A_2 corresponds to the oxidation of PEDOT chains, while A_3 is attributed to the oxidation of quinone/hydroquinone groups in lignin. The anodic process A_1, which is not presented in the single constituents CVs, is attributed to the oxidation of PEDOT as it was observed previously in EMImTFSI.[19] In the cathodic scan, the peak at 0.5 V (C_3) corresponds

to the reduction of hydroquinone groups, while the peaks at -0.3 V (C_2) and -1.1 V (C_1) are related to the reduction of PEDOT chains in the composite. PEDOT presents a broad oxidation and reduction peak at -0.3 V and -0.5 V, respectively. In this case, the potential was limited to 0.5 V to avoid oxidative breakdown of PEDOT polymer. Lignin shows an oxidation peak at 0.7 V and two reduction peaks at 0.45 V and -0.6 V, confirming that the reaction mechanism of quinone/hydroquinone groups in lignin can take place in aprotic ionic liquid such as BMPyrTFSI. These redox potentials are similar to the ones reported for hydroquinone in $BMImBF_4$ ionic liquid.[17] Both PEDOT/lignin composites present enhanced electroactivity and electrostability as compared to both constituents. A similar electrochemical response was obtained in EMImFSI ionic liquid (Figure 4.2c-d). This result demonstrates that the synergic combination between lignin and conducting polymers is also seen when ionic liquids are used as electrolytes, as observed with acidic aqueous electrolyte.[5]

Table 4.1. Anodic and cathodic potentials of the polymers investigated in BMPyrTFSI.

Polymer	A_1 (V)	A_2 (V)	A_3 (V)	C_1 (V)	C_2 (V)	C_3 (V)
PEDOTLig8020	-0.90	-0.30	0.90	-1.1	-0.30	0.50
PEDOTLig6040	-0.80	0.0	0.93	-0.95	-0.15	0.50
PEDOT		-0.25			-0.50	
Lignin			0.70		-0.60	0.45

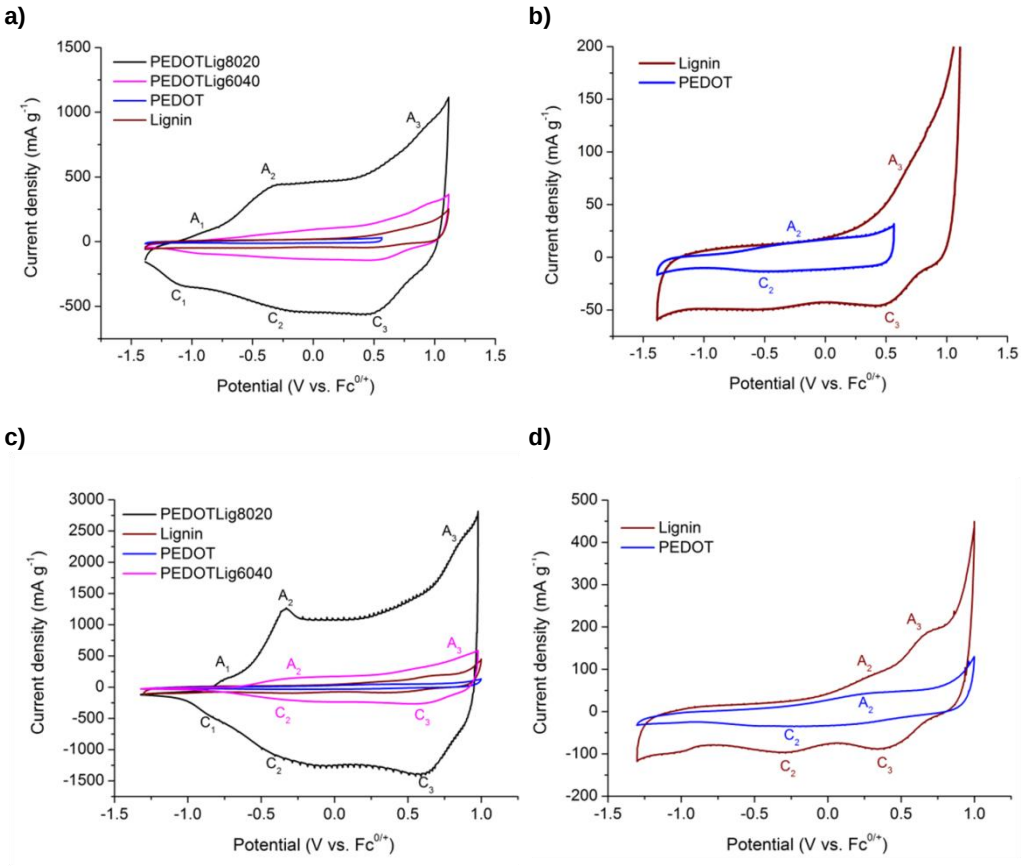

Figure 4.2. Cyclic voltammograms of PEDOTLig8020, PEDOTLig6040, PEDOT and Lignin-modified GC electrodes in BMPyrTFSI (a) and EMImFSI (c). Magnification of Lignin and PEDOT cyclic voltammograms in BMPyrTFSI (c) and EMImFSI (d). Cycle number 20. Scan rate: 20 mV s^{-1}.

As clearly observed, the presence of lignin in the biocomposites provides an extra redox process increasing the specific capacity of the PEDOT electrodes. However, it is noticeable that the current density of PEDOTLig8020 is considerately higher than PEDOTLig6040. In order to explain this result, it needs to be taken into account that the morphology and surface area can also play an important role affecting the electrochemical properties. Thus, Scanning Electron Microscopy (SEM) was used to study the surface morphology of the composites, and compared to the single constituents PEDOT and lignin (Figure 4.3). PEDOT (Figure 4.3a) presents granular-cauliflower type morphology, while a smoother solid like morphology was observed for lignin (Figure 4.3b). The morphology of the PEDOT/lignin composites depends on the weight ratio of the constituents and thus a more granular-cauliflower morphology is attained for PEDOTLig8020 (Figure 4.3c) as compared to PEDOTLig6040 (Figure 4.3d). Therefore, two competitive effects were observed in our PEDOT/lignin composites. On the one hand, the presence of lignin provides an extra redox process increasing the specific capacity of the electrodes. On the other hand, an increase of lignin in the composites leads to lower surface area, decreasing the accessible electroactive sites of the biocomposite.

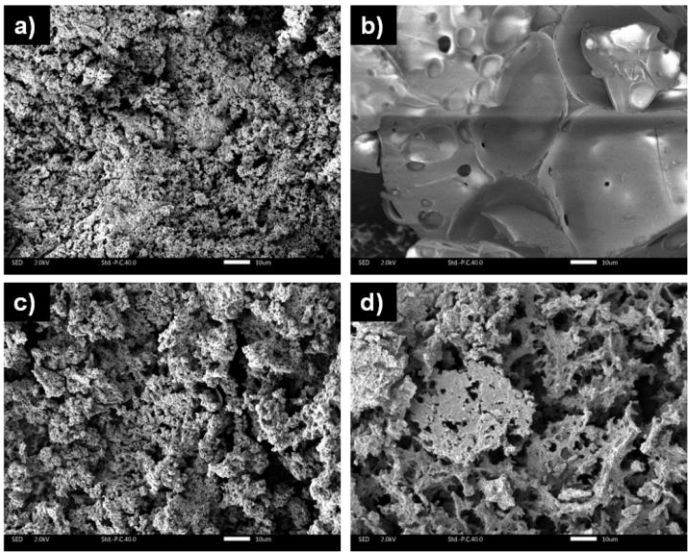

Figure 4.3. SEM images of a) PEDOT; b) Lignin; c) PEDOTLig8020 and d) PEDOTLig6040 powders.

4.3. Electrochemical characterization of PEDOTLig8020 in ionic liquids

Due to the superior redox activity in terms of current density, PEDOTLig8020 was chosen to study its electrochemical behaviour in a series of 4 different ionic liquids. Figure 4.4 shows the cyclic voltammograms of PEDOTLig8020 in pyrrolidinium and imidazolium-based ionic liquids with $TFSI^-$ and FSI^- anions. In all the cases, PEDOTLig8020 presents three redox processes (in pyrrolidinium ionic liquids oxidation reactions at -0.90 V, -0.35 V and 0.90 V and reduction reactions at 0.5 V, -0.3 V and -1.1 V). At first glance, an increase of the current density is observed in every cycle. This is clearly seen in Figure 4.4 when comparing cycles 1, 4, 12 and 20 where an increased current density is noticeable. This is associated, as discussed

below, to the activation of the film layer during the ion exchange occurring throughout the electrochemical cycling. This behaviour was previously observed for PEDOT in ionic liquids.[20] This increase of electroactivity of PEDOT films should be due to an expansion of the closed polymer structure that it is provoked by the consecutive redox processes. This indicates better swelling of the polymer and faster ion transport after long cycling. It is well known that during oxidation and reduction the polymer swells due to the transport of cations or anions of the ionic liquid that might enter the structure to compensate the charges. So the cycling leads to more active sites within the polymer which become available for the redox processes. It is important to mention that the initial counter anions of PEDOT/lignin after the synthesis are sulfonate groups. Thus, it seems that the exchange of these anions by the dominant bulky cation and anion combinations of the ionic liquids needs some activating cycles. It is worth noting that swelling of the PEDOT/lignin biocomposites by resting in the ionic liquid for three hours without cycling is not enough to activate the material (Figure 4.5).

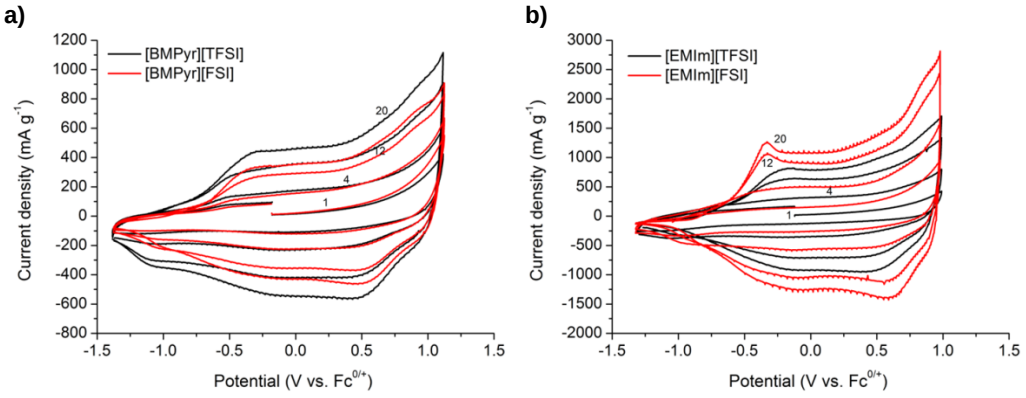

Figure 4.4. Cyclic voltammograms of PEDOTLig8020 modified GC electrodes in a) BMPyrTFSI and BMPyrFSI; b) EMImTFSI and EMImFSI ionic liquids. Cycle number 1, 4, 12 and 20. Scan rate: 20 mV s^{-1}.

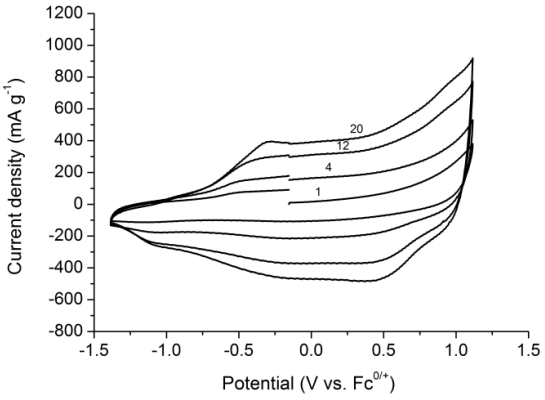

Figure 4.5. Cyclic voltammograms of PEDOTLig8020 modified GC electrodes in BMPyrTFSI, after resting 3 hours. Cycle number 1, 4, 12 and 20 at 20 mV s^{-1} scan rate.

When comparing the different ionic liquids, greater current density is seen when the cation is imidazolium (Figure 4.4b) as compared to pyrrolidinium in the electrolyte mixture (Figure 4.4a). This fact could be related by the higher ionic conductivity and fluidity of the imidazolium vs. pyrrolidinium ionic liquids as will be explained later.[9] When comparing the anions, the results obtained for pyrrolidinium ionic liquids are slightly different than for imidazolium ionic liquids. In the case of pyrrolidinium, the first four scans are identical in BMPyrTFSI and BMPyrFSI ionic liquids. However with increasing number of scans the current density for the $TFSI^-$ IL increases to a higher extent as compared to the FSI^- analogue. In the case of imidazolium ionic liquids, the FSI^- analogue shows higher electroactivity compared to the $TFSI^-$ one.

This behaviour can be explained by analyzing the redox mechanism of conducting polymers. The principle of electro-neutrality in conducting polymers is ensured by the charge compensating anions incorporated or expelled from the polymer backbone during charge/discharge. This is formally expressed by Eq. 1 and Eq. 2

$$\{P\ (C^+A^-)_y\} \rightleftharpoons \{P^{n+},\ A_n^-,(C^+A^-)_{y-n}\} + nC^+ + ne^- \qquad (1)$$

$$\{P\ (C^+A^-)_y\} + nA^- \rightleftharpoons \{P^{n+},\ A_n^-,(C^+A^-)_y\} + ne^- \qquad (2)$$

where P is the neutral polymer, P^{n+} the oxidized polymer, C^+ the cation and A^- the anion. Several studies have proved that redox mechanism involves either the egress of cations and also the ingress of anions which strongly depends on the size of the ions.[21] During the oxidation process of the polymer, anions from the bulk are incorporated into the polymer, compensating the charge along the polymeric backbone.[22] In the case of big cations and small anions, the cation exchange is unexpected. Thus, due to the big size of pyrrolidinium cation (1.1 nm radius),[23] an anionic exchange will happen in the case of BMPyrTFSI and BMPyrFSI ionic liquids; given that the $TFSI^-$ (0.8 nm radius)[23,24] anions are bigger than FSI^- (0.3 nm radius),[24] they create more accessible sites during this exchange and as a result, the current increases in greater steps with $TFSI^-$ anion. In the case of ionic liquids the transport mechanism of the ion exchange also depends on the symmetry of the ionic liquid. Although, those mechanisms are not completely understood, it is known that in the case of imidazolium-based IL due to the planarity of the cation the intercalation into the conducting polymer is easier.[25] Moreover, the $EMIm^+$ cation has a smaller size (0.3 nm radius)[26] compared with the pyrrolidinium cation and $TFSI^-$ anions, moreover, it has been reported as the main diffusing

species for one of the redox mechanisms of PEDOT.[19] Therefore, in the case of pure EMImTFSI, the small $EMIm^+$ cation will be exchanged to establish the electroneutrality in the polymer. On the other hand, pyrrolidinium-based ionic liquid is less planar and bigger in size, and therefore we hypothesise that such cation will not be involved in the electroneutrality of the conducting polymer. Thus, the TFSI and FSI anions will be responsible for the ion exchange leading to lower current density, in comparison with the imidazolium-based systems. Furthermore, as shown in Figure 4.4b, the redox peaks are sharper and the current intensity is higher in EMImFSI than in EMImTFSI ionic liquid. This behaviour can be attributed to the higher fluidity and ionic conductivity of EMImFSI ionic liquid and the smaller ionic radius of FSI^-, which makes it a more mobile species.

4.4. Effect of water

Considering the higher current density, BMPyrTFSI and EMImFSI ionic liquids combined with PEDOTLig8020 were studied in further detail. It is known that quinone/hydroquinone electrochemistry is largely affected by the presence of protic compounds such as water.[27] Therefore, the influence of water on the electrochemical performance of PEDOTLig8020 was investigated by saturating the ionic liquid with water. The cyclic voltammograms obtained in dry (<75 ppm H_2O) and wet (5100 ppm H_2O) EMImFSI are shown in Figure 4.6. The presence of water reduces the electrochemical window by 0.5 V while the current density is doubled. The polymer film is swollen during the first cycles due to the water presence which increases the electrode active area. After the 5^{th} cycle, delamination and

subsequent dissolution diminishes the performance beyond this point (see inset in Figure 4.6). As dissolution of the electrode material in the electrolyte is a drawback to obtain good battery cycling performances, wet conditions were dismissed.

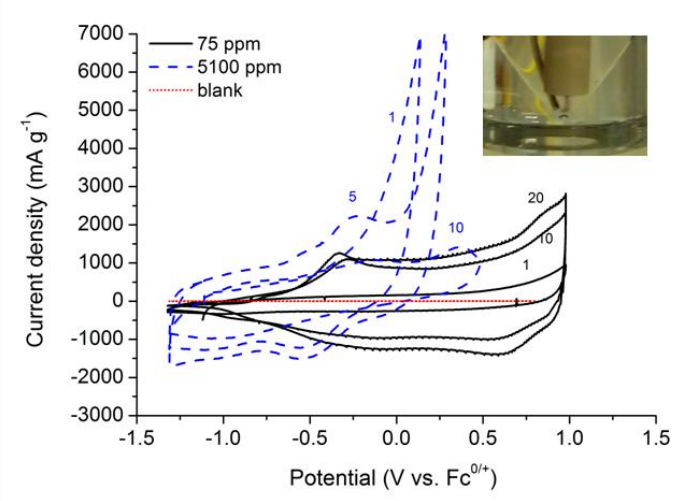

Figure 4.6. Cyclic voltammograms of GC blank electrode in wet EMImFSI and PEDOTLig8020 modified GC electrodes in dry (75 ppm H_2O) and wet (5100 ppm of H_2O) EMImFSI. Inset shows the dissolution of the polymer film from the working electrode to the electrolyte upon cycling.

4.5. Effect of sodium salt

The effect of sodium salt on the electrochemical properties of the biocomposites is crucial for well performing sodium batteries. Thus, different concentrations of sodium salts were dissolved in BMPyrTFSI and EMImFSI matching the IL anion (e.g. NaTFSI and NaFSI). Figure

4.7a depicts the 1st and 20th cyclic voltammograms of PEDOTLig8020 in BMPyrTFSI with 0, 10 and 20 mol% of NaTFSI. It is apparent that the current density decreases in presence of the salt, probably due to less favoured physicochemical performance.[11] However, the electrochemical properties of NaTFSI/BMPyrTFSI have been reported in the literature[11] exemplifying its feasibility for secondary sodium batteries even in the presence of large amount of sodium metal cation (e.g. 0.5 M NaTFSI). Redox potentials of PEDOTLig8020 are maintained and a slightly higher current density is obtained for higher NaTFSI content (20 mol %) in comparison with 10 mol % NaTFSI.

EMImFSI dissolves a larger amount of NaFSI; therefore, mixtures containing 20 and 30 mol% NaFSI were studied (Figure 4.7b). The same current density is observed for the 20 and 30 mol% NaFSI mixtures. However, the two redox potentials (A_1, A_2), which are related to PEDOT, are shifted to lower potentials only in the presence of 30 mol % NaFSI, while the process related to lignin is barely modified. Upon increasing the concentration of NaFSI in EMImFSI, the FSI^- molar concentration remains constant but the $EMIm^+$ concentration is reduced. Thus, these differences in the potential may be due to the decrease of concentration of the mobile $EMIm^+$ cation, which is consistent with the exchangeability of $EMIm^+$ during charging and discharging of the polymer.

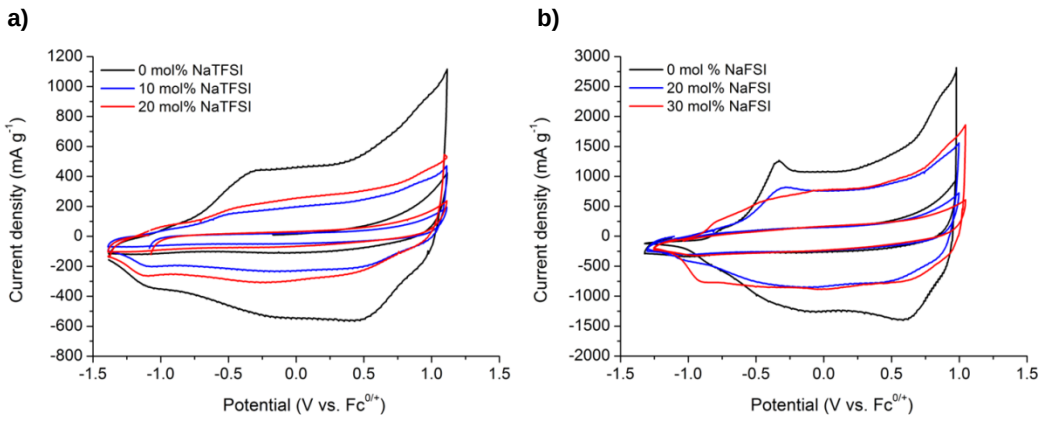

Figure 4.7. Cyclic voltammograms of PEDOTLig8020 modified GC electrodes in a) BMPyrTFSI and b) EMImFSI ionic liquids varying sodium salt concentration. Scan 1st and 20th

4.6. Cycling stability

The cycling stability of PEDOTLig8020 in sodium-ion conducting electrolytes was investigated by cyclic voltammetry, running 150 cycles for each sample. Figure 4.8 shows the cyclability of PEDOTLig8020 over several cycles in BMPyrTFSI:NaTFSI and EMImFSI:NaFSI-based electrolytes. The current density increases gradually upon cycling in BMPyrTFSI based electrolytes over the measured 150 cycles. The current density also increases upon cycling for the EMImFSI electrolyte, but it gets to a stable value after the 75th cycle. Therefore, redox activity and stability of PEDOTLig8020 is kept at least over 150 cycles in the studied sodium ion conducting electrolytes, which makes PEDOTLig8020 a good candidate for using it as a cathode material in sodium batteries.

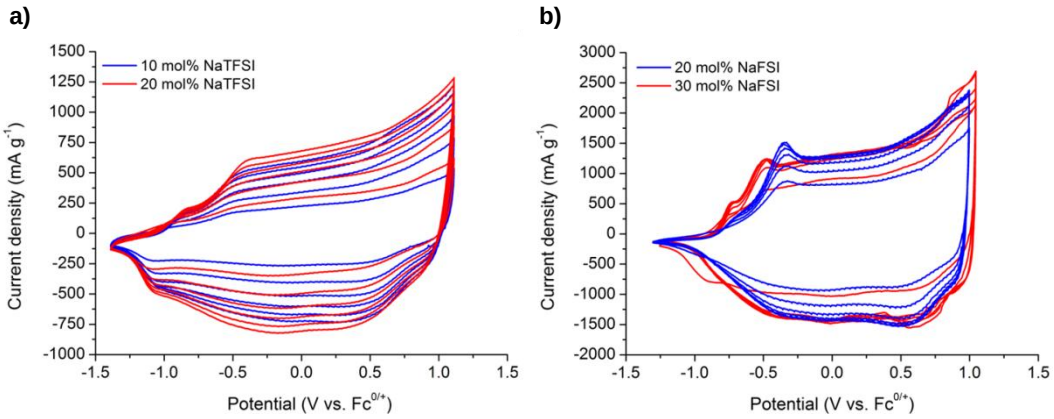

Figure 4.8. Cyclic voltammograms of PEDOTLig8020 modified GC electrodes in a) NaTFSI/BMPyrTFSI and b) NaFSI/EMImFSI electrolytes. Scans 25, 50, 75, 100, 125 and 150th

4.7. Full cell characterization

To further verify the potential of PEDOTLig8020 as cathode material, sodium coin cells were prepared using BMPyrTFSI:NaTFSI (20 mol%) and EMImFSI:NaFSI (20 mol%) electrolytes. The cathode was composed of 65 wt% PEDOTLig8020, 25 wt% PDADMA-TFSI and 10 wt% C-65, while the anode was sodium metal (Figure 4.9). It has to be mentioned that the capacities are calculated per gram of PEDOT/lignin polymer, thus, the values are related to the different redox processes in the composite material and not just the quinone/hydroquinone process taking part in lignin, which would lead to higher capacity values.

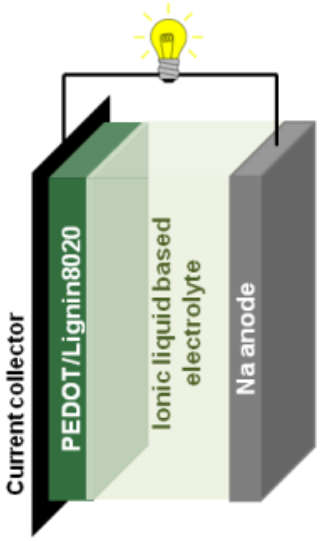

Figure 4.9. Schematic diagram of PEDOTLignin8020/sodium battery device

Figure 4.10 shows the charge and discharge profiles of pyrrolidinium (Figure 4.10a) and imidazolium based (Figure 4.10b) cells at various scan rates. The discharge profiles exhibit an almost linear decrease in potential due to the high content of PEDOT, demonstrating capacitor-like discharge behaviour. The polymer electrodes show an average discharge potential of 2.6 V and 2.8 V for pyrrolidinium and imidazolium based devices respectively, suitably serving as cathode active materials for sodium batteries.

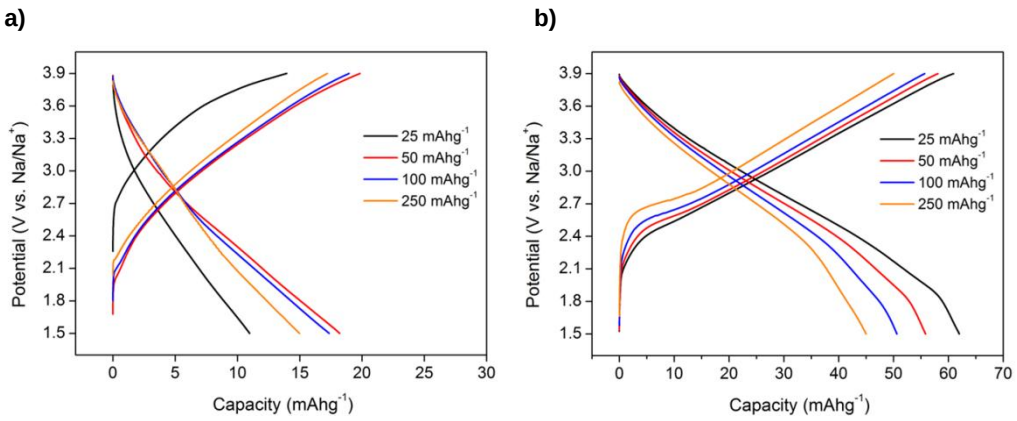

Figure 4.10. Charge-discharge profiles at different scan rates for devices based on a) BMPyrTFSI:NaTFSI(20mol%) and b) EMImFSI:NaFSI(20mol%) (voltage range 1.5 to 3.9V).

The long term cycling data is presented in Figure 4.11a. Interestingly, the capacity of the imidazolium electrolyte device stabilises rather rapidly after only 20 cycles at a capacity of 70 $mAhg^{-1}$, while the capacity increase is much slower for the pyrrolidinium sample (80 cycles, 46 $mAh\ g^{-1}$). This behaviour is in good agreement with that observed from the cyclic voltammetry experiments (see section 4.6) where the voltammograms in the pyrrolidinium-based electrolyte increased with cycling while in the imidazolium IL it stabilised more rapidly. This behaviour is believed to be due to the different ionic species exchanged during the charge and discharge of the polymer. There is a slight capacity loss of 6% observed upon long term cycling in the case of the imidazolium electrolyte. The nature of this capacity fade is unclear and still under investigation. In the case of current scan experiments (Figure 4.11b) the capacity also increases with cycle number. It should be mentioned that imidazolium device was conditioned

for 20 cycles at 25 mAg^{-1} until stable capacities were observed. As expected, with increasing current the capacity drops when the imidazolium electrolyte is used although higher capacities are attained as compared to the pyrrolidinium system (in agreement with CV and long term cycling results). As suggested before, the reason for this is mainly the higher fluidity and intrinsic ionic conductivity of the EMImFSI (15.3 mS cm^{-1})[28] compared to BMPyrTFSI (1.8 mS cm^{-1}).[24] Also after running the samples at high current rates and then switching back to the initial low current shows the capacity has regained its initial value (imidazolium sample) or shows an even larger value as a result of conditioning (pyrrolidinium), suggesting that the device performance is not compromised while exposing it to high currents.

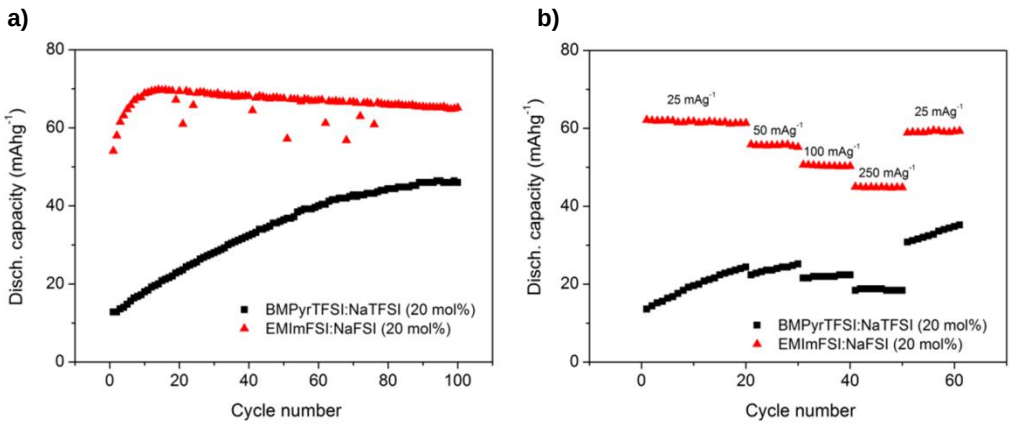

Figure 4.11. a) Long term cycling at 25 mAg^{-1} and b) current scans at 25, 50, 100, 250, 25 mAg^{-1} for devices based on BMPyrTFSI:NaTFSI(20mol%) (black) and EMImFSI:NaFSI(20mol%) (red). (Voltage range 1.5 to 3.9V).

After the long term cycling, the rate capability was studied by cycling the samples at various current densities in order to determine the nature of the conditioning (Figure 4.12). The capacity dropped during the resting period to the initial value and then increased with cycling number. The conditioning thus is highly reversible and can be related to the known rapid self-discharge of conducting polymers.[29,30]

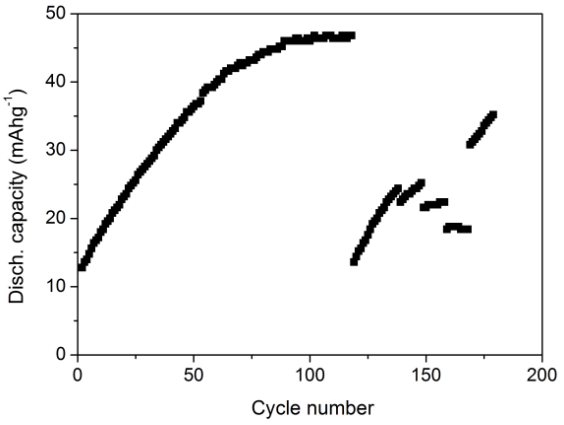

Figure 4.12. Long term cycling at 25mAg^{-1} followed by current scans (25, 50, 100, 250 mAg^{-1}) BMPyrTFSI:NaTFSI(20mol%) (voltage range 1.5 to 3.9V).

Whilst the PEDOT/lignin based electrodes perform well in Na devices shown here, it should be kept in mind that there are some inaccuracies due to the low electrode weight. Figure 4.13 show the cycling data for different pyrrolidinium cells, while the reproducibility for the imidazolium cells is shown in Figure 4.14. Despite the inaccuracies in the absolute capacities, the trend remains the same.

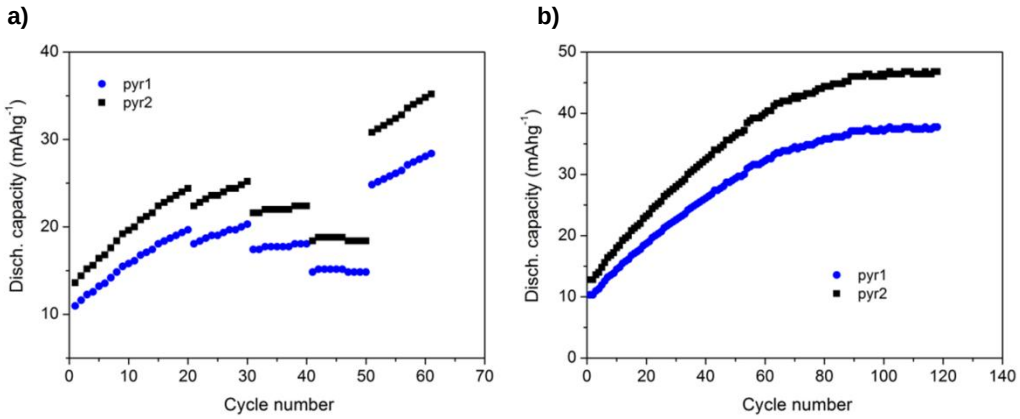

Figure 4.13. a) Current scans (25, 50, 100, 250, 25 mAg^{-1}) and b) long term cycling at 25mAg^{-1} for devices based on pyrrolidinium electrolyte (1.5 to 3.9V). The error is estimated to be less than 15%.

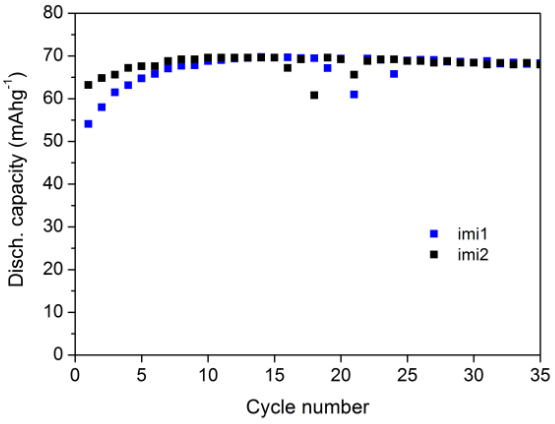

Figure 4.14. Long term cycling at 25mAg^{-1} for devices based on immidazolium electrolyte (1.5 to 3.9V).

4.8. Conclusions

In this chapter, we have demonstrated that PEDOT/lignin biocomposites combined the electroactivity of both constituents, showing an enhanced electrochemical activity and stability in ionic liquid electrolytes. The electrochemical behaviour of PEDOTLig8020 was studied in a series of pyrrolidinium and imidazolium-based ionic liquids, containing $TFSI^-$ and FSI^- anions, which demonstrated that the intrinsic properties of the ionic liquids, together with the interchangeable species taking part in the charge/discharge of the polymer, play a major role in the electrochemical performance. The addition of water and sodium salt were studied in order to get the optimum electrolyte system for sodium batteries. PEDOTLignin/Sodium metal batteries were assembled using BMPyrTFSI:NaTFSI (20 mol%) and EMImFSI:NaFSI (20 mol%) electrolytes. Discharge capacities of pyrrolidinium cells increase with cycling and get to stable values of 46 mAh g^{-1} after 100 cycles. On the other hand, imidazolium based cells stabilize faster and show higher capacity values reaching 70 mAh g^{-1}.

These encouraging findings show that PEDOT/lignin and some aprotic ionic liquids are a promising and effective cathode/electrolyte combination for developing sustainable sodium batteries. Moreover, these results open up the possibility to use other lignin derived cathodes in sodium batteries as well as PEDOT/lignin in other electrochemical devices using ionic liquids as electrolytes.

4.9. Experimental part

4.9.1. Materials

3,4-Ethylenedioxythiophene (EDOT, 99%, Acros organics), lignin alkali (Lig, Aldrich), sodium persulfate ($Na_2S_2O_8$, Aldrich), iron (III) chloride ($FeCl_3$, Aldrich) and 1-methyl-2-pyrrolidinone (NMP, 99%, Aldrich) were used without further purification. 1-butyl-1-methylpyrrolidinium bis(trifluoromethylsulfonyl)imide (BMPyrTFSI, 99.9%, Solvionic), 1-butyl-1-methylpyrrolidinium bis(fluorosulfonyl)imide (BMPyrFSI, 99.9%, Solvionic), 1-ethyl-3-methylimidazolium bis(trifluoromethylsulfonyl)imide (EMImTFSI, ≥98%, Aldrich), 1-ethyl-3-methylimidazolium bis(fluorosulfonyl)imide (EMImFSI, 99.9%, Solvionic), sodium(I) bis(trifluoromethanesulfonyl)imide (NaTFSI, 99.5%, Solvionic), sodium(I) bis(fluorosulfonyl)imide (NaFSI, 99.7%, Solvionic) were used as received. Those chemicals were opened and stored in a glovebox. The moisture content of the ionic liquids was < 150 ppm, as determined via Karl Fisher titration (Metrohm).

4.9.2. Methods

Electrochemical measurements were performed on a Biologic SP-200 potentiostat in an Ar-filled glove box in a conventional 3 electrode set up. A platinum wire (99.95%, APS) was used as counter electrode and a glassy carbon electrode (GC, 1mm diameter, ALS Co., Ltd. Japan) as working electrode, which was modified with a slurry of the redox active polymer. The reference electrodes were fabricated by immersing a silver wire into 5 mM AgOTf BMPyrTFSI and 5 mM AgOTf EMImDCA solutions, both separated from the bulk by a glass frit and used

respectively for pyrrolidinium and imidazolium based electrolytes. The reference electrodes were calibrated against ferrocene/ferrocinium couple and all potentials were referenced against Fc/Fc^+ couple. The slurry modified working electrodes were allowed to rest for 30 min inside the ionic liquid before running the electrochemical measurements.

Scanning electron microscopy (SEM) images were acquired on a JSM IT 300 series SEM at an accelerating voltage of 2 kV.

4.9.3. Synthesis of PEDOT/lignin composites

PEDOT/Lignin composites were synthesized via chemical oxidative polymerization of EDOT in presence of lignin, using an aqueous mixture of $Na_2S_2O_8$ and a catalytic amount of $FeCl_3$, accordingly to Chapter 3.[5] The obtained PEDOT/lignin dispersions were dialyzed with deionized water for 2 days using 12000 - 14000 g/mol cut-off membranes and freeze-dried to obtain PEDOT/lignin composites as powder. The initial EDOT:lignin mass ratios used were 100:0, 80:20 and 60:40 yielding to the composites named PEDOT, PEDOTLig8020 and PEDOTLig6040, respectively.

4.9.4. Synthesis of p-DADMA-TFSI binder

p-DADMA-TFSI binder was synthesized by anionic exchange reaction from the commercially available polymer poly(diallyldimethylammonium) chloride (p-DADMAC, Aldrich, average Mw 400,000–500,000, 20 wt.% in H_2O) with lithium bis(trifluoromethanesulfonyl)imide (LiTFSI, Solvionic, 99.9%), following the synthetic procedure previously reported.[31]

4.9.5. Preparation of GC modified electrodes

Redox active polymer (0.0136 g) and carbon black (0.0017 g, Timcal C_{65}) were gently mixed in a hand mortar and added to a solution of PDADMA-TFSI (0.0017g, Solvet) in NMP to obtain a composition of 80 wt % of redox active polymer, 10 wt % of C_{65} and 10 wt % of PDADMA-TFSI binder. The dispersion was stirred at r.t. for 2h and 0.3 µL of the slurry were drop-casted into the 1 mm GC electrode. The electrode was allowed to dry in the fume hood for 30 min and further drying at 50 °C/vacuum for 12h.

4.9.6. Sodium cells assembly

Coin cell prototypes were prepared using CR2032 Hohsen setup (2x 0.3 mm spacer, 1.4 mm spring). Sodium electrodes were prepared rolling sodium metal (Merck) in a glovebox and cutting out 0.9 cm diameter discs using a hole puncher. Cathodes were prepared by applying a formulation of 65% PEDOTLignin, 25% PDADMA-TFSI, and 10% C-65 (Timcal) in N-methyl-2-pyrrolidine (Sigma Aldrich) onto battery grade aluminium substrate (Targray) using a #40 wire coating bar. After evaporation of the solvent the foils were dried at 100°C overnight. Discs were cut using a 7/16th inch hole puncher. The weight of each individual electrode was determined. Before assembly the cathodes were vacuum dried inside the glovebox. A solupor separator was used (Lydall). The electrolytes for these experiments were prepared by adding 20 mol% NaTFSI and NaFSI to BMPyrTFSI and EMImFSI, respectively.

The cells were cycled at room temperature in a potential range of 1.5 to 3.9 V. The two experiments performed were *(i)* a current scan experiment changing the current from 25 (20

cycles), 50 (10 cycles) 100 (10 cycles), 250 (10 cycles) and 25 mAg^{-1} (10 cycles) and *(ii)* a long term experiment were the cells were cycled for 100 cycles at $25mAg^{-1}$. The capacities and scan rates are calculated per gram of PEDOT/lignin biopolymer in the electrode.

4.10. References

(1) Larcher D., Tarascon J. M. Towards greener and more sustainable batteries for electrical energy storage. *Nat Chem*. **2015**;7:19-29.

(2) Casado N., Hernández G., Sardon H., Mecerreyes D. Current trends in redox polymers for energy and medicine. *Prog. Polym. Sci.* **2016**;52:107-35.

(3) Nagaraju D. H., Rebis T., Gabrielsson R., Elfwing A., Milczarek G., Inganäs O. Charge Storage Capacity of Renewable Biopolymer/Conjugated Polymer Interpenetrating Networks Enhanced by Electroactive Dopants. *Adv. Energy Mater.* **2014**;4:n/a-n/a.

(4) Rębiś T., Milczarek G. A comparative study on the preparation of redox active bioorganic thin films based on lignosulfonate and conducting polymers. *Electrochim. Acta*. **2016**;204:108-17.

(5) Ajjan F. N., Casado N., Rebis T., Elfwing A., Solin N., Mecerreyes D., Inganas O. High performance PEDOT/lignin biopolymer composites for electrochemical supercapacitors. *J. Mater. Chem. A*. **2016**;4:1838-47.

(6) Leguizamon S., Diaz-Orellana K. P., Velez J., Thies M. C., Roberts M. E. High charge-capacity polymer electrodes comprising alkali lignin from the Kraft process. *J. Mater. Chem. A*. **2015**;3:11330-9.

(7) Rebis T., Nilsson T. Y., Inganas O. Hybrid materials from organic electronic conductors and synthetic-lignin models for charge storage applications. *J. Mater. Chem. A*. **2016**;4:1931-40.

(8) Milczarek G. Synthesis and Electroanalytical Performance of a Composite Material Based on Poly(3,4-ethylenedioxythiophene) Doped with Lignosulfonate. *Int. J. Electrochem.* **2012**;2012.

(9) Armand M., Endres F., MacFarlane D. R., Ohno H., Scrosati B. Ionic-liquid materials for the electrochemical challenges of the future. *Nat Mater*. **2009**;8:621-9.

(10) Osada I., de Vries H., Scrosati B., Passerini S. Ionic-Liquid-Based Polymer Electrolytes for Battery Applications. *Angew. Chem. Int. Ed.* **2016**;55:500-13.

(11) Mohd Noor S. A., Howlett P. C., MacFarlane D. R., Forsyth M. Properties of sodium-based ionic liquid electrolytes for sodium secondary battery applications. *Electrochimica Acta*. **2013**;114:766-71.

(12) Monti D., Ponrouch A., Palacín M. R., Johansson P. Towards safer sodium-ion batteries via organic solvent/ionic liquid based hybrid electrolytes. *J. Power Sources*. **2016**;324:712-21.

(13) Guerfi A., Trottier J., Gagnon C., Barray F., Zaghib K. High rechargeable sodium metal-conducting polymer batteries. *J. Power Sources*. **2016**;335:131-7.

(14) MacFarlane D. R., Forsyth M., Howlett P. C., Kar M., Passerini S., Pringle J. M., Ohno H., Watanabe M., Yan F., Zheng W., Zhang S., Zhang J. Ionic liquids and their solid-state analogues as materials for energy generation and storage. *Nat. Rev. Mater.* **2016**;1:15005.

(15) Österholm A. M., Shen D. E., Dyer A. L., Reynolds J. R. Optimization of PEDOT Films in Ionic Liquid Supercapacitors: Demonstration As a Power Source for Polymer Electrochromic Devices. *ACS Appl. Mater. Inter.* **2013**;5:13432-40.

(16) Karlsson C., Nicholas J., Evans D., Forsyth M., Strømme M., Sjödin M., Howlett P. C., Pozo-Gonzalo C. Stable Deep Doping of Vapor-Phase Polymerized Poly(3,4-ethylenedioxythiophene)/Ionic Liquid Supercapacitors. *ChemSusChem*. **2016**;9:2112-21.

(17) Bhat M. A. Mechanistic, kinetic and electroanalytical aspects of quinone–hydroquinone redox system in N-alkylimidazolium based room temperature ionic liquids. *Electrochim. Acta*. **2012**;81:275-82.

(18) Pandey M. P., Kim C. S. Lignin Depolymerization and Conversion: A Review of Thermochemical Methods. *Chemical Engineering & Technology*. **2011**;34:29-41.

(19) Randriamahazaka H., Plesse C., Teyssié D., Chevrot C. Ions transfer mechanisms during the electrochemical oxidation of poly(3,4-ethylenedioxythiophene) in 1-ethyl-3-methylimidazolium bis((trifluoromethyl)sulfonyl)amide ionic liquid. *Electrochem. Commun.* **2004**;6:299-305.

(20) Wagner K., Pringle J. M., Hall S. B., Forsyth M., MacFarlane D. R., Officer D. L. Investigation of the electropolymerisation of EDOT in ionic liquids. *Synth. Met.* **2005**;153:257-60.

(21) Heinze J., Frontana-Uribe B. A., Ludwigs S. Electrochemistry of Conducting Polymers—Persistent Models and New Concepts. *Chem. Rev.* **2010**;110:4724-71.

(22) Robert Hillman A., Daisley S. J., Bruckenstein S. Solvent effects on the electrochemical p-doping of PEDOT. *PCCP*. **2007**;9:2379-88.

(23) Balducci A., Dugas R., Taberna P. L., Simon P., Plée D., Mastragostino M., Passerini S. High temperature carbon–carbon supercapacitor using ionic liquid as electrolyte. *J. Power Sources*. **2007**;165:922-7.

(24) Tiruye G. A., Muñoz-Torrero D., Palma J., Anderson M., Marcilla R. Performance of solid state supercapacitors based on polymer electrolytes containing different ionic liquids. *J. Power Sources*. **2016**;326:560-8.

(25) Sandoval A. P., Feliu J. M., Torresi R. M., Suarez-Herrera M. F. Electrochemical properties of poly(3,4-ethylenedioxythiophene) grown on Pt(111) in imidazolium ionic liquids. *RSC Adv.* **2014**;4:3383-91.

(26) Tokuda H., Hayamizu K., Ishii K., Susan M. A. B. H., Watanabe M. Physicochemical Properties and Structures of Room Temperature Ionic Liquids. 2. Variation of Alkyl Chain Length in Imidazolium Cation. *J. Phys. Chem. B*. **2005**;109:6103-10.

(27) Chambers J. Q. Electrochemistry of quinones. The Quinonoid Compounds (1988): John Wiley & Sons, Inc.; 2010. p. 719-57.

(28) Armel V., Pringle J. M., Forsyth M., MacFarlane D. R., Officer D. L., Wagner P. Ionic liquid electrolyte porphyrin dye sensitised solar cells. *Chem. Commun.* **2010**;46:3146-8.

(29) Olsson H., Jämstorp Berg E., Strømme M., Sjödin M. Self-discharge in positively charged polypyrrole–cellulose composite electrodes. *Electrochem. Commun.* **2015**;50:43-6.

(30) Olsson H., Strømme M., Nyholm L., Sjödin M. Activation Barriers Provide Insight into the Mechanism of Self-Discharge in Polypyrrole. *J. Phys. Chem. C*. **2014**;118:29643-9.

(31) Pont A.-L., Marcilla R., De Meatza I., Grande H., Mecerreyes D. Pyrrolidinium-based polymeric ionic liquids as mechanically and electrochemically stable polymer electrolytes. *J. Power Sources*. **2009**;188:558-63.

CHAPTER 5

High conductive PEDOT/PSTFSI dispersions for Lithium-ion battery electrodes

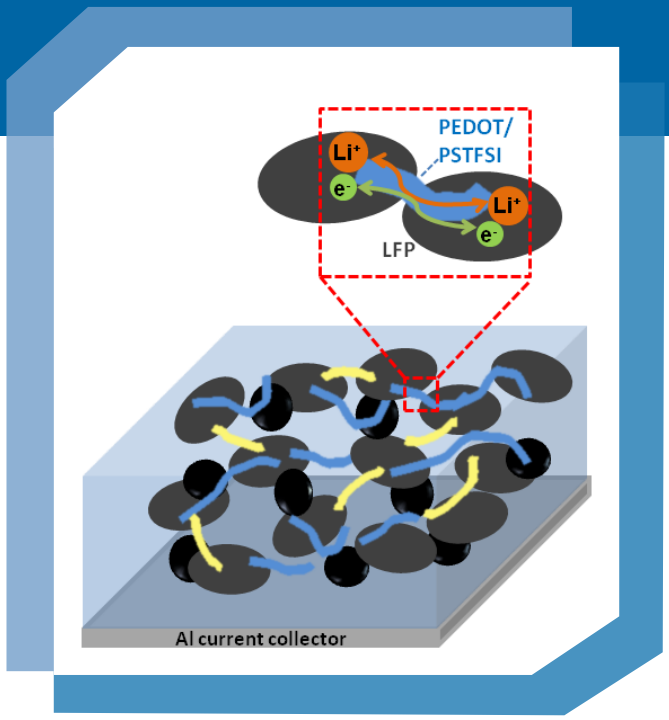

Chapter 5. High conductive PEDOT/PSTFSI dispersions for Lithium-ion battery electrodes

5.1. Introduction

One of the most important energy storage devices nowadays is the lithium ion battery, which is the current choice for powering portable electronic devices.[1] Lithium iron phosphate ($LiFePO_4$ or LFP) is highly regarded by its environmental friendliness and cost effective synthetic routes.[2] However, its main downside is its low electronic conductivity, leading to poor rate capability.[3] Nowadays, LFP is coated with carbon to enhance the electronic conductivity.[4] Moreover, in order to ensure good electronic connection between the particles, electrode formulations include apart from the active material, carbon additives and a polymeric binder.

As mentioned in the state of the art, conducting polymers are attractive materials to implement in the configuration of electrodes due to their excellent electronic conductivity and mechanical stability.[5] Recently, various methods have been employed to design composite electrodes of LFP and conducting polymers, which include the blending of LFP with conducting polymers or the chemical or electrochemical polymerization in presence of the phosphate.[6-8] For example, Tirado and Ahmad's groups studied different preparation methods, such as electropolymerization and blending, to obtain LFP composite cathode materials with PEDOT.[8]

Between the studied methods, direct electropolymerization of EDOT onto the LFP cathode showed the best cycling performances. PEDOT:PSS has also been used in LFP cathodes, which was able to act as conducting additive and binder.[9] In this case, $LiFePO_4$ was added to the conductive PEDOT:PSS dispersion for the preparation of the slurry.

As electrodes require the transport of both ions and electronic charge, the objective of this chapter is to develop highly conductive PEDOT dispersions, which might be able to improve also the ionic transport between the components of the electrode. For this, EDOT is polymerized in presence of a soft ionic conductor polyanion. This polyanion would be able not only to act as dispersant and counter-ion of doped PEDOT but also to provide ionic conductivity. In this way, the lithiation/delithiation processes and the electronic conductivity of LFP cathodes will be improved.

The anionic (trifluoromethylsulfonyl)imide groups (TFSI), as opposed to sulfonates, are highly dissociated because of the extended delocalisation, improving greatly the ionic conductivity.[10] Therefore, these anionic groups have been widely implemented to improve the ionic conductivity in different applications such as polymer electrolytes. Copolymers containing a methacrylate bearing TFSI anion[11] or the grafting of TFSI anions to nanoparticles[12,13] for the development of solid polymer electrolytes are some of the examples. Moreover, Armand and Bonnet pioneered the synthesis of a polystyrene bearing TFSI anion (PSTFSI polyanion), applying it as single-ion polymer electrolyte in lithium batteries.[10] PSTFSI and PSS polyanions were mixed with poly(ethylene oxide) to prepare composite membranes and they observed that the ionic conductivity was about ten times higher for the membrane with PSTFSI compared to the one with PSS.

Therefore, the aim of this chapter is to synthesize and characterize an ionic/electronic conducting network, where doped-PEDOT is stabilized by the ionic conductor PSTFSI polyanion. For that purpose, EDOT is polymerized by oxidative chemical polymerization in presence of PSTFSI, achieving highly conducting PEDOT/PSTFSI dispersions. The final goal is to apply this polymer in LFP electrodes to improve the interconnection of LFP particles and thus, enhance their cycling performance.

Recently, similar PEDOT/PSTFSI dispersions have been studied by Hofmann *et al.*[14], also obtained by polymerization of EDOT in presence of a PSTFSI-K polyanion, to be used as electrode materials in organic light-emitting diodes and organic photovoltaics, but not for electrochemical energy storage applications.

5.2. PEDOT/PSTFSI synthesis

PEDOT/PSTFSI dispersions were synthesized by oxidative chemical polymerization of EDOT in an aqueous solution of PSTFSI-Li, as illustrated in Figure 5.1. In order to analyse the effect of each component in the physical properties of PEDOT/PSTFSI, the polymerization was carried out containing different EDOT:PSTFSI mass ratios (40:60, 50:50, 60:40). First, the polyelectrolyte PSTFSI-Li was dissolved in degassed water and stirred for 30 min at 0 ºC. Then, EDOT monomer was added and after 10 min, a degassed solution containing the oxidant $(NH_4)_2S_2O_8$ and a catalytic amount of $FeCl_3$ were added. After finishing the reaction, the reaction solution turned from colourless to deep blue coloured solution. The final polymer is

an ionic complex where PSTFSI acts as dispersant and counter-ion of the positively doped PEDOT chains.

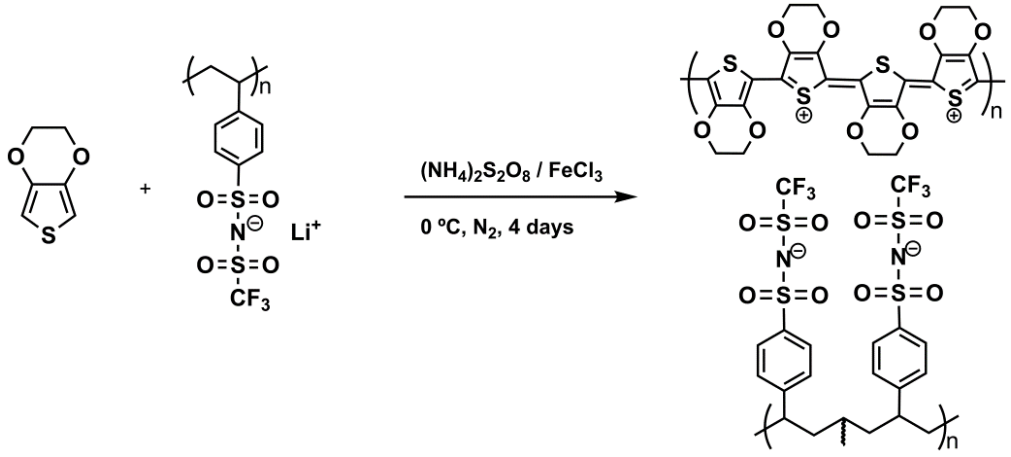

Figure 5.1. Synthesis of PEDOT/PSTFSI by oxidative chemical polymerization of EDOT in the presence of PSTFSI-Li.

5.3. Characterization of PEDOT/PSTFSI dispersions

PEDOT/PSTFSI dispersions were characterized by UV/Vis spectroscopy. The UV/Vis spectra of the dispersions obtained from different EDOT:PSTFSI ratios are shown in Figure 5.2. The three different compositions show similar spectra. The absorbance spectra of PEDOT/PSTFSI dispersions show two main peaks, one at 800 nm related to the polaronic

states and another one at wavelengths higher than 1000 nm ascribed to the bipolaronic states of PEDOT.[15]

Although no significant differences were observed in the UV-Vis spectra using different EDOT:PSTFSI ratios, its appearance confirms that EDOT has been successfully polymerized in presence of PSTFSI polyelectrolyte, achieving a doped PEDOT stabilized with PSTFSI.

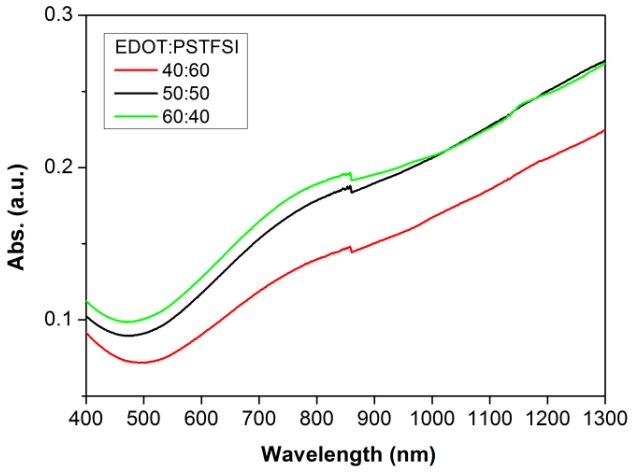

Figure 5.2. UV–Vis-NIR absorption spectra of PEDOT/PSTFSI dispersions, obtained from different EDOT:PSTFSI weight ratios (40:60, 50:50, 60:40).

PEDOT/PSTFSI films were obtained by drop-casting of the dispersions onto glass slides. Then, the electronic conductivity of PEDOT/PSTFSI films was measured by four-point probe. The values obtained for the films with different PSTFSI contents and thicknesses are shown in Figure 5.3. As expected, thinner films lead to higher conductivity values, with an

increase of one order of magnitude from the thickest to the thinner film in each composition. This occurs because when the thickness is decreased, the connectivity of the PEDOT/PSTFSI domains in the film is higher, providing better connecting pathways through the film and thus, the conductivity values are increased.

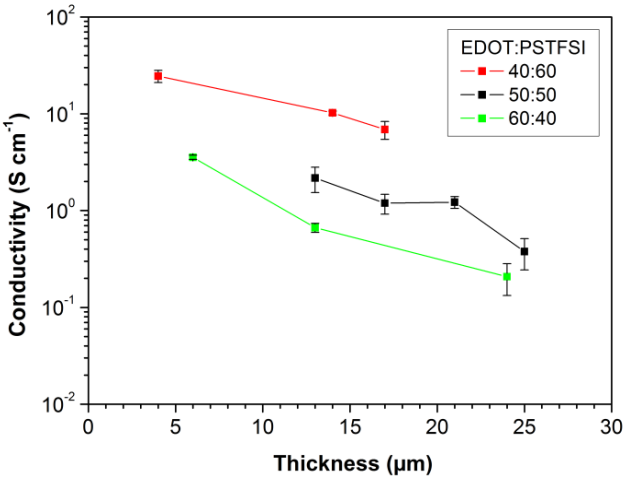

Figure 5.3. Conductivity as a function of thickness of PEDOT/PSTFSI films, obtained from different EDOT:PSTFSI weight ratios (40:60, 50:50, 60:40).

On the other hand, we would expect a decrease on the electronic conductivity with higher ratios of PSTFSI, due to its insulating behaviour.[16] However, comparing the films of similar thicknesses (13-15 µm), an increase of almost two orders of magnitude is observed from lowest (40 wt%) to highest PSTFSI ratio (60 wt%) (Table 5.1). As mentioned before, the PSTFSI polyanion acts as counter ion of the positively charged PEDOT chains, which are the

responsible of the electronic conduction. Thus, if PSTFSI is not in excess, as in this case, an increase of PSTFSI content allows a higher doping level of PEDOT, enhancing the conductivity of the material. It is worth to mention that the conductivity values of PEDOT/PSTFSI films are similar or even higher than the ones obtained for commercial PEDOT:PSS (Clevios P) before adding any secondary dopant.[17,18]

It is known that the content of the polyanion (PSTFSI or PSS) affects the particle size of the dispersions.[19] Thus, PEDOT/PSTFSI dispersions were characterized by dynamic light scattering (DLS) and transmission electron microscopy (TEM). The results obtained by DLS showed that the average particle size of PEDOT/PSTFSI decreases with the increase of PSTFSI content (Table 5.1). The dispersion obtained using a EDOT:PSTFSI ratio of 40:60 shows the smallest average particle size. Moreover, TEM images of this dispersion (Figure 5.4) showed almost spherical domains with more than one core in each and diameter sizes smaller than 2 μm, which are in agreement with the values obtained by DLS. These domains might be formed by the aggregation of various particles, as more than one core is observed in each domain, which have a PEDOT rich inner core (dark part) and a PSTFSI rich outer part (light part).

Table 5.1. Particle size and conductivity data of PEDOT/PSTFSI dispersions or films.

Number	EDOT (wt%)	PSTFSI (wt%)	Z average particle size (nm)	Film thickness (μm)	Film conductivity (S cm^{-1})
1	40	60	1386	14	10.2 ± 0.5
2	50	50	2724	13	2.17 ± 0.64
3	60	40	2969	13	0.67 ± 0.07

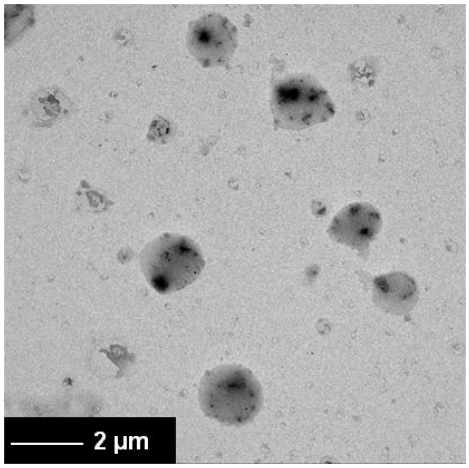

Figure 5.4. TEM image of PEDOT/PSTFSI dispersion obtained with EDOT:PSTFSI weight ratio of 40:60.

The thermal behaviour of the different PEDOT/PSTFSI was investigated by thermogravimetric analysis (TGA), performed under nitrogen atmosphere, measuring the weight loss as a function of temperature (Figure 5.5). TGA curves show that PEDOT/PSTFSI composites are stable up to 200 ºC. A weight loss of around 10% is observed between 200 and 300 ºC for 40:60 and 60:40 EDOT:PSTFSI ratios, which can be attributed to the first degradation step of PSTFSI.[10] The second degradation of PSTFSI is reported to begin at about 400 ºC and the third one at around 450 ºC. However, these steps are not noticeable in PEDOT/PSTFSI, instead a gradual degradation is observed above 400 ºC. The most pronounced degradation occurs between 300 °C and 400 °C, which is attributed to the decomposition of PEDOT.[20]

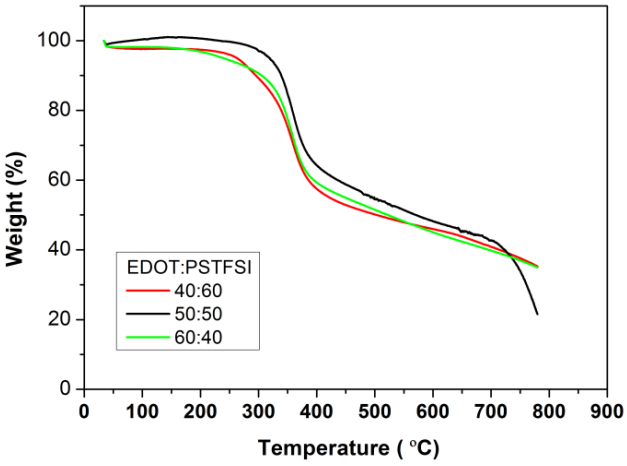

Figure 5.5. Thermogravimetric analysis (TGA) of previously lyophilized PEDOT/PSTFSI dispersions, obtained from different EDOT:PSTFSI weight ratios (40:60, 50:50, 60:40).

5.4. Electrochemical characterization

The electrochemical characterization of PEDOT/PSTFSI was carried out by casting the dispersions onto the platinum working electrodes to obtain the corresponding films. Cyclic voltammetry measurements of different PEDOT/PSTFSI compositions were performed in 0.1 M $LiClO_4$ acetonitrile solutions in order to examine the electrochemical properties. The voltage range was held from −0.6 to 1.2 V and a scan rate of 100 mV s^{-1} was employed. The resulting cyclic voltammograms are shown in Figure 5.6. PEDOT/PSTFSI films exhibited reversible oxidation and reduction during cycling, with shapes typical for polythiophene derivatives.[21] The film containing higher PSTFSI content (40:60) showed the most pronounced redox peaks, with oxidation and reduction peaks at -0.12 V and -0.28 V, respectively. However, the capacitance

current for the PEDOT/PSTFSI with the lowest PSTFSI content (60:40) was found to be lower and more sloping, which might be attributed to the lower conductivity of the material. It has to be mention that PEDOT/PSTFSI 40:60 film presented electrochromic properties being dark blue in the reduced state and sky blue transparent coloured in the oxidized state.

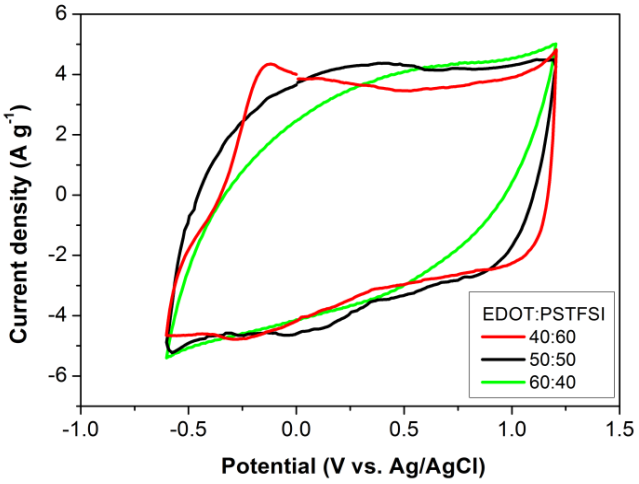

Figure 5.6. Cyclic voltammograms in 0.1 M $LiClO_4$ acetonitrile solution of drop-casted PEDOT/PSTFSI films obtained from different EDOT:PSTFSI weight ratios (40:60, 50:50, 60:40). Scan rate: 100 mV s^{-1}

Due to the superior conductivity and electrochemical properties, PEDOT/PSTFSI obtained from EDOT:PSTFSI 40:60 (wt %) was chosen to study as conducting additive in lithium-ion batteries.

5.5. Application in Li-ion batteries

PEDOT/PSTFSI with the highest conductivity value (EDOT:PSTFSI 40:60) was used in $LiFePO_4$ (LFP) cathodes to improve both the electronic and ionic conductivity of the electrode. As comparison, a standard electrode without any conducting polymer additive and another electrode with commercial PEDOT:PSS were used. The standard electrode was composed of 89% LFP, 7% PVDF and 4% carbon, while the configuration of the electrodes containing conductive polymers was 84% LFP, 7% PVDF, 4% carbon and 5% conducting polymer (PEDOT:PSS or PEDOT/PSTFSI).

The cell performance at C/2 rate of the three studied cathodes is shown in Figure 5.7b. The discharge capacities of the cells containing 5% of PEDOT/PSTFSI and PEDOT/PSS are higher than the standard electrode, with stable capacity values of 153, 157 and 148 mAh g^{-1}, respectively. The three electrodes showed high coulombic efficiency, all above 97 %. This confirms that the addition of a minimum amount of PEDOT/PSTFSI can improve the performance of conventional LFP cathodes; moreover, comparable capacity values to PEDOT/PSS were obtained.

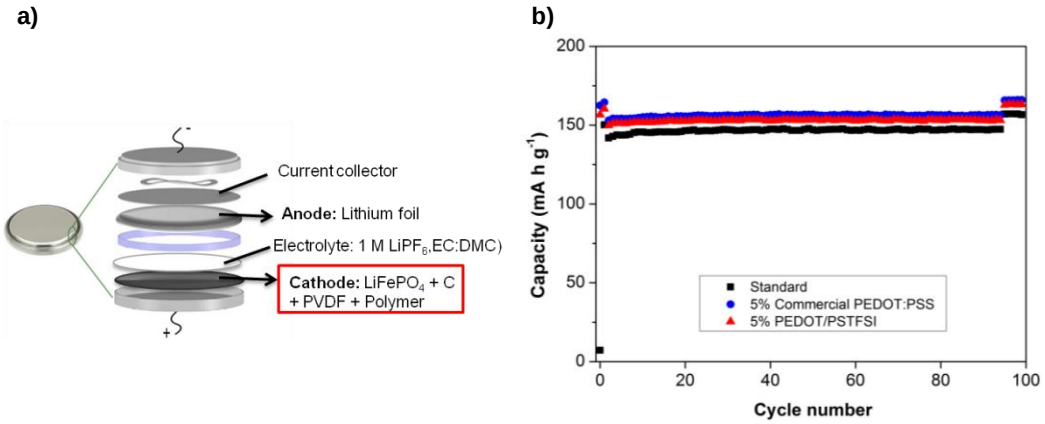

Figure 5.7. a) Schematic diagram of the battery components. b) Discharge capacities at C/2 rate except first 2 and last 5 cycles (C/10) for the studied LFP cathodes: standard (89% LFP / 7% PVDF / 4% CB, black), 5% PEDOT:PSS (84% LFP / 7% PVDF / 4% C / 5% PEDOT:PSS, blue) and 5% PEDOT:PSTFSI (84% LFP / 7% PVDF / 4% C / 5% PEDOT:PSTFSI, red).

One of the main limitations of LFP batteries is the rate capability, due to its low intrinsic conductivity.[3] Therefore, the rate capability of the three cells was also investigated. As shown in Figure 5.8a, the rate capability of the standard LFP cathode is improved by the addition of both conducting polymers, which provide higher specific discharge capacity values at every studied rate. The voltage profiles at different rates are shown in Figure 5.8b where the polarization of the standard cathode at high rates is noticeable. When the cells containing conducting polymers are compared, enhanced rate capability is observed for the cathode with commercial PEDOT:PSS, while the polarization is similar in both cases. It is worth to mention that the formulation of the PEDOT:PSS used, as opposed to PEDOT/PSTFSI, includes secondary dopants to increase its conductivity up to 1000 S cm^{-1} and thus, its improved rate capability is reasonable. Therefore, the results obtained with pristine PEDOT/PSTFSI are promising and leave the door open for future investigations and improvements.

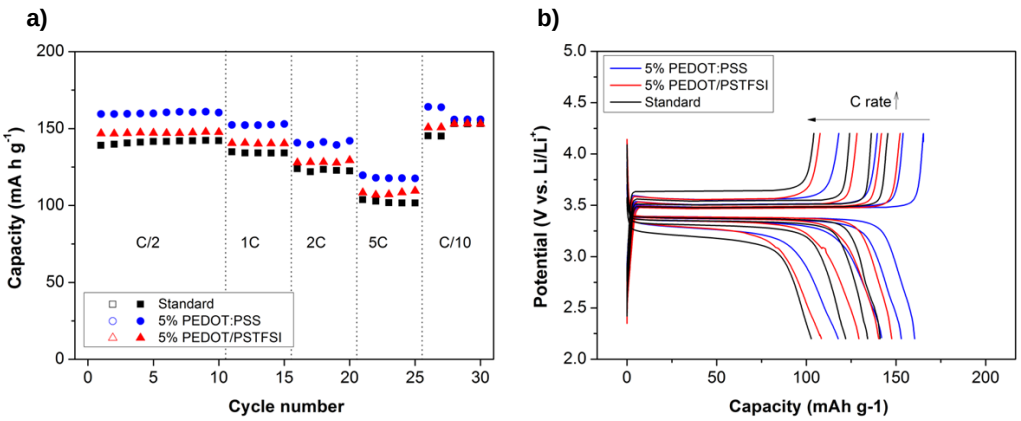

Figure 5.8. a) Discharge capacity and b) voltage profile at different rates for the studied LFP cathodes: standard (89% LFP / 7% PVDF / 4% CB, black), 5% PEDOT:PSS (84% LFP / 7% PVDF / 4% C / 5% PEDOT:PSS, blue) and 5% PEDOT:PSTFSI (84% LFP / 7% PVDF / 4% C / 5% PEDOT:PSTFSI, red).

5.6. Conclusions

In conclusion, the synthesis and characterization of PEDOT/PSTFSI dispersions has been presented in this chapter. EDOT has been polymerized by oxidative chemical polymerization in presence of PSTFSI polyanion using different EDOT:PSTFSI weight ratios. In this way, the obtained dispersions posses combined properties, the electronic conductivity of PEDOT and the ionic conductivity of PSTFSI. Interestingly, a higher content of PSTFSI leaded to a more conducting and electroactive polymer. These properties make PEDOT/PSTFSI a good candidate to be used in lithium iron phosphate batteries to improve its cycling performance. It was proved that by an addition of only 5 % of PEDOT/PSTFSI, the cycling performance at C/2 rate of LFP cathodes was enhanced, with high coulombic efficiencies. Moreover, the rate capability of $LiFePO_4$ batteries was also improved due to the decrease in

the polarization of the electrodes. Therefore, it was demonstrated that PEDOT/PSTFSI can improve the cycling performance of $LiFePO_4$ electrodes and thus, further steps should be taken in order to replace as much as possible the conventional inactive binder and high surface area carbon additive generally used in insulating cathode materials.

5.7. Experimental part

5.7.1. Materials

3,4-Ethylenedioxythiophene (EDOT, 99%, Acros organics), ammonium persulfate ($(NH_4)_2S_2O_8$), iron (III) chloride ($FeCl_3$), anhydrous acetonitrile (ACN) and dry lithium perchlorate ($LiClO_4$, 99.99%), were obtained from Sigma-Aldrich and used as received. The aqueous solutions were prepared with ultrapure deionised water (Millipore).

5.7.2. Methods

UV-Vis spectra were acquired at room temperature on a PerkinElmer UV/Vis/NIR Lambda 950 spectrometer.

Conductivity measurements were performed on a four-point probe Veeco/Miller FPP5000 using layer resistivity function, sampling in different zones of the film more than three times. Polymer films were prepared by drop-casting of the dispersions onto glass coverslips

and drying at r.t. overnight. Thickness of polymer film was measured with a Digimatic micrometer from Mitutoyo Corporation.

Particle size was measured with dynamic light scattering (DLS) using a Zetasizer Nano Series (Malvern Instrument) at 20 ºC. A fraction of PEDOT/PSTFSI dispersion was diluted with deionized water for the analysis and the reported average particle size values represent an average of three repeated measurements.

Transmission electron microscopy (TEM) images were collected using a FEI TECNAI G2 20 TWIN TEM, operating at an accelerating voltage of 200 KV in a bright-field image mode. Dispersions were diluted and then dried using a UV lamp before the analysis.

The thermal stability of the samples was investigated by thermo-gravimetric analysis (TGA) performed on a TGA Q500 from TA Instruments. Measurements were carried out by heating the sample at 10 °C min^{-1} under nitrogen atmosphere from 40 ºC to 800 °C.

The electrochemical characterization of PEDOT/PSTFSI was performed on an Autolab PGSTAT302N by using the standard three-electrode configuration where platinum sheets (with an area of 1 cm^2) were used as working (WE) and counter electrodes (CE) and an Ag/AgCL (3 M KCl) as reference electrode (RE). The potential window of the cyclic voltammetry (CV) was cycled from -0.6 V to 1.2 V vs Ag/AgCl by applying 20 cycles at 100 mV s^{-1}.

5.7.3. Synthesis of PSTFSI-Li

The synthetic route followed for the synthesis of lithium poly[(4-styrene-sulfonyl)-(trifluoro-methane-sulfonyl)imide] (PSTFSI-Li) is shown in Figure 5.9. First, 4-styrene sulfonyl chloride was synthesized starting from oxalyl chloride and through the Vilsmeier–Haack complex, as already described by Meziane *et al.*[10] Then, the solution of 4-styrene sulfonyl chloride in acetonitrile anhydrous was cooled down to 0 ºC and then, a mixture of trimethylamine (58.1 mmol), trifluoromethanesulfonamide (19.4 mmol) and DMAP (4-dimethylaminopyridine, 1.7 mmol) in acetonitrile (previously prepared uner argon atmosphere) was added dropwise. The reaction was placed under vigorous stirring overnight. At that point, the acetonitrile was removed in order to make the work-up of the reaction in dichloromethane using an aqueous solution of $NaHCO_3$ 4 wt.% (2 x 20 mL), and then HCl 1 M (1 x 20 mL). At that point, the solvent was removed being the resulting product dissolved in ethanol. STFSI-Li was obtained by adding an excess of lithium hydroxide over this solution. Finally, it was filtrated to remove the excess of LiOH, and the final product was washed with acetonitrile in order to remove any unmodified styrene sulfonyl chloride (global yield 38.7%).

The polymerization reaction was carried out by dissolving 1.0 g of STFSI-Li monomer (3.1 mmol) in 20 mL of deionized and deoxygenated water with 2.0 wt.% of ammonium persulfate (0.09 mmol) and leaved stirring at 80 ºC under argon flow for at least one day. Finally, the acetonitrile was evaporated in a rotatory evaporator and the final product was dissolved in dimethyl sulfoxide and precipitated with ethyl acetate (several times) obtaining a yellowish powder.

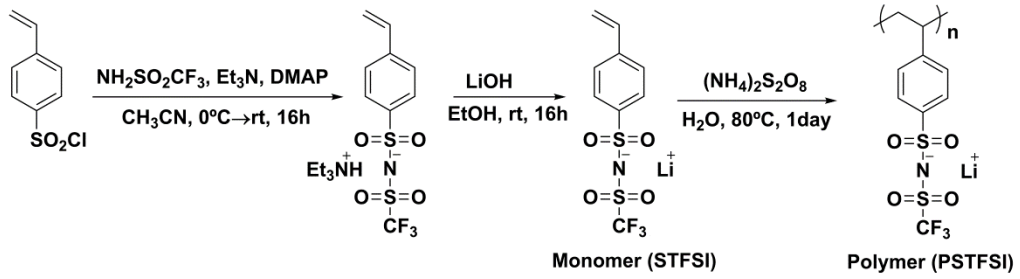

Figure 5.9. Synthetic route followed for PSTFSI preparation.

5.7.4. Synthesis of PEDOT/PSTFSI dispersions

The polymerization of PEDOT/PSTFSI dispersions was carried out containing different EDOT:PSTFSI mass ratios (40:60, 50:50, 60:40). First, the polyelectrolyte PSTFSI-Li was dissolved in previously deoxygenized water and stirred for 30 min at 0 ºC. Then, EDOT monomer was added and after 10 min, a deoxygenized water solution containing the oxidant $(NH_4)_2S_2O_8$ and a catalytic amount of $FeCl_3$ were added. The oxidative polymerization was carried out under mechanical stirring at 0 ºC for 4 days and the concentration of the solution was kept constant at 2% (w/v). After finishing the reaction, the reaction solution turned from colourless to deep blue coloured solution. Finally, the obtained PEDOT/PSTFSI dispersions were dialyzed with deionised water for 48 hours using a 12000-14000 g/mol cut-off membrane and freeze-dried, yielding PEDOT/PSTFSI as a dark bluish powder.

5.7.5. Lithium cells assembly

Carbon Black (Csp-Imerys®), lithium iron phosphate ($LiFePO_4$, Alees3, Taiwan) and the PEDOT/PSTFSI or PEDOT:PSS (Clevios^{TM} PH 1000) powders, if it is applicable, where mixed together by hand-milling and added to the dissolved polyvinylene fluoride (PvdF, Sigma-Aldrich) in N-methyl pyrrolidone (NMP, Sigma-Aldrich). Dr. Blade was used to laminate the different slurries over carbon coated aluminium foil.

The laminates were dried under vaccuum at 100ºC overnight and then pressed at 1.5 ton cm^{-2}. Coin cells (CR2032) were assembled in an argon-filled glove box (M-Braun). The anode was a disk of lithium metal foil (Rockwood lithium) and it was separated from the cathode by a glass fiber (Glass fiber GFD/55, Whatman) soaked in a solution of 1 M $LiPF_6$ in EC:DMC (1:1 vol. %) (Solvionic). Batteries were tested in a Biologic VMP3 between 2.2 V and 4.2 V. Two different experiments were performed: (i) large cycling (100 cycles) at C/2 and (ii) short cycling at different scan rates, C/2 (10 cycles), 1C (5 cycles), 2C (5 cycles), 5C (5 cycles) and C/10 (5 cycles). Previous to each experiment, two cycles at C/10 were performed first as a formation step.

5.8. References

(1) Armand M., Tarascon J. M. Building better batteries. *Nature*. **2008**;451:652-7.

(2) Zhang Y., Huo Q.-y., Du P.-p., Wang L.-z., Zhang A.-q., Song Y.-h., Lv Y., Li G.-y. Advances in new cathode material LiFePO4 for lithium-ion batteries. *Synth. Met.* **2012**;162:1315-26.

(3) Delacourt C., Laffont L., Bouchet R., Wurm C., Leriche J.-B., Morcrette M., Tarascon J.-M., Masquelier C. Toward Understanding of Electrical Limitations (Electronic, Ionic) in LiMPO4 (M = Fe , Mn) Electrode Materials. *J. Electrochem. Soc.* **2005**;152:A913-A21.

(4) Ravet N., Chouinard Y., Magnan J. F., Besner S., Gauthier M., Armand M. Electroactivity of natural and synthetic triphylite. *J. Power Sources*. **2001**;97–98:503-7.

(5) Kim J., Lee J., You J., Park M.-S., Hossain M. S. A., Yamauchi Y., Kim J. H. Conductive polymers for next-generation energy storage systems: recent progress and new functions. *Mater. Horiz.* **2016**;3:517-35.

(6) Boyano I., Blazquez J. A., de Meatza I., Bengoechea M., Miguel O., Grande H., Huang Y., Goodenough J. B. Preparation of C-LiFePO4/polypyrrole lithium rechargeable cathode by consecutive potential steps electrodeposition. *J. Power Sources*. **2010**;195:5351-9.

(7) Lepage D., Michot C., Liang G., Gauthier M., Schougaard S. B. A Soft Chemistry Approach to Coating of LiFePO4 with a Conducting Polymer. *Angew. Chem. Int. Ed.* **2011**;50:6884-7.

(8) Cintora-Juarez D., Perez-Vicente C., Ahmad S., Tirado J. L. Improving the cycling performance of LiFePO4 cathode material by poly(3,4-ethylenedioxythiopene) coating. *RSC Adv.* **2014**;4:26108-14.

(9) Das P. R., Komsiyska L., Osters O., Wittstock G. PEDOT: PSS as a Functional Binder for Cathodes in Lithium Ion Batteries. *J. Electrochem. Soc.* **2015**;162:A674-A8.

(10) Meziane R., Bonnet J.-P., Courty M., Djellab K., Armand M. Single-ion polymer electrolytes based on a delocalized polyanion for lithium batteries. *Electrochim. Acta*. **2011**;57:14-9.

(11) Porcarelli L., Shaplov A. S., Salsamendi M., Nair J. R., Vygodskii Y. S., Mecerreyes D., Gerbaldi C. Single-Ion Block Copoly(ionic liquid)s as Electrolytes for All-Solid State Lithium Batteries. *ACS Appl. Mat. Interfaces*. **2016**;8:10350-9.

(12) Lago N., Garcia-Calvo O., Lopez del Amo J. M., Rojo T., Armand M. All-Solid-State Lithium-Ion Batteries with Grafted Ceramic Nanoparticles Dispersed in Solid Polymer Electrolytes. *ChemSusChem*. **2015**;8:3039-43.

(13) Villaluenga I., Bogle X., Greenbaum S., Gil de Muro I., Rojo T., Armand M. Cation only conduction in new polymer-SiO2 nanohybrids: Na+ electrolytes. *J. Mater. Chem. A*. **2013**;1:8348-52.

(14) Hofmann A. I., Smaal W. T. T., Mumtaz M., Katsigiannopoulos D., Brochon C., Schütze F., Hild O. R., Cloutet E., Hadziioannou G. An Alternative Anionic Polyelectrolyte for Aqueous PEDOT Dispersions: Toward Printable Transparent Electrodes. *Angew. Chem. Int. Ed.* **2015**;54:8506-10.

(15) Park B.-w., Yang L., Johansson E. M. J., Vlachopoulos N., Chams A., Perruchot C., Jouini M., Boschloo G., Hagfeldt A. Neutral, Polaron, and Bipolaron States in PEDOT Prepared by Photoelectrochemical Polymerization and the Effect on Charge Generation Mechanism in the Solid-State Dye-Sensitized Solar Cell. *The Journal of Physical Chemistry C*. **2013**;117:22484-91.

(16) Stöcker T., Köhler A., Moos R. Why does the electrical conductivity in PEDOT:PSS decrease with PSS content? A study combining thermoelectric measurements with impedance spectroscopy. *J. Polym. Sci., Part B: Polym. Phys.* **2012**;50:976-83.

(17) Cruz-Cruz I., Reyes-Reyes M., Aguilar-Frutis M. A., Rodriguez A. G., López-Sandoval R. Study of the effect of DMSO concentration on the thickness of the PSS insulating barrier in PEDOT:PSS thin films. *Synth. Met.* **2010**;160:1501-6.

(18) Cruz-Cruz I., Reyes-Reyes M., López-Sandoval R. Formation of polystyrene sulfonic acid surface structures on poly(3,4-ethylenedioxythiophene): Poly(styrenesulfonate) thin films and the enhancement of its conductivity by using sulfuric acid. *Thin Solid Films*. **2013**;531:385-90.

(19) Kirchmeyer S., Reuter K. Scientific importance, properties and growing applications of poly(3,4-ethylenedioxythiophene). *J. Mater. Chem.* **2005**;15:2077-88.

(20) Lei Y., Oohata H., Kuroda S.-i., Sasaki S., Yamamoto T. Highly electrically conductive poly(3,4-ethylenedioxythiophene) prepared via high-concentration emulsion polymerization. *Synth. Met.* **2005**;149:211-7.

(21) Roncali J. Conjugated poly(thiophenes): synthesis, functionalization, and applications. *Chem. Rev.* **1992**;92:711-38.

CHAPTER 6

Conclusions

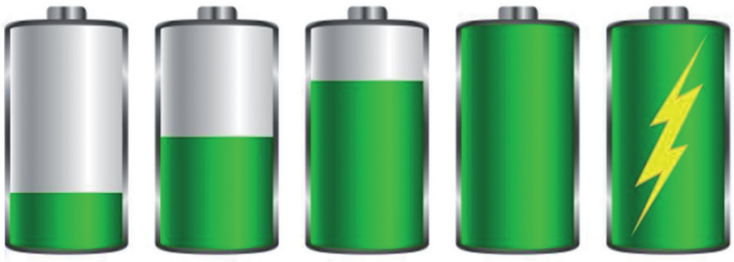

Chapter 6. Conclusions

In this PhD thesis we synthesized innovative PEDOT derivatives for the area of electrochemical energy storage systems. Overall, we demonstrated that conducting polymer PEDOT can be modified to develop electroactive polymers, which can be employed in various energy storage devices including lithium-ion batteries, sodium batteries and supercapacitors.

In the first part of this thesis, a novel PEDOT radical polymer was presented with combined redox and electrical properties, named PEDOT-TEMPO. The functionalization of EDOT monomer with a TEMPO nitroxide radical was the key to obtain the synergetic properties. Moreover, electrochemical techniques allowed to obtain the polymer and to tune its properties depending on the polymerization conditions. Taking advantage of its processability, PEDOT-TEMPO polymer was applied as conductive binder in lithium-ion batteries. It was demonstrated that it can effectively be used as conductive binder, replacing the conventional inactive binder and reducing the amount of high surface area carbon additive generally required in insulating cathode materials.

In the second part of the thesis, sustainable organic electrode materials were synthesized by the polymerization of EDOT in presence of lignin biopolymer. PEDOT/Lignin biocomposites were synthesized by oxidative chemical polymerization and their charge storage

properties were studied in acidic aqueous media. It was demonstrated that the incorporation of lignin provided enhanced energy storage properties to PEDOT by means of its redox active quinone moieties. PEDOT/Lignin composites exhibited high capacitance values and higher stability values than the previous polypyrrole/lignin composites, where strong degradation was observed upon cycling. Moreover, it was proved that oxidative chemical polymerization can be used to scale up PEDOT/Lignin production, satisfying the requirements of inexpensiveness, environmental friendliness and easy processability, for the preparation of electrode materials in supercapacitors.

On the other hand, it was demonstrated that PEDOT/lignin biopolymers are electroactive in aprotic ionic liquid electrolytes by studying their electrochemical properties in a series of pyrrolidinium and imidazolium-based ionic liquids. The investigations about the effects of water and sodium salt addition allowed achieving an optimum electrolyte system for sodium batteries. The concept of a new battery cell was proved by using PEDOT/Lignin as cathode material, the optimized ionic liquid as electrolyte and a sodium anode for the first time. Thus, it was demonstrated that PEDOT/lignin and some aprotic ionic liquids are a promising and effective cathode/electrolyte combination for the development of sustainable sodium batteries. Moreover, these findings open up the possibility to use other lignin derived cathodes in sodium batteries, as well as PEDOT/lignin in other electrochemical devices using ionic liquids as electrolytes.

Finally, the synthesis and characterization of high conductive PEDOT/PSTFSI dispersions were presented. EDOT was polymerized by oxidative chemical polymerization in presence of PSTFSI using different EDOT:PSTFSI weight ratios. In this way, the obtained

dispersions possessed the electronic conductivity of PEDOT and the ionic conductivity of PSTFSI. It was proved that a higher content of PSTFSI leaded to a more conducting and electroactive polymer. Taking advantage of its high conductivity, PEDOT/PSTFSI was used in intrinsically insulating $LiFePO_4$ electrodes to improve its cycling performance. It was demonstrated that the addition of only 5 % of PEDOT/PSTFSI was able to improve the cycling performance and rate capability of $LiFePO_4$ batteries.

Resumen

La sostenibilidad energética y medioambiental son hoy en día dos de los mayores retos de nuestra sociedad. Durante el último siglo, se ha intensificado la búsqueda por mejorar los sistemas de almacenamiento de energía actuales para poder resolver los problemas relacionados con la contaminación y la disminución de combustibles fósiles, así como para poder abastecer el rápido desarrollo de dispositivos electrónicos portátiles, vehículos eléctricos y estaciones de almacenamiento de energía. En el futuro, las tecnologías de almacenamiento de energía que se elijan, consistirán en dispositivos más seguros y con mayores capacidades de almacenamiento, además de materiales rentables y fáciles de procesar.

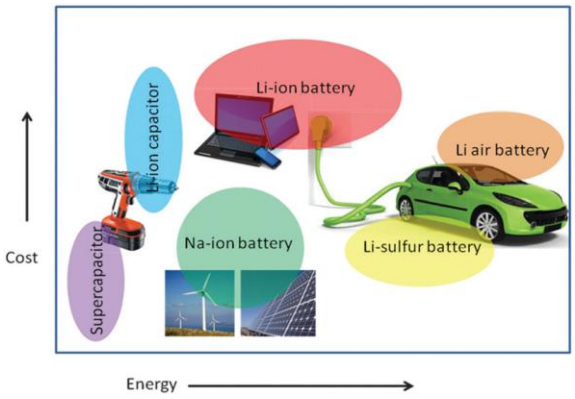

Figura R.1. Gráfico de coste vs. energía de varios sistemas de almacenamiento de energía.

En este contexto, los polímeros conductores son buenos candidatos para implementarlos en dispositivos de almacenamiento de energía, debido a su fácil procesamiento, alta conductividad, bajo peso y buenas propiedades electroquímicas. Además, pueden desempeñar varias funciones a la hora de mejorar las propiedades electroquímicas del dispositivo, por ejemplo, como material de electrodo redox activo o como aglutinante conductor. Entre los diferentes polímeros conductores, poli(etilendioxitiofeno) (PEDOT) es el más prometedor debido a su alta conductividad y estabilidad ambiental. Por ello, el objetivo principal de esta tesis es sintetizar nuevos materiales basados en PEDOT para el área de almacenamiento de energía electroquímica.

En la primera parte de esta tesis, se ha presentado la síntesis y caracterización de un nuevo polímero radical de PEDOT con propiedades redox y eléctricas sinérgicas, denominado PEDOT-TEMPO. Para ello, primeramente se realizó la funcionalización del monómero EDOT con el radical nitroxido TEMPO. Después, se polimerizó el monómero mediante técnicas electroquímicas como la voltametría cíclica. Curiosamente, la electropolimerización en acetonitrilo derivó en un polímero soluble. Estas propiedades hacen que PEDOT-TEMPO sea ideal para utilizarlo como aglutinante conductor en baterías. Se estudió su función como aglutinante en baterías de litio hierro fosfato y se comparó con los resultados obtenidos con un aglutinante convencional (no conductor). Se demostró que el nuevo polímero puede actuar como aglutinante conductor, remplazando así el aglutinante inactivo convencional y reduciendo la cantidad de carbón añadido. Este carbón generalmente es requerido para mejorar la conductividad eléctrica del material catódico, pero a su vez disminuye la densidad energética del cátodo debido a su gran volumen.

En la segunda parte de la tesis, se han preparado materiales de electrodos sostenibles mediante la polimerización de EDOT en presencia del biopolímero lignina. La lignina es el segundo biopolímero más abundante en la tierra y contiene una gran variedad de grupos fenólicos, los cuales son redox activos y así permiten el almacenamiento de carga. La obtención de los polímeros PEDOT/lignina, se realizó mediante polimerización química utilizando varios porcentajes de EDOT/lignina, pudiendo así estudiar el efecto de cada componente en las propiedades de almacenamiento de carga en medio acuoso ácido. Se ha demostrado que la incorporación de lignina aumenta las propiedades de almacenamiento de energía del PEDOT, por medio de sus grupos quinona. Además, se lograron valores más altos de capacitancia y mayor estabilidad de ciclado que en el caso de los anteriores compuestos de polipirrol/lignina, los cuales sufrían una fuerte degradación durante el ciclado. Asimismo, se ha demostrado que la polimerización química es adecuada para la producción de PEDOT/lignina a gran escala, satisfaciendo los requisitos de bajo coste, compatibilidad medioambiental y fácil procesamiento, para finalmente utilizarlo como material de electrodo en supercondensadores.

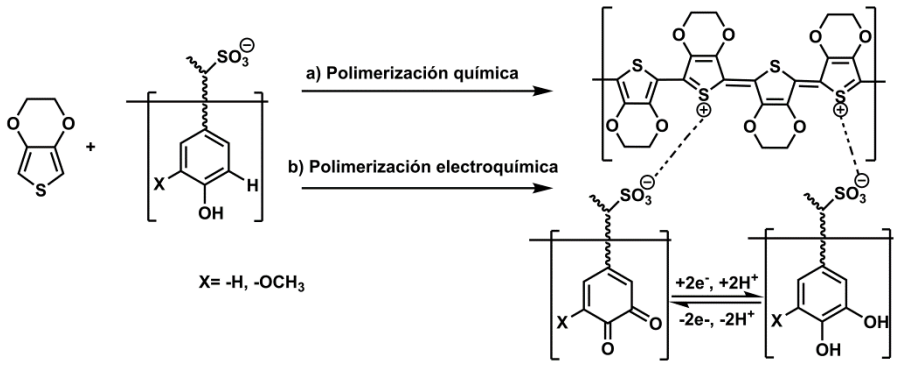

Figura R.2. Rutas de polimerización para la preparación de PEDOT/lignina.

Por otra parte, se ha demostrado la electroactividad de los biopolímeros PEDOT/lignina en electrolitos líquidos apróticos, al estudiar sus propiedades electroquímicas en una serie de líquidos iónicos de pirrolidonio e imidazolio. Los estudios sobre el efecto del agua y la adición de sal sódica en las propiedades electroquímicas del polímero permitieron lograr un electrolito óptimo para realizar baterías de sodio. Así, el concepto de una nueva batería ha sido presentado por primera vez, utilizando PEDOT/lignina como material catódico, el líquido iónico optimizado como electrolito y sodio como ánodo. De tal modo, se ha demostrado que PEDOT/lignina y algunos líquidos iónicos apróticos son una prometedora y eficaz combinación de cátodo/electrolito para el desarrollo de baterías sostenibles de sodio. Además, mediante este estudio se abren nuevas posibilidades para utilizar otros cátodos derivados de lignina en baterías de sodio, así como PEDOT/lignina en otros dispositivos electroquímicos utilizando líquidos iónicos como electrolitos.

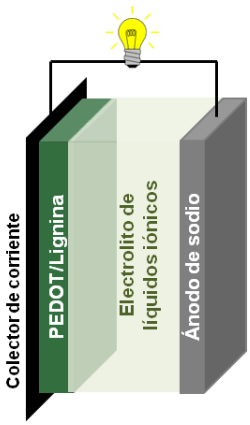

Figura R.3. Esquema de la batería constituida de un cátodo de PEDOT/lignina, un ánodo de sodio y electrolito basado en líquidos iónicos.

Por último, se ha presentado la síntesis y caracterización de las dispersiones PEDOT/PSTFSI con conductividad electrónica e iónica. Para su síntesis, EDOT fue polimerizado por polimerización química oxidativa en presencia del polímero PSTFSI usando diferentes relaciones de peso EDOT:PSTFSI. De este modo, las dispersiones obtenidas poseían propiedades combinadas, la conductividad electrónica del PEDOT y la conductividad iónica del polímero PSTFSI. El polímero más conductor y electroactivo fue obtenido con un mayor contenido de PSTFSI en la dispersión. Aprovechando su alta conductividad, PEDOT/PSTFSI fue utilizado en electrodos de litio hierro fosfato, debido a su carácter aislante, para mejorar su rendimiento durante el ciclado de la batería. Así, ha quedado demostrado que la adición de sólo un 5% de PEDOT/PSTFSI es capaz de aumentar la capacidad de carga y la capacidad de ciclar a velocidades más altas de los cátodos de litio hierro fosfato.

En conclusión, en esta tesis doctoral se han sintetizado nuevos polímeros derivados del PEDOT para el campo de almacenamiento de energía electroquímica. En general, se ha demostrado que el polímero conductor PEDOT puede ser modificado para desarrollar polímeros electroactivos, los cuales pueden ser empleados en varios dispositivos de almacenamiento de energía, como pueden ser las baterías de litio ion, las baterías de sodio o los supercondensadores.

List of acronyms

ACN	Acetonitrile
ATR	Attenuated Total Reflectance
BMImBF4	1-butyl-3-methylimidazolium tetrafluoroborate
BMPyr	1-butyl-1-methylpyrrolidinium
BMPyrFSI	1-butyl-1-methylpyrrolidinium bis(fluorosulfonyl)imide
BMPyrTFSI	1-butyl-1-methylpyrrolidinium bis(trifluoromethylsulfonyl)imide
CE	Counter electrode
CP	Conducting Polymer
CV	Cyclic Voltammetry
DCC	Dicyclohexylcarbodiimide
DCM	Dichloromethane
DLS	Dynamic Light Scattering
DMAP	Dimethylaminopyridine
DMC	Dimethyl carbonate
EC	Ethyl carbonate
EDLC	Electric Double Layer Capacitor
EDOT	3,4-Ethylenedioxythiophene
EDOT-MeOH	2,3-Dihydrothieno[3,4-b][1,4]dioxin-3-ylmethanol
EES	Electrochemical Energy Storage

EMIm	1-Ethyl-3-methylimidazolium
EMImFSI	1-Ethyl-3-methylimidazolium bis(fluorosulfonyl)imide
EMImTFSI	1-Ethyl-3-methylimidazolium bis(trifluoromethylsulfonyl)imide
ESR	Electron Spin Resonance
EtOAc	Ethyl acetate
FSI	Bis(fluorosulfonyl)imide
FTIR	Fourier Transform Infrared Spectroscopy
GC	Glassy Carbon
HMW	High Molecular Weight
IL	Ionic Liquid
LFP	Lithium Iron Phosphate
LMW	Low Molecular Weight
MALDI-TOF	Matrix-ssisted laser desorption/ionization time of flight
MMD	Molar Mass distribution
MS	Mass spectrometry
NMP	1-Methyl-2-pyrrolidinone
PANI	Polyaniline
PEDOT	Poly(3,4-ethylenedioxythiophene)
PEDOT/Lig	PEDOT/lignin
Ppy	Polypyrrole
PSS	Polystyrenesulfonate
PSTFSI	Poly[(4-styrene-sulfonyl)-(trifluoro-methane-sulfonyl)imide]
PT	Polythiophene

PVDF	Poly(vinylidene fluoride)
RE	Reference electrode
SEM	Scanning Electron Microscopy
$TBAPF_6$	Tetrabutylammonium hexafluorophosphate
TEM	Transmission Electron Microscopy
TEMPO	2,2,6,6-Tetramethylpiperidine-1-oxyl
TFSI	Bis(trifluoromethylsulfonyl)imide
TGA	Thermogravimetric analysis
UV/Vis	Ultraviolet/Visible
VPP	Vapour-phase polymerization
WE	Working electrode

List of publications, conference presentations and collaborations

PUBLICATIONS

(1) Polímeros innovadores para almacenamiento de energía. **N. Casado**, G. Hernández, D. Mecerreyes, M. Armand. *cicNetwork*. 2013;14:52-55.

(2) Redox-active polyimide-polyether block copolymers as electrode materials for lithium batteries. G. Hernandez, **N. Casado**, R. Coste, D. Shanmukaraj, L. Rubatat, M. Armand, D. Mecerreyes. *RSC Advances*. 2015;5:17096-103.

(3) Current trends in redox polymers for energy and medicine. **N. Casado**, G. Hernández, H. Sardon, D. Mecerreyes. *Progress in Polymer Science*. 2016;52:107-35.

(4) PEDOT Radical Polymer with Synergetic Redox and Electrical Properties. **N. Casado**, G. Hernández , A. Veloso, S. Devaraj, D. Mecerreyes, M. Armand. *ACS Macro Letters*. 2016;5:59-64.

(5) High performance PEDOT/lignin biopolymer composites for electrochemical supercapacitors. F. N. Ajjan, **N. Casado**, T. Rebis, A. Elfwing, N. Solin, D. Mecerreyes, O. Inganas. *Journal of Materials Chemistry A*. 2016;4:1838-47.

(6) Electrochemical behavior of PEDOT/Lignin in Ionic Liquid Electrolytes: Suitable Cathode/Electrolyte System for Sodium Batteries. **N. Casado**, M. Hilder, C. Pozo-Gonzalo, M. Forsyth, D. Mecerreyes. Accepted in *ChemSusChem.* 2017. DOI: 10.1002/cssc.201700012.

(7) Full-Cell Quinone/Hydroquinone Supercapacitors Based on Partially Reduced Graphite Oxide and Lignin/PEDOT Electrodes. A. M. Navarro-Suárez, **N. Casado**, J. Carretero-González, D. Mecerreyes, T. Rojo. *Submitted*. 2017

(8) New Carboxylic Acid Dioxythiophene (ProDOT-COOH) for easy functionalizable conductive polymers. D. Mantione, **N. Casado**, A. Sanchez-Sanchez, H. Sardon, D. Mecerreyes. *Submitted*. 2017

CONFERENCE PRESENTATIONS

(1) New PEDOT derivative redox polymer for electrochemical energy storage. **N. Casado**, G. Hernández, M. Armand and D. Mecerreyes, 2nd International Forum on Progress and Trends in Battery and Capacitor Technologies-Power our future 2014, Vitoria-Gasteiz, Spain (poster presentation).

(2) PEDOT eratorri berria energia elektrokimikoa gordetzeko. **N. Casado**, G. Hernández, M. Armand and D. Mecerreyes, II Materialen Zientzia eta Teknologia Kongresua, 2014, Donostia-San Sebastián, Spain (oral presentation).

(3) PEDOT bearing TEMPO moieties for Electrochemical Energy Storage. **N. Casado**, G. Hernández, M. Armand and D. Mecerreyes, 2014, XIV International Symposium on Polymer Electrolytes, Geelong, Australia (poster and flash presentation).

(4) PEDOT bearing TEMPO moieties for electrochemical energy storage. **N. Casado**, G. Hernández, S. Devaraj, M. Armand and D. Mecerreyes, 2015, Conducting Polymeric Materials EUPOC 2015, Gargnano, Italy (oral presentation).

(5) PEDOT bearing TEMPO moieties for electrochemical energy storage. **N. Casado**, G. Hernández, S. Devaraj, M. Armand and D. Mecerreyes, 2015, 8th International Conference on Advanced Lithium Batteries for Automobile Applications, Bilbao, Spain (poster presentation).

(6) High performance PEDOT/Lignin biopolymer composites for electrochemical supercapacitors. **N. Casado**, F. N. Ajjan, T. Rębiś, A. Elfwing, N. Solin, O. Inganäs and D. Mecerreyes, 2016, Frontiers in Green Materials, London, United Kingdom (oral presentation).

COLLABORATIONS

This thesis has been done in close collaboration with various universities and research centres. The electrochemical characterizations related to the devices of Chapter 2 and Chapter 5 have been carried out in CIC energiGUNE (Vitoria-Gasteiz, Spain) under the supervision of Prof. Michel Armand and Dr. Devaraj Shanmukaraj, where I regularly moved to perform the experiments.

On the other hand, Chapter 3 was carried out in collaboration with Prof. Inganäs's group of Linköping University (Linköping, Sweeden). PEDOT/lignin composites were synthesized by chemical polymerization at POLYMAT and by electrochemical polymerization at Linköping University. Moreover, some of the electrochemical characterization of Chapter 3 was performed at Linköping University.

Finally, Chapter 4 has been developed at Deakin University (Melbourne, Australia) during 3 months secondment at the Institute for Frontier Materials under the supervision of Dr. Cristina Pozo-Gonzalo and Prof. Maria Forsyth.